# Optimization of LED-based agrivoltaic system

Combining photovoltaic and light emitting diode technology in a horticultural system to improve space and energy efficiency of crop cultivation

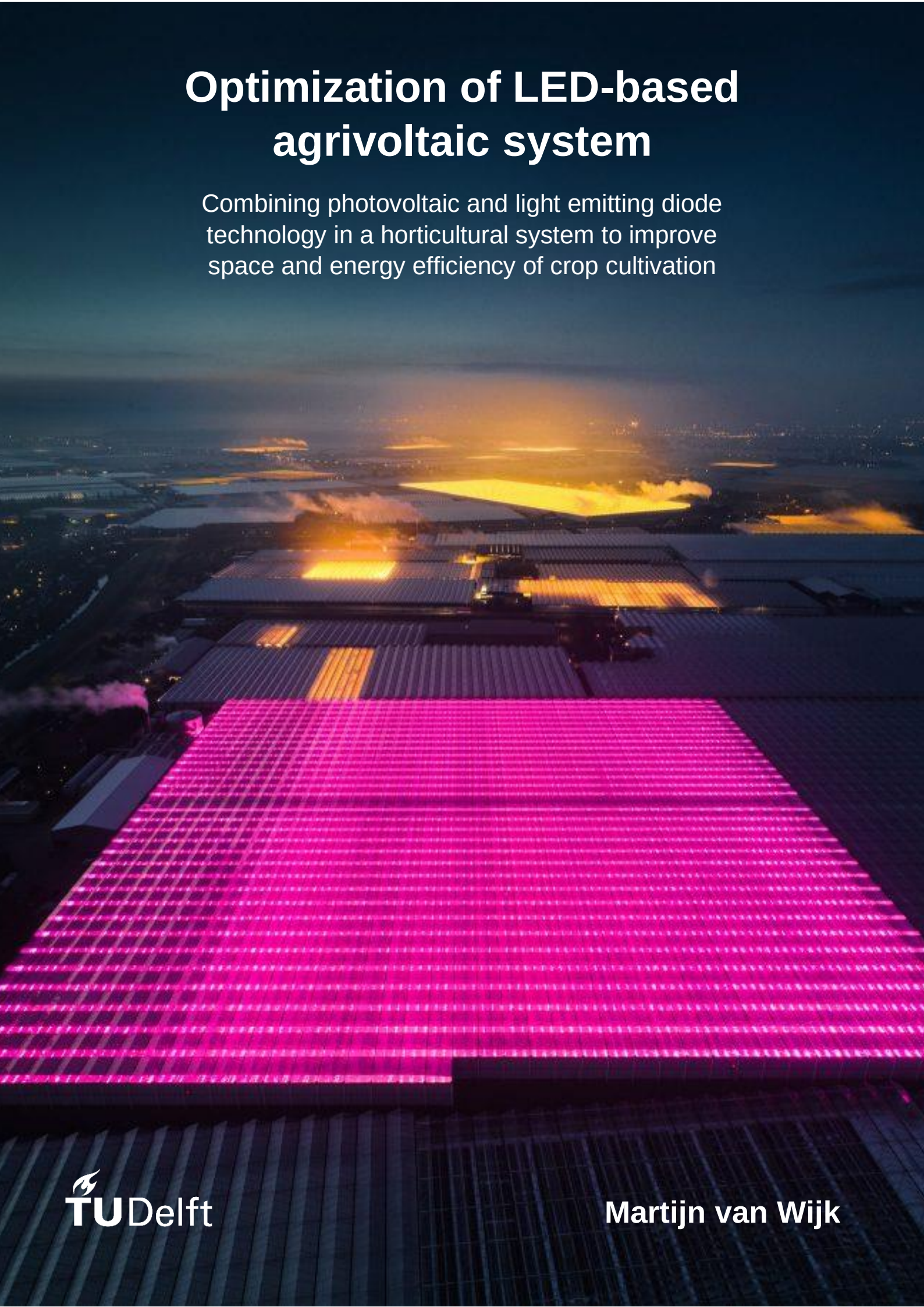

TU Delft

Martijn van Wijk

# Optimization of LED-based agrivoltaic system

## Combining photovoltaic and light emitting diode technology in a horticultural system to improve the space and energy efficiency of crop cultivation

by

Martijn van Wijk

to obtain the degree of Master of Science in Sustainable Energy Technology
at the Delft University of Technology,
to be defended publicly on Wednesday September 23, 2020 at 10:00 am.


| | | |
|---|---|---|
| Student number: | 4354257 | |
| Project duration: | January 6, 2020 – September 16, 2020 | |
| Thesis committee: | Dr. O. Isabella, | TU Delft, supervisor |
| | Dr. H. Ziar, | TU Delft, daily supervisor |
| | Dr. ir. R. Santbergen, | TU Delft |
| | Dr. E. Kaiser, | Wageningen University & Research |


TU Delft

# Preface

This thesis was written as the graduation project for my Sustainable Energy Technology master's program at Delft University of Technology. Several people have contributed academically and practically to this master thesis. Therefore, I would like to thank my main supervisor dr. Olindo Isabella and my daily supervisor dr. Hesan Ziar for their time, valuable input and support throughout the master thesis period. Furthermore, I would like to thank my family and friends for being helpful and supportive during my time at Delft University of Technology. Lastly, may this thesis be useful for readers and for future research about similar topic or any related field.

*Martijn van Wijk*
*Delft, September 2020*

# Abstract

By 2050, the global demand for food and energy is expected to grow by 70% and 50%, respectively, as a result of the increase of the world's population. Despite the significant growth of the food demand, the agricultural land can only be increased by another 2%. Besides that, the agricultural sector is heavily dependent on fossil fuels. Over the coming decades, the share of fossil fuels in the energy mix has to be reduced drastically to decrease the negative impact of the world energy use on the environment. However, the land area needed to produce renewable energy is significantly higher per unit produced than for traditional energy sources. At some places, this results in competition between food and energy production for the use of available land. It is clear that significant changes have to take place in the agricultural sector, regarding land and energy use, to keep up with the growing world population and to reduce its impact on the environment. During the last decades, significant improvements have been made in horticulture. This research combines two of these developments, namely: the integration of photovoltaic (PV) modules in a horticultural system (agrivoltaics) and the use of light emitting diodes (LEDs) as supplemental lighting source for crops.

The main objective of this study is to find the most space and energy efficient *LED-based agrivoltaic system* for the cultivation of lettuce and tomato in three different climates. In order to understand the dynamics of an LED fixture and the optimal lighting conditions for the specified crops, a light simulation model is developed in the Matlab environment. With this simulation model, one is able to determine the characteristics of an LED fixture required for optimal crop growth. The performance of this model is verified by comparing the output of the model with practical measurements with an LED bar. Furthermore, four greenhouse systems and a plant factory are designed. The first scenario is a reference greenhouse that uses High Pressure Sodium (HPS) lighting as an addition to sunlight. The second scenario is comparable to the reference greenhouse, but uses LED lighting instead of HPS lighting. The third scenario is a greenhouse that uses LED lighting and has a checkerboard PV array configuration installed on the roof. In this greenhouse, the amount of sunlight reaching the crops is reduced and the LED lamps ensure that a sufficient amount of light reaches the crops. The fourth scenario is a greenhouse that is fully covered with PV modules and therefore no sunlight is able to enter the greenhouse. LED lamps are the sole source of light for the crops. In contrast with the semi-closed greenhouse systems, the plant factory is a closed insulated system and therefore uses LEDs as the only source of light. The roof of the plant factory is covered with PV modules. Also, it has five storeys of crops, while the greenhouse scenarios only have one layer. For the systems that include a PV system, it is assumed that the electricity produced by the PV systems is dumped on the grid. Besides that, the electricity needed for the systems driven by electricity, is drawn from the grid. There is no storage system present in these systems. The performance regarding space and energy efficiency is analyzed for these five systems for both lettuce and tomato and for three different climate zones and latitudes (24-68°N). The locations are Kiruna (Sweden), Delft (the Netherlands) and Abu Dhabi (United Arab Emirates).

This study shows that the purpose of a horticultural system is important to determine which configuration is optimal. When the productivity per area is the most important requirement, the plant factory has the best performance in all locations, mainly because of the multiple storeys of crops. The combined productivity of the crops and PV energy is six times higher compared to a conventional greenhouse. In case both the productivity and the energy use are important, the greenhouse that uses LED lighting and has a checkerboard PV module configuration installed on the roof has the best performance of all systems in Delft. Compared to a conventional greenhouse, the efficacy of this LED-based agrivoltaic greenhouse is increased by 56%. In more extreme climates, like in Abu Dhabi and Kiruna, a plant factory produces the most crops per unit of energy required. The efficacy in these locations is 6.3 and 1.8 times higher, respectively, compared to the conventional greenhouse. In general, this works shows that the production of food and renewable energy do not have to be in competition for the same piece of land; they can be combined in one system while increasing the cumulative productivity per square meter and the total efficacy of the system.

# Contents

# 1 Introduction

By 2050, the world's growing population will require an estimated 60% more food than is produced today [1, 2]. The arable land available, however, is finite and therefore it is not possible to meet the growing food demand by just increasing the use of land. Global projections show that up to 2040, the amount of agricultural land can only be increased with another 2% [3]. Parallel to the increasing demand for food, the global energy usage is expected to grow with 50% by 2050 [4]. In order to reduce the impact of energy consumption on the environment, the share of renewable energy in the total energy mix needs to increase significantly. The land area needed to produce the same amount of energy as traditional energy sources, is at least four times higher for renewable energy technologies [5]. These trends in the agricultural and energy sector can lead to a conflict in land-use [6]. Also, the agricultural sector itself is heavily dependent on fossil fuels, which are often even subsidized by the local government [7, 8]. It is clear that significant changes have to take place in the agricultural sector, regarding land and energy use, to keep up with the growing world population and to reduce its negative impact on the environment.

The introduction of the cultivation of crops inside greenhouses to ensure year-round production, has been an important development in the agricultural sector. Besides these greenhouses, a lot of other developments have contributed to a more space and energy efficient production of food. For example, the integration of photovoltaic (PV) modules in a greenhouse system (agrivoltaics) contributes to an increased productivity of a certain piece of land. Furthermore, during the last two decades, light emitting diodes (LEDs) have made their entry into the agricultural sector [9]. The use of LEDs in a horticultural system leads to a higher crop yield by being able to specifically target the light conditions that are optimal for a certain plant type. The combination of these two technologies in one system, however, has not been part of research yet. That is why this study focuses on the potential of integrating both PV and LED technology in one horticultural system used for the cultivation of lettuce and tomato, specifically. This leads to the following main research question:

*What is the most space and energy efficient LED-based agrivoltaic system for the cultivation of lettuce and tomato in three different climates?*

In order to understand the state of the art regarding the cultivation of crops and the most important technological developments in the agricultural sector, the next part of this chapter is used to review the relevant literature related to these subjects. At the end of this review, the research gap that forms the core of this study, is explained. Furthermore, the other research questions that support the main research question are presented.

## 1.1. Literature review

In this section the state of the art of the available research relevant for this thesis is described. Scientific publications and relevant previous work form the foundation of this review. The system that is the central element in this research consists of three main parts: the crops, the light emitting diode system (hereafter called LED system) and the photovoltaic system (hereafter called PV system). The state of the art regarding these three components is elaborated on in the paragraphs of this section.

Firstly, this literature review discusses the characteristics of light that are important for plant growth. Secondly, the main developments within the agricultural sector, regarding supplemental lighting technologies and the concept of agrivoltaics are described. Lastly, the state of the art regarding crop cultivation in plant factories is touched upon.

### 1.1.1. Light for crop cultivation

In order to design a system that is optimal for crop growth, it is important to understand how light affects chemical processes within a plant. This section firstly describes the photosynthetic process and the role light plays within this process. Subsequently, the two parameters that have a significant effect on plant growth are discussed: light quality and light quantity.

#### Photosynthesis

Photosynthesis consists of two stages: the light-dependent and light-independent reactions [10]. The light reaction uses two photosystems: photosystem I and photosystem II (hereafter PSI and PSII, respectively) [11]. Both systems are located in the thylakoid membrane. PSI and PSII are named for the order of which they were discovered, not for the order in which they participate in photosynthesis. The light reaction starts in PSII. Chlorophyll pigments in PSII absorb photons. This causes electrons in the photosystem to become energized, after which they leave PSII [12]. Electrons are transported through the electron transport chain towards PSI. To replace the electrons that left PSII, water molecules are split, releasing oxygen, two hydrogen ions and two electrons. The electrons that arrive in PSI, have released stored energy in the transport chain as they moved. This energy is used to create a hydrogen ion gradient across the thylakoid membrane [13]. This gradient is used for the creation of ATP [14]. The electrons moving through the electron transport chain end up in PSI. In PSI the electrons are energized again by the light that is absorbed by the photoreceptors present in PSI. After being energized, the electrons leave PSI, and form NADPH together with a hydrogen ion [10]. NADPH is used in the Calvin cycle reactions together with ATP and $CO_2$ to create carbohydrates. The reactions in the Calvin cycle are not directly driven by light. The final product, carbohydrate, is used as an immediate source of energy for cells in a plant [15]. This energy is used for production of structural compounds and is important to plant growth. The overall photosynthetic reaction for photosynthesis is [16, 17]:

$$CO_2 + 2H_2O + (energy) \rightarrow (CH_2O)_n + H_2O + O_2 \tag{1.1}$$

In this chemical reaction, $CH_2O$ represents a carbohydrate. The synthesis of carbohydrate from carbon ($CO_2$) and water ($H_2O$) requires light energy. The energy needed to fix one $CO_2$ molecule is equal to 9 mole photons with a wavelength of $680nm$ [16, 17]. The energy of a photon depends on the wavelength of the photon and can be determined with the following relation:

$$E_{ph} = \frac{hc}{\lambda}, \tag{1.2}$$

where $E_{ph}$ is the photon energy in $eV$, $h$ is Planck's constant in $Js$, $c$ is the speed of light in $m/s$ and $\lambda$ is the wavelength of the photon in $m$. Despite the fact that photons with a short wavelength (like blue light) contain more energy than photons with a longer wavelength, 9 photons of blue light cannot fix more $CO_2$ than 9 photons of red light. This is why photosynthetic calculations should always use quantum units [18]. The next sections will further elaborate on this.

#### Photosynthetically Active Radiation

Sunlight is the primary source of light for plants. The spectral distribution of solar radiation reaching the earth's surface has a broad wavelength range, from 100 $nm$ to about $1mm$ [19]. In figure 1.1, the most significant wavelengths of the broad AM1.5 solar spectrum are displayed. However, only 47% of the radiant energy can be used by plants [14]. This part is called the Photosynthetically Active Radiation (PAR) and ranges from 400 to 700 $nm$ [20]. This wavelength range is approximately the same as the for human visible spectrum, as can be seen in figure 1.1.

In the leaves of plants, specialized photoreceptors are present that are able to capture photons from the PAR region and convert the radiant energy into chemical energy in the photosynthetic process. This process is explained in more detail in section 1.1.1. High frequency photons (UV photons), with wavelengths below the

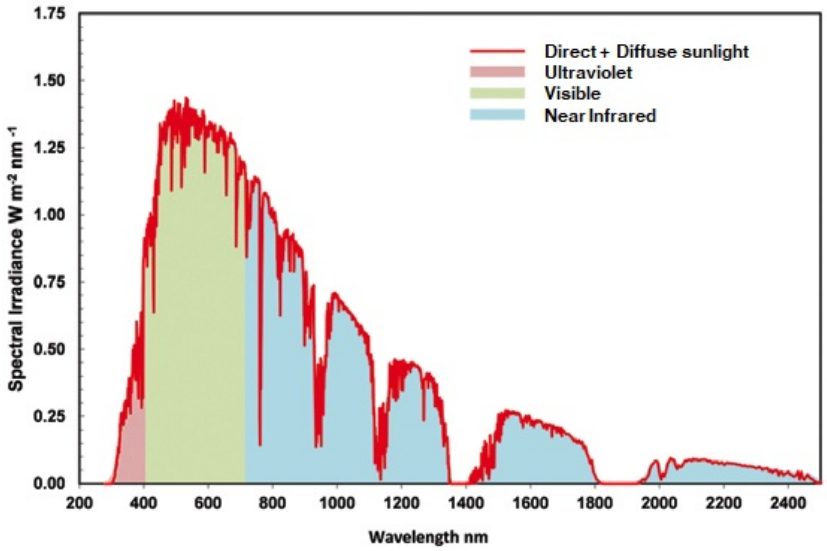


Figure 1.1: Air Mass 1.5: ASTMG-173-03 [19]

PAR range, contain too much energy for the plant to utilize them. UV light can be subdivided into three types: UV-A, UV-B and UV-C. The UV-C region includes wavelengths below 280 $nm$. These high energetic photons are not present in sunlight reaching the earth's surface, since they are absorbed by ozone in the stratosphere [21]. UV-A and UV-B radiation are known to damage various plant processes, because of their high energy. They cause damage to DNA and damage to physiological processes within plants [21, 22]. At the same time, other plant photopigments do have a positive response on UV light and respond under dimmed light conditions. However, these are likely suppressed under high light conditions [23]. On the other hand, low energetic photons with wavelengths higher than the PAR range (in the infrared part of the spectrum), do not contain enough energy to start the photosynthetic process. However, in combination with photons within the PAR range, infrared (IR) photons can have a positive effect on photosynthesis [24]. This is called the Emerson effect. This is why in 2020, Zhen and Bugbee [25] presented an argument in favor of redefining the PAR region, to also include far red wavelengths (400 - 750 $nm$). The concept of the Emerson effect is further explained in the next section.

## Spectral quality

In the section *Photosynthesis* it was discussed that 9 mole photons of blue light cannot fix more $CO_2$ molecules than 9 mole photons of red light. Therefore, not all photons in the PAR range are used equally efficient in the photosynthetic process. It can be concluded that the photosynthetic responses of a plant to light are wavelength-dependent [24, 26–30]. It has been shown that plants essentially utilize the blue, red and infrared portions of the spectrum for the photosynthetic process and for the regulation of various adaptive and developmental processes. Figure 1.2 shows the typical absorption spectra of the most common photomorphogenic and photosynthetic photoreceptors. The photomorphogenic responses are regulated by three types of photoreceptors, namely: phototropins, cryptochromes and phytochromes. The photomorphogenic responses include leaf expansion, flowering, shade avoidance, stomatal development and chloroplast mitigation. As displayed in figure 1.2, it can be concluded that these photoreceptors mainly have a response on photons with a wavelength between 400 to 500 $nm$ and from 600 to 750 $nm$ approximately.

Clorophyll $a$ and $b$ absorb photons and use the energy for the photosynthetic process [32]. Just like the photoreceptors for photomorphogenesis, the main absorption peaks of chlorofyll lie in the blue and red regions. Both, photosynthesis and photomorphogenesis are important processes for plant growth. In 1972, McCree [30] tested the actual plants metabolism as a response to light at different wavelengths. McCree created a plant sensitivity curve, also known as the McCree curve. This curve, depicted in figure 1.3, shows the efficiency of photons reaching the crops in driving photosynthesis at different wavelengths. He used 22 different plant species and grew them under various testing conditions. In his research, McCree determined the $CO_2$ assimilation rates of different crops for specific wavelength regions. In figure 1.3, the relative action spectrum

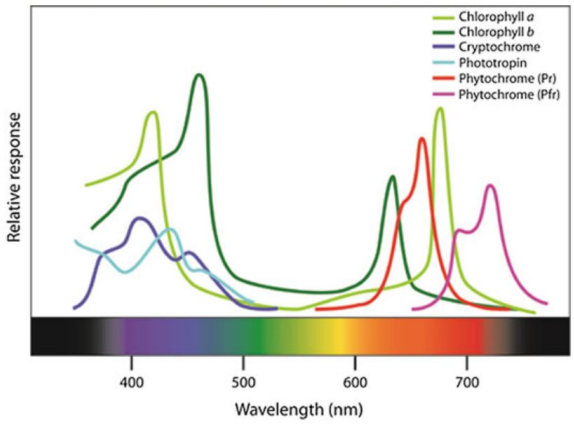


Figure 1.2: Wavelengths of light used by chlorophylls for photosynthesis, by phytochrome, cryptochrome and phototropin for photomorphogenesis [31]

found by McCree is shown. The relative action spectrum is the relative photosynthetic rate, which is the rate at which $CO_2$ is taken up divided by the rate at which energy is received by the plant. McCree's results indicate that red light between 625-675 $nm$ is used most efficiently, followed by a lower blue peak around 450 $nm$. These peaks are approximately equal to the absorption peaks of chlorophyll (shown in figure 1.2). Besides the chlorophyll pigments, other pigments are also involved in the absorption of photons [33]. These photoreceptors can absorb light that is poorly absorbed by the chlorophyll receptors and transfer the excitation energy to chlorophylls. This process allows plants to use much of the light with wavelengths in the PAR region in the photosynthetic process. This utilization of the PAR region is in line with the findings of McCree.

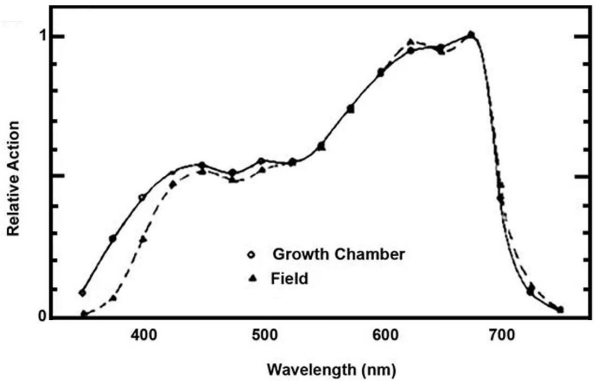


Figure 1.3: Action spectrum McCree: relative photosynthetic rate at different wavelengths [30]

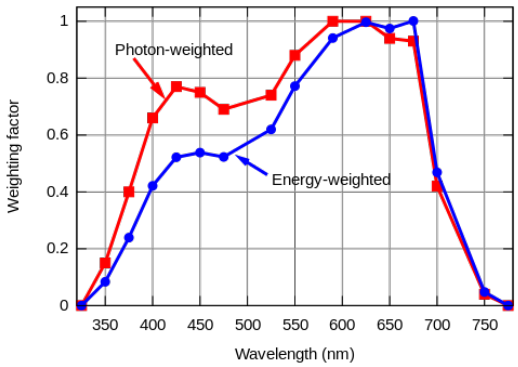


Figure 1.4: Energy weighted and photon weighted action spectrum [34]

As mentioned above, the action spectrum is the rate at which $CO_2$ is taken up divided by the rate at which energy is received by the plant. This action spectrum is therefore energy weighted. However, it has been discussed that measuring light in the number of photons is more commonly used as the predictor of photosynthesis by horticulturalists. Using equation 1.2, the energy weighted action spectrum can be scaled to a photon weighted action spectrum [34]. This is shown in figure 1.4. The blue curve shows the energy weighted action spectrum and the red curve shows the photon weighted action spectrum. From the blue curve, it can be concluded that the highest photosynthetic rate per incident unit of energy is at around 660 $nm$. However, the red curve shows that the highest amount of photosynthesis per photon is for photons with a wavelength of around 610$nm$, since short-wavelength photons carry more energy per photons.

Three major reasons for the wavelength dependence of the efficiency of absorbed photons in driving photosynthesis have been found. First of all, photosynthetic carotenoids have their absorption peaks in the blue wavelength region (not shown in figure 1.2). Carotenoids are essential photoreceptors in photosynthesis and after they absorb photons, they transfer the absorbed energy to chlorophylls to expand the wavelength range

of light that is able to drive photosynthesis [35]. Photosynthetic carotenoids differ in their efficiency (from 35 to 90%) for excitation energy transfer to chlorophylls. The efficiency of this transfer depends on the type of carotenoid and the location in the photosynthetic apparatus [27]. On the other hand, the energy transfer efficiency of chlorophyll to chlorophyll is 100 % [36]. Secondly, nonphotosynthetic photoreceptors, like the so-called flavonoids and free carotenoids, also absorb light. Their absorption maxima are mainly in the UV region, but also in the blue and green part of the spectrum. These nonphotosynthetic photorecepters do not transfer this absorbed energy to the photosynthetic apparatus [27]. In order words, these receptors absorb photons in the PAR region, but these photons are not used for photosynthesis. Thirdly, the photoreceptor composition and absorbance characteristics differ between photosystem I and photosystem II. Because of this, the balance of excitation between photosystem I and II is wavelength dependent [37]. An imbalance in excitation of the two systems causes quantum yield losses. These three causes explain why the photosynthetic rate is not 100% at all wavelengths. However, the understanding of the contribution of each of these factors to the losses in the efficiency is still lacking [27].

Nowadays, the McCree curve is still used as a standard in the agricultural sector by horticulturists and suppliers [31, 38]. However, the shortcomings in the creation of this curve have to be taken into account when applying it. The results were found by analysing single leaves at a low photon flux and over a short time interval of several minutes [30]. This method simplifies the way of measuring, but more realistic results would have been found by measuring the chemical processes of the whole plant at a high photon flux (comparable to a realistic environment) for a longer interval. Furthermore, McCree tested each color individually. The McCree curve shows all the individual results of the different colors in one graph, whereas in reality, plants are exposed to a broader spectrum (for example the solar spectrum). Also, by measuring the effect of each color individually, McCree found that infrared light is almost not used by plants. In 1957, however, Emmerson [39] already showed that if a plant is exposed to two different wavelengths at the same time, the photosynthetic rate in a plant can increase. This extra boost of photosynthesis is called the Emerson effect. This phenomena occurs when any wavelength in the PAR region is combined with infrared light. It is the product of photosystem I and II. As mentioned in section 1.1.1, PSI and PSII work together and share light to boost photosynthesis. First, PSII absorbs wavelengths below 680 *nm*. It uses this light to split an electron from water and sends it to PSI. PSI then takes that elecron and uses infrared light (wavelengths higher than 700 *nm*) to increase photosynthesis.

McCree's study should not be considered to be the definitive reference for the optimal spectral distribution for plants. Since the publication of McCree in 1972, many other researches have been done to find the effects of different spectral distributions and lighting combinations on plant growth. A significant part of this research focuses on the effect of using different ratios of blue and red light to grow plants [40–45]. Promising results have been found by using only red and blue light at different intensity ratios, but the results lack consistency. The differences in photosynthetic efficiencies might be explained by the Emerson effect as discussed before. For example, in 2017, Zhen and van Iersel [46], compared the net photosynthesis of lettuce under white and blue/red LED light. They found that the net photosynthesis was consistently higher under the white lighting than under the blue/red lighting, measured at the same photon flux. This shows that a broader spectrum is used more efficiently than just a blue and red peak. However, an in-depth understanding of this synergism of multiple wavelengths is still limited.

The conclusion after years of research is still that the effects of light quality on plant growth are complex and mixed results have been reported over time [47]. Also, different plant species can react differently on the same lighting setup [48]. Spectral distributions are not yet custom-made, nor optimized. Nevertheless, it can be concluded that McCree [30] created an important foundation for the understanding of the role of the spectral quality of light on chemical processes within plants.

### Light quantity

Plant growth and development are not solely influenced by the qualitative aspect of light. Besides the spectral distribution, also the amount of light falling on a certain surface over a certain time interval is important. This section describes the relevant parameters for the determination of the quantity of light.

**Photosynthetic Photon Flux Density**
Despite the fact that certain wavelengths are more efficiently absorbed by plants than other wavelength, photosynthesis is a quantum process [49]. This means that the chemical reactions of photosynthesis are more dependent on the number of photons than the energy the photons contain. That is why in plant biology, the flux of light that reaches the crops is quantified using the number of photons reaching a specific surface for a specific amount of time. The flux of PAR photons falling on a square meter each second is called the Photosynthetic Photon Flux Density (PPFD) (in $\mu mol/(m^2 s)$). For most plants, the photosynthetic process starts at a PPFD of 20 $\mu mol/(m^2 s)$. Figure 1.5 shows the relation between the PPFD and the Electron Transport Rate (ETR): a measure for the rate of photosynthesis.

In this figure, the rate of photosynthesis is given as the number of electrons travelling through PSII every second: the electron transport rate (ETR). Weaver and van Iersel [13] determined this rate of electron transport by measuring the fluorescence emitted by chlorophyll *a* before and during a short exposure to light. First it is important to understand that light absorbed by chlorophyll can undergo one of three fates. First of all, because the accumulation of excess light energy in the chlorophyll can lead to damage of PSII, plants have evolved several protective mechanisms that can dissipate excess absorbed photons as heat [50]. Secondly, it can be used to drive photosynthesis. Lastly, absorbed light can be re-emitted as light, which is called chlorophyll fluorescence [51]. These processes happen in competition: when the yield of one increases, the yield of the other two decrease. By measuring the chlorophyll fluorescence, Weaver and van Iersel were able to determine the ETR at different PPFD's. Figure 1.5 shows this relation. It can be seen that as the PPFD increases, a greater part portion of absorbed light energy is dissipated as heat, leaving a smaller part of the energy to drive photosynthesis [50, 52]. The measurements follow an exponential rise to an asymptote. An important conclusion that can be drawn from this graph is that the lower the PPFD reaching the crops, the higher the efficiency is at which plants utilize absorbed light energy.

**Photoperiod**
Another important factor affecting plant growth is the photoperiod. This is the amount of time during a day crops are exposed to light [53]. The photoperiod can affect biomass accumulation of many crops [54]. Berkovich et al (2017) found that by extending the photoperiod from 16 to 24$h$ per day, doubled the weight of all cultivars of loose leave lettuce. With the same amount of photons that have reached the plants after a day, plants under 24$h$ radiation weighted 30 to 50% more than plants with a 16$h$ photoperiod [55, 56]. The effects of the photoperiod on plant growth, however, depends on the species. Short day plants grow best when there is less than 12$h$ of daylight. On the other hand, long day plants grow best when they receive light for at least 12$h$ per day [57]. Together with the PPFD, the photoperiod determines the total amount of photons received by the plant per day. This quantity is called the Daily Light integral.

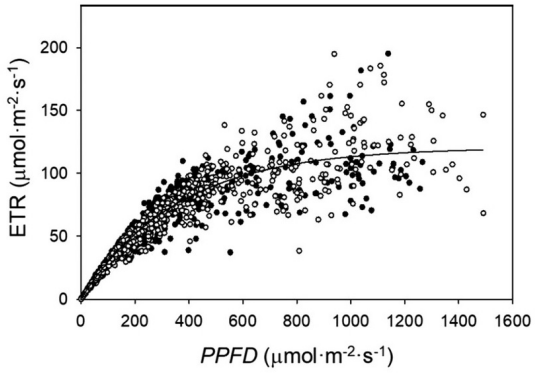


Figure 1.5: Electron Transport Rate in PSII at different PPFD's for lettuce [13]

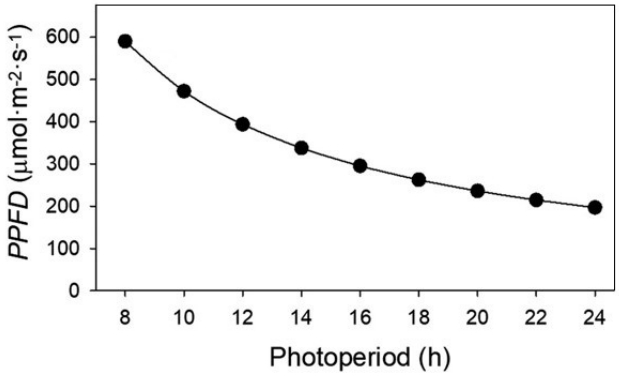


Figure 1.6: Relation between the PPFD and the photoperiod for lettuce [13]

**Daily Light Integral**
The Daily Light Integral (DLI) is the total amount of PAR photons that fall on a square meter in a day and has the unit $mol/(m^2 day)$. Each plant species has its own optimal value for the DLI. As an example, the optimal

DLI for lettuce is 17 $mol/(m^2 day)$ [13, 58, 59]. The DLI can be determined with the following equation:

$$DLI = 3600 \times PPFD \times Photoperiod \tag{1.3}$$

The factor 3600 is used to convert the PPFD from photons per second to photons per hour. Figure 1.6 displays this relation for the crop lettuce. From this graph it can be concluded that the longer the photoperiod is, the lower the PPFD needs to be to meet the optimal daily lighting integral. Combining the conclusions from figure 1.5 and figure 1.6 and the fact that lettuce is a long-day plant, the optimal values for the photoperiod and PPFD are 24 *hours* and 197 $mol/(m^2 day)$ respectively.

### 1.1.2. Developments in agriculture

This paragraph describes a number of important developments within the agricultural sector. Because agriculture has had a enormous evolution over time, only the developments relevant for this research are discussed in this section. First of all, the concept of cultivation within greenhouses is touched upon. Secondly, the idea behind and developments around supplemental lighting are presented. Lastly, the concept of agrivoltaics and the cultivation of crops in plant factories is explained.

#### Greenhouses

A greenhouse, normally consisting of a structure of glass and metal, is a semi-closed environment in which plants are cultivated. The idea behind indoor cultivation, or greenhouses and the need for year round crop production already exists for centuries. However, greenhouses were only commonly used by the end of the 19th century [60]. Greenhouses have several advantages compared to open-field farming. First of all, in greenhouses, one is able to grow crops all year round, because the temperature within a greenhouse is regulated. Also plants within a greenhouse are protected against a variety of diseases, birds and insects and extreme weather conditions like hail and snow [61, 62]. Because the plants are less affected by fluctuations of the external environment, the annual yield of crops per square meter within a greenhouse is normally higher compared to the same area of open-field agriculture.

On the other hand, the cultivation of plants within greenhouses demands more energy. Cooling and heating systems help to regulate the internal climate and demand a significant amount of energy. The amount of heating and cooling needed is dependent on the region and climate a greenhouse is located in. In the Netherlands, greenhouses have the problem of overheating during the summer, caused by the external air temperature and solar irradiation. A common solution for overheating in summer is to open windows of the greenhouse for natural ventilation or the use of light blocking screens on top of the greenhouse to prevent too much light energy from entering the greenhouse [63]. This concept can be seen in figure 1.7.

Figure 1.7: Sun blocking screen to control the amount of sunlight that enters the greenhouse [64]

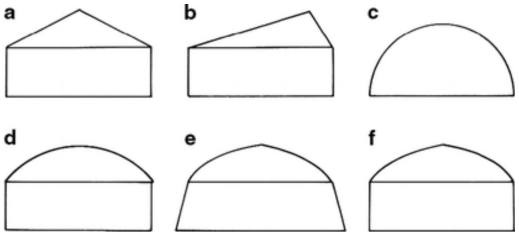


Figure 1.8: Most frequently used shapes of greenhouses worldwide [62]

World wide, a variety of greenhouse designs exist. Figure 1.8 shows cross sections of multiple types of greenhouses [62]. It is dependent on the geographical location and the possible investment which greenhouse type has the best shape. For example, the arch shaped greenhouses like example *c, d* and e, are often made of plastic film and therefore need a low investment. Some designs allow for better natural or mechanical ventilation and others are more suitable for capturing light.

In the Netherlands, the Venlokas is the most commonly used type of greenhouse (type *a* in figure 1.8) [65]. In figure 1.9, an example of common dimensions is given. The design of the Venlokas changed over time. The main improvement made is the significant increase in span length. The roof of the greenhouse is titled to increase the amount of sunlight reaching the crops. Most of the sunlight beams reaching the earths surface have an inclination angle significantly lower than 90 *degrees*. When the greenhouse would have a flat roof, the angle of incidence would be relatively large most of the time. The larger the angle of incidence with respect to a surface is, the more light is reflected. This is why the covering glass forming the roof of a greenhouse is normally tilted at and angle around 25 *degrees* [66]. This triangle roof design also helps to get rid of excess heat more easily. The warm air rises and is captured in the roof-ridges. This phenomena is shown in figure 1.10. In this figure an arch shaped greenhouse is shown, but the concept is the same as in a Venlokas. When the heat builds up in the roof-ridge, the windows present in the roof can be opened and excess heat can be removed via natural ventilation [67].

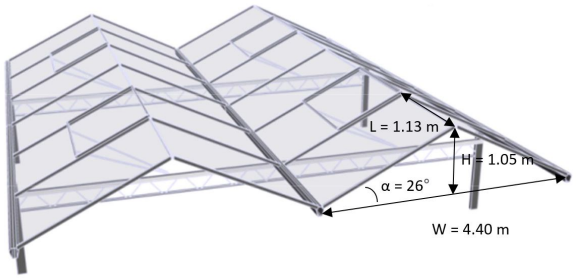


Figure 1.9: Venlokas with dimensions that are commonly used nowadays [66]

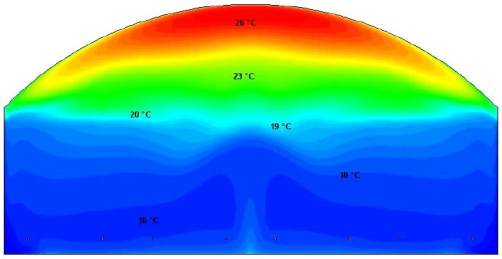


Figure 1.10: Temperature gradient over cross-section of arch shaped greenhouse [67]

## Supplemental lighting

As discussed above, greenhouses form a protection for the plants against bad conditions from the environment. In the winter season the temperature does not drop significantly within the greenhouse and plants can still grow. However, the yield in greenhouses in the winter season is suboptimal because the amount of available sunlight reaching the crops is insufficient. In the Netherlands, a DLI of 2 $mol/(m^2 day)$ is not a rare event on winter days. As discussed, the optimal DLI value for lettuce is 17 $mol/(m^2 day)$ and thus crop productivity would be low when only using sunlight as the source of light energy.

In order to mitigate this low crop productivity, artificial light sources are used to augment insufficient sunlight. The first report of plant growing under artificial light was published in the 1861 by Mangon [68]. The commercial application of artificial light to grow crops, however, started only after the development of more long-lasting and robust lamps, in the first half of the twentieth century [69]. In greenhouses, artificial light is used as a supplemental light source to boost plant growth. Artificial light structures within a greenhouse are turned on in case not enough sunlight reaches the crops over a day time. Before the conventionally used artificial lighting technologies in greenhouses are explained, it is first important to understand how the productivity of artificial light sources is measured. Although, the efficiency of a lamp fixture can be calculated in watts of output per watt of input, plant growth is determined by moles of photons and not by watts of power. This is why the efficacy is a more appropriate way to quantify the productivity of lighting systems. This quantity has the unit $\mu mol/Joule$. The input energy of the lamp is measured in Joule and the number of PAR photons emitted by the lamp are measured in $\mu mol/s$. Both the terms efficiency and efficacy are widely used in lighting, and care must be taken not to confuse them.

### Traditional lighting techniques

Over the years, several different lighting techniques have been used, including: incadescent, fluorescent, high-pressure mercury, high-pressure sodium and metal-halide lamps [31]. These traditionally used lamps are discussed in this paragraph. The next section describes more about the relatively new technique used in agriculture, namely Light Emitting Diodes (LEDs).

Incadescent lamps make use of the incandescence mechanism to emit light. This mechanism is produced by an electric current flowing through the tungsten filament. Tungsten has been the only metal used for producing the filament for incadescent lamps since the twentieth century . It has the characteristics of having a high melting point and a low coefficient of thermal expansion [31]. As the filament heats up because of the electric current, its gradually starts dissipating energy as electromagnetic radiation. Only around 10 % of the input power is converted to PAR photons and the rest is emitted at heat [70]. The poor efficacy and unbalanced spectrum (shown in figure 1.12) are the main causes why incandescent lights are barely used anymore as supplemental lighting in greenhouses. Besides these two disadvantages, these lamps also have a relatively low lifetime expectancy of around 2000$h$.

A more frequently used lighting technique in horticulture is the fluorescent lamp [70]. This lamp consists of a hollow glass tube filled with a mixture of argon and mercury vapors in a low pressure environment. By sending a current through the tungsten cathode, it heats up and starts emitting electrons [71]. These electrons cause the excitation of other electrons in the outer orbitals of the mercury atoms. The excited electrons fall back to the ground state and doing so they emit UV radiation. The high energy UV photons are absorbed by the phosphor coating with fluoresces or starts emitting photons within the visible range by the down-conversion of high energy to low energy photons. A significant part of the input is lost during the conversion of UV photons into PAR where almost half of the energy of each photons is lost as heat [31]. The working principle as described above is visualized in figure 1.11. The reason why fluorescent lamps were used more often in horticulture than incadescent lamps is mainly because of the higher efficacy, longer lifetime expectancy and a more balanced spectral output. This spectral output is shown in figure 1.12. Typically, 90% of the spectrum is within the PAR region, with a peak in the blue region. Primary UV emissions are down-converted by layers of phosphor materials present in the inner surface of the glass tube.

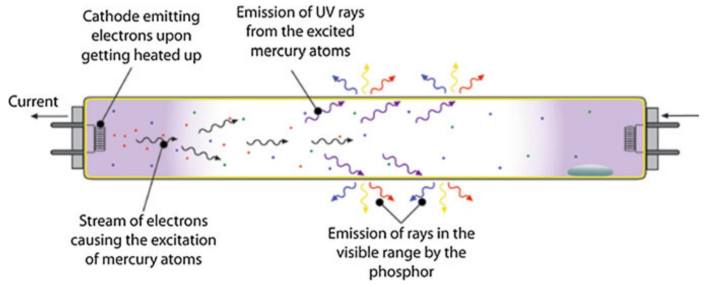


Figure 1.11: Functioning of a fluorescent lamp [31]

A third lighting technique that has been commonly used is the high-intensity discharge (HID) lamp. The working principle of the lamps is comparable to the fluorescent lamps. However, the HID lamps work at a high operating pressure and temperature, to improve the spectral output and efficacy [70]. The gas mixture is maintained in a quartz arc tube to the high pressure that is 200,000 times higher than in fluorescent lamps [31]. Also in this lamp, mercury atoms are ionized by the emission of electrons from the tungsten electrodes. However, because of the high pressure, the frequency of the collisions between electrons and mercury atoms becomes very high. This creates a lot of heat, resulting in the electrons to get ionized to higher excitation states. This leads to the emission of photons at wavelengths in the visible and UV range. The metal halide lamps falls under the HID lamps and used metal halides along with mercury vapor and inert gas to optimize the spectral output quality. Metals like scandium, sodium and indium are used because of their typical emission spectra in the visible range. An extra feature of these lamps is that the outer casing is made of UV-filtering glass to block UV radiation of mercury. The output spectrum can be tuned by changing the combinations of the metal vapor mixture [71]. Metal halide lamps have a spectral output mainly in the PAR region. Furthermore, the lamp has a relatively high efficacy and a long lifetime expectancy of around 20,000 *hours*.

The most commonly used lighting technique in greenhouses in northern latitudes is high-pressure sodium (HPS) lamps. HPS lamps operate at very high pressures and temperatures [31]. As in fluorescent lamps, HPS lamps contain a mixture of gasses, namely sodium vapors along with mercury. The tube is pressurized with xenon. They have the same working principle as fluorescent with electric discharge through a gas. However, the high pressure and temperature improve the spectral output and increase the efficacy of the lamp. The excitation of sodium and mercury occurs by the collision with electrons from the tungsten electrodes.

Thermal ionization in combination with the electron impact ionization causes electrons to jump to various higher energy states. While falling back to the ground state, the electrons emit light covering a wide range in the visible spectrum. The main advantages are that the lamp is low cost, the largest part of the emission is in the PAR region, it has a relatively long lifetime expectancy and a high efficacy. Despite the fact that most of the photons have a wavelength in the PAR region, HPS lamps have a poor spectral quality since the photons are predominantly in the yellow-green and infrared regions of the spectrum. In winter, when there is little sunlight available, plants growing under these lamps may suffer from unbalanced morphology resulting in excessive leaf and stem elongation [72].

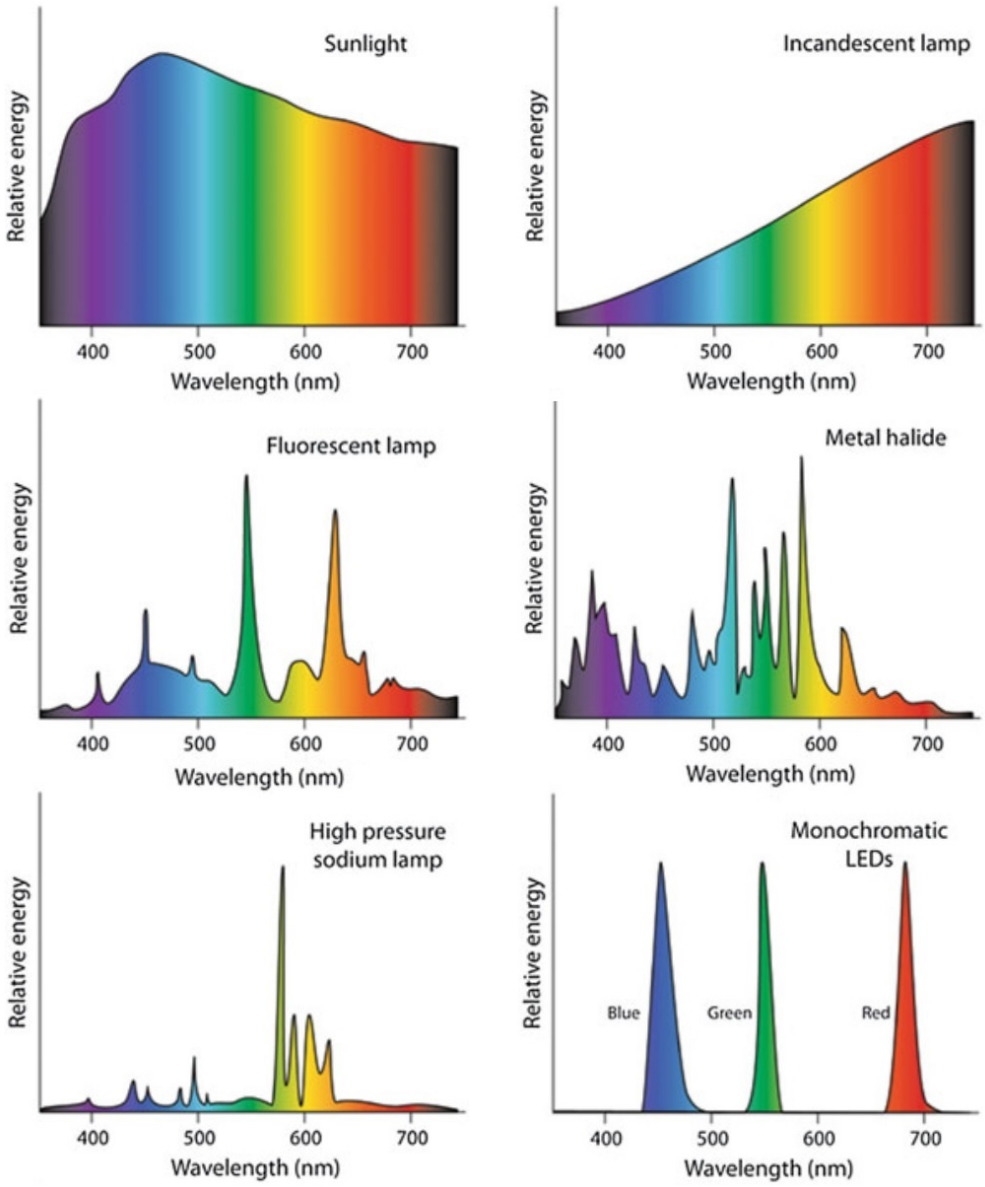


Figure 1.12: Spectral output in PAR region of different light techniques [31]

## Light Emitting Diodes

LEDs are categorized as solid state light sources, because they emit light from a semiconductor diode chip [31]. This technology has a high potential in crop cultivation and has already been introduced in agriculture. This section describes the major landmarks in the development of LEDs, the working principle of the diode and the benefits of LEDs compared to the traditional lamps as light source to grow plants.

**Delevelopment of LED technology**
The first light emitting diode was patented in 1961 by Biard and Pittman [73]. While working on solar cells, they accidentally discovered the emission of infrared radiations from gallium arsenide (GaAs) semiconductor during the passage of electrcity. In the decades after that, the LED technology is significantly improved. However, the lack of viable blue LEDs delayed the utilization of LED technology to grow crops. Finding suitable materials for making blue devices proved difficult [74]. In 1994, Nakamura [75], presented the first design of a high-brightness blue LED using an indium gallium nitride (InGan). This LED had a peak emission wavelength of 450 $nm$, a wavelength that was found to be suitable for use in studies on plant growth. This invention also enabled the development of energy-efficient and high brightness white light sources and was awarded with the Nobel Prize in Physics in 2014. Over the years, further developments in LED technology has led to a further reduction in the cost and significant increase in efficacy ($\mu mol/J$).

**Structure and working principle**
As mentioned above, an LED consists of a semiconductor chip. This chip is housed within an epoxy or plastic lens, with connecting wires to direct the electrical current [31]. The so called dual in-line package (DIP) LED has been the most commonly used LED type and the components of this design can be seen in figure 1.13a. In figure 1.13b, the components of the newly developed high power LED is displayed. Compared to the DIP-LED, this LED has a higher luminosity, because of the higher current flow that is able to flow through it.

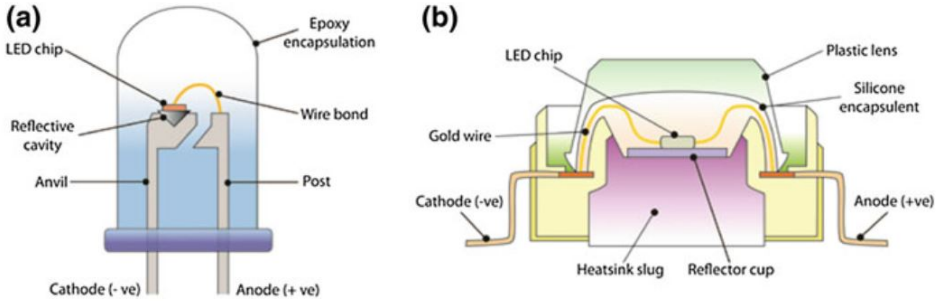


Figure 1.13: (a) Dual in-line package LED and (b) high power LED [31]

The semiconductor wafer, having a size of approximately 1 $mm^2$, has been impregnated with specific dopants or impurities. Two types of dopants exist: $n$-type (elements having a high number of valence electrons) and $p$-type (having a high number of holes in the valence shell. The $p$-type and $n$-type are fused together and form a $p$-$n$ heterojunction [31]. The PN-junction is a structure that, under certain circumstances, can spacely seperate electrons and holes. By forward biasing the device, which occurs by applying a higher voltage in the $P$ than in the $N$ material, the current flows through the structure causing the electrons and holes to meet in the same region of the space. This process is known as carrier injection. When there are many electrons and holes in a region of space, more than those corresponding to their equilibrium values, carrier recombination is enhanced and energy is emitted. This process is shown in figure 1.14.

In semi-conductors, free electrons always have higher energies than those electrons forming the bonds between atoms [76]. The range of energy values that free electrons have, is called conduction band. The energy values that bound electrons have is called valence band. Since the holes are the absence of electrons in the atomic bonds, holes have energies corresponding to the valence band. There can be no electrons in the semiconductor with energies between both bands. Therefore, this interval is called bandgap. When a free electron recombines with a hole in the valence band, the free electron ends up occupying a bond in the structure filling the empty state in the bond. In this process, the electron releases energy as heat or as electromagnetic radiation [76]. The wavelength of the radiation corresponds to the difference in valence shell energies of the $p$ and $n$ dopants (shown in figure 1.14 [31]). This can be mathematically expressed with the following equation.

$$\Delta E = \frac{hc}{\lambda}, \tag{1.4}$$

where $\Delta E$ is the change in energy of an electron in $eV$, $h$ is Planck's constant in $Js$, $c$ is the speed of light in $m/s$ and $\lambda$ is the wavelength of light in $m$. Because of the LEDs dopants, and LED is capable to emit light at

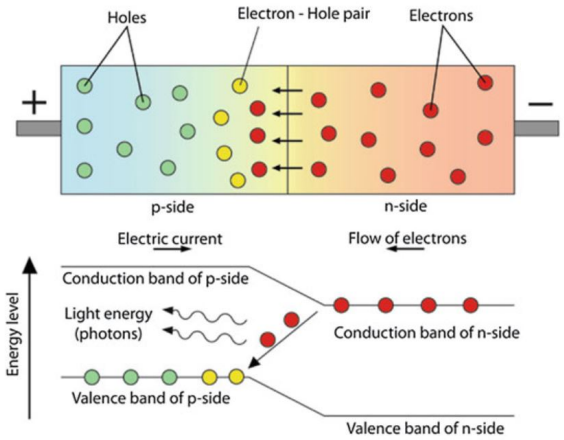


Figure 1.14: The working principle of the *p-n* junction inside an LED [31]

a fixed wavelength only. This is shown in figure 1.12, in the bottom right corner. Since Planck's constant and the speed of light are constants, the following statement goes:

$$\Delta E \propto \frac{1}{\lambda} \tag{1.5}$$

In words, the wavelength at which the light is emitted is inversely proportional to the forbidden bandgap.

In order to make recombination more effective, heterostructures and quantum wells were used. Improvements in epitaxial crystal growth techniques made the formation of customized heterostructures and quantum wells in LED chips possible [77]. An active zone composed by several thin layers of materials having different bandgap widths is embedded in it. The bandgap width in some layers is lower than in the surroundings. Electrons tend to occupy the lower energy levels available in these layers. Therefore, that region becomes a kind of well for electrons. Once the electrons are inside these lower energy levels, it is relatively unlikely to escape, because they would need extra energy for that. Holes, considered as the absence of electrons, behave in the opposite way. This structure brings electrons and holes to the same region of space. This increases the probability of radiative recombination. The intermediate region is designed to be narrow to obtain a high concentration of electron and holes therein. This leads to a higher efficacy of the LED, because the major part of the electric energy supplied is converted into light.

**Advantages of LED lighting**

For the utilization in crop cultivation, LEDs have important advantages compared to the conventional lamps described above. First of all, LEDs have a small size compared to other lighting techniques. This minimizes the interception of sunlight when they are used as supplemental lighting system in greenhouses and thereby maximizing the sunlight received by the plants. Also, because LEDs have a low emittance of heat, they can be placed close to the plants without burning them. LEDs are also suitable for intracanopy lighting, in which lamps are placed inside the plant canopy [78]. Besides that, when the optimal light spectrum is known for a plant, one is able to specifically create this spectrum with individual LEDs, which can provide light of a narrow bandwidth. Fourthly, LED lamps can be easily controlled by regulating the electrical current [70]. This controllability is an important characteristic when the lamp is used as light source supplemental to the varying solar radiation. Furthermore, the efficacy of LED light is higher compared with the conventional light types. As discussed before, the efficacy of a lighting system is the number of photons emitted per Joule input electricity. Because of the continuing developments in LED technology, the efficacy of LED lamps keeps increasing over time. At the moment of writing, the efficacy of LED fixtures used in greenhouses is approximately 2.5 $\mu mol/J$, while the efficacy of HPS lamps is around 1.7 $\mu mol/J$ [79–82]. Lastly, LEDs light have a lifetime expectancy of more than 50,000 *hours*, which is significantly higher than the lifetime expectancy of the conventional lighting techniques [79].

The main disadvantage of LED lights is the high investment costs. In 2014, Nelson and Bugbee [80] analyzed the economics of different lighting fixtures used in greenhouses. One of their conclusions was that the

five-year electric plus fixture cost per mole of photons output is 2.3 times higher for LED fixtures. However, it should be taken into account that this analysis in performed 2014 and that the investment cost of LED fixtures has decreased while the efficacy has increased. At the time of writing, the investment in LED lighting is still higher than the conventional lamps. Another concern limiting the prevalence of LEDs for crop growth is the inconsistent information available about optimal LED lighting parameters for different plant species. The inconsistent experimental conditions in combination with the variety of plant species that is analyzed without systematic research approach, makes it hard to compare and combine current knowledge on the effect of various LED parameters on plants.

## Agrivoltaics

In order to increase the efficacy of land use, in 1981, Goetzberger and Zastrow [83] came up with the idea of solar energy collection and agricultural activities on the same piece of land. They proposed a configuration with solar collectors at a height of two meters above the ground. Later, this concept got the name agrivoltaics. The term agrivoltaics, build up from the words agriculture and photovoltaics (PV), was firstly introduced by Dupraz et al. in 2011 [84]. Figure 1.15 displays the concept of agrivoltaics. One can either use 100% of a piece of land for crop (Wheat) production or 100% for electricity production with PV modules. However, by combining the two concepts on the same piece of land, the net productivity might be increased.

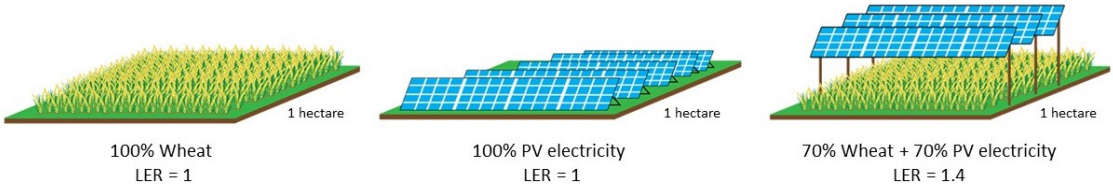


Figure 1.15: Concept of agrivoltaics [85]

Dupraz et al. introduced an indicator to measure the productivity of a certain piece of land: the Land Equivalent Ratio (LER). The LER of an agrivoltaic system is defined with the following equation:

$$LER = \frac{Y_{\text{AV-crop}}}{Y_{\text{mono-crop}}} + \frac{Y_{\text{AV-electricity}}}{Y_{\text{mono-electricity}}}, \tag{1.6}$$

where $Y_{\text{AV-crop}}$ is the yield of the crops in the mixed agrivoltaic system, $Y_{\text{mono-crop}}$ refers to the yield of the sole cultivation of crops, $Y_{\text{AV-electricity}}$ is the electricity produced by the PV modules in the mixed agrivoltaic system and $Y_{\text{mono-electricity}}$ stand for the electricity that can be produced in a normal PV plant with the same area available. It is important to note that caution must be taken when using the measure LER. The ratio does not differentiate the value of one yield over the other [86]. As an example: in agrivoltaics, an LER with a value over 1 would be obtained where PV modules are to completely cover the surface while the crop yield was only a small part of the monosystem. As a result, a higher LER, despite a potentially lower crop yield, is a disadvantage of relying on this measure to draw conclusions for the success of an agrivoltaic system.

Dupraz et al. showed that the combination of cultivation (durum wheat) and PV modules (59% ground coverage) lead to an LER of 1.73. This means that a 100 $m^2$ area with a combination of PV and cultivation produces as much electricity and crops as a 173 $m^2$ are with separate productions. The research also showed that a 57% reduction in sunlight availability resulted in only a 19% decrease in wheat yield. This means that the light efficiency of wheat crop is increased in the reduced radiation because of the PV module shading. In 2018, Amaducci et al. [87] showed a comparable result. They found that the shading of PV modules actually resulted in multiple additive and synergistic benefits for certain species. The prevention of direct sunlight reaching the crops (maize) reduced drought stress in the plant and the amount of biomass produced was higher. Also heat stress on PV modules was reduced, leading to a higher PV module efficiency. Beside the more efficient land use when applying the concept of agrivoltaics, the economic value of a piece of land also increases. In 2017, Prannay et al. [88] showed that the economic value of a grapefarm deploying an agrivoltaic system could increase more than fifteen times as compared to the sole farming of grapes, while the grape production is approximately maintained.

The concept of agrivoltaics has also been implemented in greenhouses, where PV modules are placed on the greenhouse roof. PV greenhouses have been installed worldwide, but many installations are currently underutilized or empty [89]. Instead of focussing on both crop and PV energy production, these new PV farms preferred to concentrate on the PV energy production. This is mainly because of the negative shading effects of the PV modules on crops. In 2013, Marrou et al found that tomatoes grown under a partly shaded situation in southern France ripen later and yield fruit with a significantly lower mean mass compared to a traditional greenhouse configuration. They discuss that less than 10% of the roof space should be covered with PV modules in cases where food yield is weighted as the priority over electricity generation. Allardyce et al. (2017) showed the effect of the integration of PV modules on top of greenhouses. They found several disadvantages with the integration of PV modules in greenhouses. Full or partial shading causes differences in growth and development of crops. Cossu et al. concluded that the available global radiation for crops decreased by 0.8% for each additional 1.0% PV area. It is dependent on the plant species and the geographical location what the maximum PV coverage could be to have the right balance between crop production and PV energy production.

The geometrical arrangement of PV arrays drastically affects the growth of plants cultivated under PV arrays. In order to get a better spatial distribution of sunlight, different PV arrangements have been tested on greenhouse rooftops. It has been found that for PV modules placed in a checkerboard arrangement, the plant growth was better compared to a straight-line arrangement. It has been concluded that a checkerboard arrangement improves the unbalanced spatial distribution of received sunlight energy in the greenhouse [90, 91]. These two arrangements are shown in figure 1.16. Figure 1.16a shows PV modules arranged in a straight line and figure 1.16b show PV modules having a checkerboard arrangement. Figure 1.17 shows the light distribution maps of the two greenhouses showed in figure 1.16. These maps show the ratio between the cumulative available global radiation inside the PV greenhouse and the cumulative global radiation inside the same greenhouse with no PV modules on the roof [89]. For the straight line arrangement, there is an area that receives less than 40% of the radiation that would normally reach the greenhouse floor. This significantly reduced amount of light is detrimental to the plants located in this area. The conclusion that can be drawn from figure 1.17 is that the checkerboard configuration leads to a better light distribution in the greenhouse, which is in line with previous research [90–92].

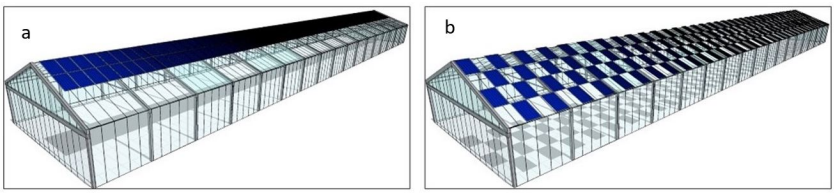


Figure 1.16: Straight line (a) and Checkerboard (b) PV module arrangement on greenhouse rooftop [89]

Several studies have analysed the change in internal conditions -other than the reduction in radiation- in PV greenhouses compared to greenhouses without PV modules [89, 93]. It has been concluded that PV modules placed on a greenhouse roof act as a passive cooling system during the summer. The internal temperature of the greenhouse decreases with the increase in the shading percentage. This means that less energy is needed for ventilation. On the other hand, the coverage with PV modules might have a negative effect during the winter, because of the increased energy needed for heating. However, PV modules placed on a greenhouse roof might have, to a certain extent, also an insulating function. The area under the PV modules that cover the roof, can be covered with insulation screens. Fatnassi et al (2014) and Fatnassi et al (2015) also studied the air temperature when covering the roof of a Venlo greenhouse for 50% with PV modules. They found that the internal air temperature was -3$^{\circ}C$ on both a typical day in summer and the same value for a typical day in winter.

A further development in agrivoltaics is the implementation of suntracking PV modules. In 2019, Gao et al. found that for a greenhouse in the Netherlands, suntracking PV modules could increase the electricity production with almost 7% compared to a PV system with fixed modules. Also the amount of global radiation

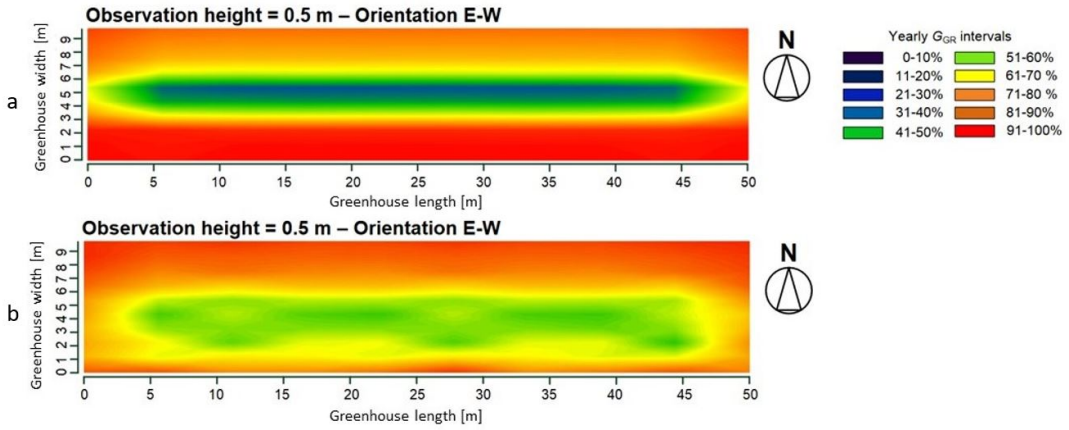


Figure 1.17: Light distribution maps of two greenhouse types (Straight line (a) and Checkerboard (b) PV module arrangements) showing the ratio between the annual available global radiation inside the PV greenhouse and the annual global radiation inside the same greenhouse without PV modules on the roof [89]

reaching the crops increased with almost 11%. These results were found with a 50% roof coverage and a single axis suntracking mechanism. The conclusions of this study are in line with a study done by Valle et al. in 2017. They also showed that by using suntracking PV modules the electricity generation was increased compared to stationary PV modules and also the transmitted radiation increased slightly, hence crop biomass. However, other studies showed that solar tracking systems on greenhouses led to a negative ratio between the minimum and maximum light transmission compared to a system with fixed modules [94]. Using solar tracking modules results in a lower light transmission for direct light. This effect is mainly significant at the edge of the day.

### Plant factory

Another system for the indoor cultivation of crops is a plant factory. In contrast with greenhouses, plant factories, also known as vertical farms, are closed, multi-storey crop production systems which are designed to maximise production density [95]. Since the crops inside are not exposed to extreme weather conditions, it produces vegetables year round by controlling environmental conditions like light, temperature, $CO_2$ concentration, humidity and nutrient solutions [96]. Because plant factories are a closed system, the plants inside are solely dependent on artificial light technologies and since this way of cultivation is relatively new, mainly LED technology is used. Figure 1.18 shows an example of a vertical farm having multiple levels of crops and lighting systems.

Figure 1.18: Example of multi-storey vertical farm [97]

## 1.2. Research gap & questions

Summarizing the sections described in this literature review, it can be concluded that there have been various important developments in agriculture. First of all, a lot of research has been done finding the optimal lighting conditions for crops. It can be concluded that the optimal conditions have not been fully determined

yet and that research is still ongoing to better understand the reaction of plants under different lighting conditions. This literature shows, however, that LED seems to be the right lighting technology to grow crops in an efficient way. Research has been done and is still going on regarding the optimization of LED technology. This is expected to bring down the costs and energy consumption of the lamp. Furthermore, research has been done finding the right balance between the amount of PV modules used and the amount of light that reaches the crops in an agrivoltaic setup. It was found that a checkerboard PV module arrangement led to the best spatial distribution of light at the crop level in greenhouses.

The interaction between these main developments (LED technology and agrivoltaics) and the optimization of a combined system has not been studied yet. Therefore, the purpose of this study is to optimize the cultivation of lettuce and tomato in greenhouses in different geographical locations by integrating both PV technology and LED technology. This study will make a trade-off with on the one hand, the amount of freely available sunlight with suboptimal light conditions and on the other hand the energy consuming LED fixtures with optimal light conditions in combination with PV modules to supply (a part of) this energy. The main difference between this study and studies done before related to agrivoltaics, is that this study takes into account the spectral response of plants, instead of only looking at the quantity of light that reaches the plants.

This research gap leads to the main research question of this study:

*What is the most space and energy efficient LED-based agrivoltaic system for the cultivation of lettuce and tomato in three different climates?*

In order to support this research question, the following sub-questions are formulated to give structure to this study:

1. *What is the state of the art of the developments of crop cultivation within greenhouses?*
   It is important to understand the state of the art of crop cultivation in greenhouses. This question has been answered in the previous section. In this review, the most important developments of the last decades regarding cultivation in greenhouses have been described.

2. *What are the requirements for an artificial lighting system for optimal crop cultivation?*
   To better understand the lighting conditions crops need, a light simulation model is worked out. Besides the right lighting conditions for crops, this model gives more insight into the characteristics of lamps and the behaviour of light.

3. *How can LED and PV technology be arranged in a greenhouse system?*
   Because the combination of a PV system and LED technology has not been part of research yet, this question is formulated. To answer this question, multiple greenhouse designs are presented and the important components of such a system are discussed.

4. *What is the optimal LED-based agrivoltaic greenhouse design for different climates?*
   While the previous question focused on the design of multiple LED-based agrivoltaic greenhouses, to answer this question, the performance of the greenhouse designs is analysed based on certain performance indicators for three different climates.

5. *What is the potential of plant factories compared to greenhouses?*
   For this sub-question, the focus is shifted to the cultivation of crops within plant factories. To answer this question, the performance of plant factories is compared to the results found to answer the previous question.

## 1.3. Report structure

In this introducing chapter, the motivation for this study is given. Also, the literature review described the state of the art knowledge on the optimal lighting requirements for crops and the developments in LED and PV technology applied in greenhouses. Lastly, the research gap and research questions that form the core of this study were touched upon. Hereby, the first sub-question, regarding the state of the art of crop cultivation within greenhouses, has been covered.

In chapter 2, the second sub-question is discussed. To better understand the characteristics of lighting systems for crop cultivation, a light simulation model is designed in this chapter. The most important requirements and parameters of this model are discussed. The results of the model are finally compared with practical measurements with an actual lamps used to grow crops. Chapter 3 focuses on the third sub-question and presents different greenhouse designs in which LED and PV technology as discussed in the literature review are integrated. Also the approach and main indicators to analyse the performance of the various systems is elaborated on. In chapter 4, the performance of the greenhouse scenarios designed in chapter 3 is analysed and compared using certain indicators. This comparison is done for two different crops and three locations, discussing sub-question 4. Chapter 5 switches the focus from the greenhouse scenarios to plant factories. In this chapter, the design with the most relevant components of the plant factory is worked out and the performance is compared with the results for the greenhouses discussed in chapter 4. In the last chapter, the main conclusion and answer to the main research question is given. Also an outlook to future and possible improvements for crop cultivation in the future is presented.

# 2

# Light simulation model

The central question that is discussed in this chapter is: what are the requirements for an artificial lighting system for optimal crop cultivation? In order to better understand the lighting conditions crops need, a light simulation model is worked out in this chapter. This chapter firstly explains the purpose of this light simulation model in greater detail. Then, the requirements of the simulation model and the lighting requirements for specific crops are discussed. Subsequently, the characteristics of light and the approach used to design the model are elaborated on. Furthermore, the performance of the simulation tool is analysed and the output results are presented and discussed. Finally, the light simulation model is compared with practical measurements done with an LED bar used to grow crops.

## 2.1. Purpose of light simulation model

In order to get an idea about how to place a light source to achieve the required light distribution with the right spectrum, light planning tools can be used. For human applications, the lighting design software DIALux [98] is commonly used. It can be used to plan, calculate and visualize light for indoor and outdoor areas. The downside of this software is that it is not directly applicable for horticultural applications. DIALux designs lighting systems for human applications and uses $Lux$ as the unit for measuring the light intensity. The unit $Lux$ is adopted to the spectral sensitivity of the human eye, which is different from the plants spectral response as shown in figure 1.2. $Lux$ has no relevance for plant photosynthesis. DIALux does not support the light intensity with the unit $mol/m^2s$. Conversion factors to convert the light intensity in $Lux$ to $mol/m^2s$ exist for specific light sources having a defined spectral output. But in order to be able to measure the light intensity in $mol/m^2s$ for every possible spectral output, another model is needed.

The company Valoya designed a light planning tool for horticultural purposes [99]. This tool is an addition to DIALux and uses the PPFD, the photoperiod and the right light spectrum to design a lighting plan for specific crops. A visualisation of the output of this tool is shown in figure 2.1. This tool, however, is not freely available and only meant for Valoya's customers. Besides that, this model uses a selected amount of light spectra. These are the reasons for the design of a new lighting model meant for crop cultivation. This model is designed in the Matlab environment. The following section elaborates on the various design criteria for this model.

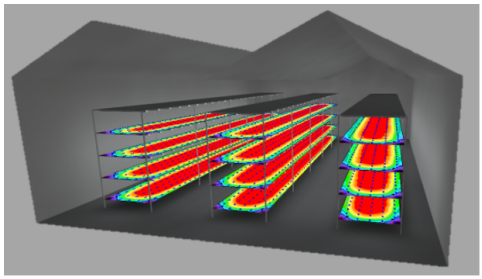

Figure 2.1: Example of an output of Valoya's light planning tool used to design lighting systems for crop cultivation [99]

## 2.2. Requirements for simulation model

First of all, it is important to understand the requirements that a lighting model used for cultivation purposes has to fulfill. As discussed in the literature review, the artificial light source should have the right spectral output for plants. Furthermore, the lamp should be able to output the right light intensity, i.e. the PPFD that matches the crops needs. Also, the distribution of light on the illuminated surface should be homogeneous with respect to the intensity and the spectral distribution. In this way, the crops that are distributed over a certain illuminated surface, get the same amount and quality of light. This is necessary to ensure the same growing cycle for crops illuminated with the same light fixture. In order to be able to design a light system, plant specific data is needed. Because different plants can respond differently to the same lighting conditions, for this research, two plant species are chosen and the light simulation tool is initially designed for these plant specifically. The plant species that are used to design the model are lettuce and the tomato plant. The next section elaborates on the lighting characteristics that these crops need.

## 2.3. Crops

As mentioned in the literature review, research on the optimal lighting conditions for crops is still ongoing. In this section, assumptions are made regarding the optimal lighting conditions for lettuce and the tomato plant. Firstly, the conditions for lettuce are described. Subsequently, the light characteristics for tomato plants are elaborated on.

### 2.3.1. Lettuce

Supplemental lighting for greenhouse lettuce production has been the subject of a great deal of research, and some of the most advanced supplemental lighting strategies developed to date have focused on lettuce production [13]. Because of this, a lot of information is available on the light spectrum and intensity that lettuce needs. Lettuce is an important greenhouse crop, since there is a continuous demand for a supply of fresh leafy greens. Furthermore, production cycles of lettuce are relatively short and lettuce can be produced year-round in greenhouses in case the appropriate conditions are available.

In this study, the AP673L spectrum of Valoya is assumed to be optimal to produce lettuce with a high biomass [100]. This spectrum is shown in figure 2.2. The spectral distribution contains all wavelengths in the PAR region and also infrared light. The relative output of each color is shown in table 2.1. The AP673L spectrum has been designed to grow well-balanced, high biomass plants [101]. The effect that photons of different wavelengths have on the development of lettuce specifically is discussed below. It was found that blue light (425-440 $nm$) led to an improved leaf expansion [102] and compact plant morphology [103, 104]. The use of green light (490-550 $nm$) in combination with red and blue light improved the fresh weights of lettuce shoots with 61% compared to those under red and blue light [45]. Furthermore, red light (620-700 $nm$) increases chlorophyll $a$ and $b$ and carotenoids concentrations [40]. Lastly, far-red light (700-850 $nm$) in combination with photons with wavelengths in the PAR region, improved shoot and root growth, stem length and leaf length and increased the number of leaves [102, 105, 106].

Furthermore, as discussed in section 1.1.1, the optimal DLI of lettuce is 17 $mol/m^2day$ [58, 59, 107]. Using the relation between the PPFD and the photoperiod as described in equation 1.3 and displayed in figure 1.6 and the fact that lettuce is a long day plant with highest production found with a photoperiod 24 $hours$, the corresponding PPFD is 197 $\mu mol/m^2s$. An overview of these data is shown in table 2.2.

### 2.3.2. Tomato

While the AP673L spectrum is assumed to be optimal for lettuce, the G2 spectrum of Valoya is used for the tomato plant. This spectrum is shown in figure 2.2. Compared to the AP673L spectrum, the G2 spectrum has a larger share of red and infrared light, as shown in table 2.1. It was found that red (620 - 700 $nm$) enhanced the tomato yield of tomato plants [108]. Furthermore, the combination of blue, red and far red LEDs was shown to have a positive effect on tomato growth [109]. On the other hand green and yellow light (520 - 600 $nm$) was used less efficiently, but is to a lesser extend important for the penetration through the plants canopy.

Focussing on the optimal light quantity characteristics for tomato plant, studies have shown that the optimal photoperiod is 16$h$ [110, 111]. Tomato plants need at least six to eight hours of darkness per day. They

use this dark period to properly absorb carbon dioxide and to work through the dark cycle of energy production [112]. Keeping the plant under lighting for too long, can cause slower growth and smaller fruit yields, because of the lack of carbon dioxide that the plant has absorbed. The optimal DLI is found to be in the range of 22 to 30 $mol/m^2day$ [113–115]. For this study, it is assumed that the optimal DLI is 22 $mol/m^2day$. Using equation 1.3, it can be determined that the corresponding PPFD is 381 $\mu mol/m^2s$. These data are presented in table 2.1.

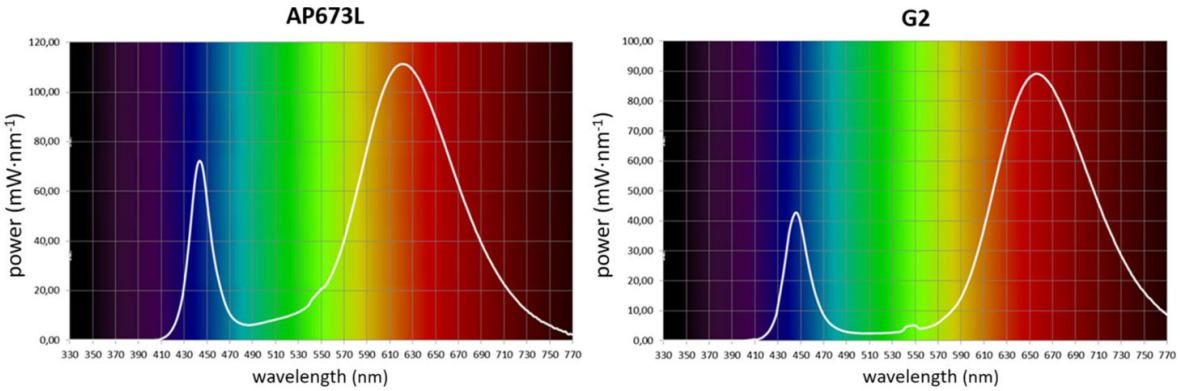


Figure 2.2: AP673L spectrum (left) for optimal biomass production for lettuce and G2 spectrum (right) for optimal biomass production for tomato [100]

Table 2.1: Shares of wavelength regions present in the AP673L spectrum and G2 spectrum [100]

| Color | Wavelength range (nm) | AP673L (%) | G2 (%) |
|---|---|---|---|
| Ultraviolet | <400 | 0 | 0 |
| Blue | 400 - 500 | 12 | 8 |
| Green | 500 - 600 | 19 | 2 |
| Red | 600 - 700 | 31 | 65 |
| Far-red | 700 - 800 | 8 | 25 |
| PAR | 400 - 700 | 92 | 75 |

Table 2.2: Lighting requirements of lettuce and tomato plants

| Crop | Spectrum | PPFD (µmol/m$^2$s) | Photoperiod (hour/day) | Optimal DLI (mol/m$^2$ day) |
|---|---|---|---|---|
| Lettuce | AP673L | 197 | 24 | 17 |
| Tomato | G2 | 381 | 16 | 22 |

## 2.4. Light simulation model

This section describes the main parameters taken into account in the design of the light simulation model. Primarily, this model is designed for LED lamps. The characteristics of the LEDs implemented in the model and the most important variables of the model are discussed in this section. As mentioned before, this model is designed in the Matlab environment.

### 2.4.1. Single wavelength LEDs

LED fixtures used for horticultural application normally consist of multiple individual LEDs. These LEDs together form a certain spectral output. By changing the ratios between the colors, specific processes within a plant can be triggered. This model take the AP673L and the G2 spectrum as example spectra. As displayed in figure 2.2 and table 2.1, both spectra span the whole PAR region and a part of the far-red region. For the sake of simplicity, the spectra are replicated using on the shelf, single wavelength LEDs. The colors blue, green, red and infrared (IR) are used. The corresponding peak wavelengths are shown in table 2.3 and table 2.4. Figure 2.3 shows an example of the relative spectral output of four types of LEDs.

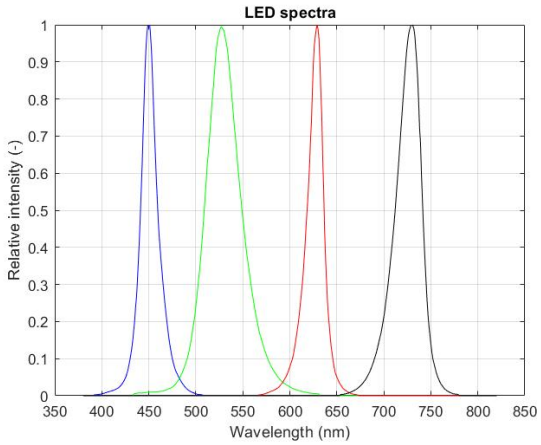


Figure 2.3: Relative spectral output of four single wavelength LEDs

Table 2.3: Characteristics of individual LEDs lights used to recreate the AP673L spectrum

| **Color** | **Wavelength Peak (nm)** | **Wavelength range (nm)** |
|---|---|---|
| Blue | 450 | 400 - 510 |
| Green | 520 | 430 - 630 |
| Red | 630 | 570 - 680 |
| IR | 740 | 650 - 780 |
| PAR | - | 400 - 700 |

Table 2.4: Characteristics of individual LEDs lights used to recreate the G2 spectrum

| **Color** | **Wavelength Peak (nm)** | **Wavelength range (nm)** |
|---|---|---|
| Blue | 445 | 416 - 493 |
| Green | 545 | 455 - 655 |
| Red | 650 | 570 - 735 |
| IR | 750 | 690 - 790 |
| PAR | - | 400 - 700 |

### 2.4.2. Photon flux LEDs

This section elaborates on the approach used to implement the photon flux output by the LEDs in the model. As describe by equation 1.2, a photon with a certain wavelength, has his own energy. From this follows that each of the four LEDs has its own photon flux. This photon flux can be determined by using equation 1.2 and the radiant flux (radiant power) of an LED. The following equation can be noted [116]:

$$\phi_{photon} = \phi_{radiant} \frac{\lambda}{hcN_A}, \tag{2.1}$$

where $\phi_{photon}$ is the photon flux in $mol/s$ and $\phi_{radiant}$ the radiant power in $W$. The radiant power is calculated by multiplying the input power with the conversion efficiency of the LED:

$$\phi_{radiant} = IV\eta \tag{2.2}$$

In this equation, $I$ is the forward current in $A$, $V$ the operating Voltage in $V$ and $\eta$ the conversion efficiency of the LED. These data can be found in the operation manual of an LED. A single wavelength LED emits a certain range of wavelengths around the peak wavelength, as can be seen in figure 2.3. This is why the total photon flux in a given spectral range is defined as:

$$\phi_{photon} = \phi_{radiant} \int_{\lambda_{min}}^{\lambda_{max}} \frac{\lambda}{hcN_A} d\lambda \tag{2.3}$$

By implementing this equation in the model, the contribution of each wavelength in the total photon flux output of the spectral range of the LED is accounted for.

In order to create a light spectrum with the four single peak LEDs that has the right ratio between the different colors and is comparable to the desired spectrum, the light output per color of the whole LED fixture has to be adjusted. The spectrum of the tuned LEDs is shown in figures 2.4 and 2.5 for the AP673L and G2 spectrum, respectively. It must be noted that these spectra are given in $W/nm$ and are therefore energy weighted. In the following analysis however, the photon weighted spectra are used. This conversion is done with equation 2.1.

The output of the LEDs are tuned by matching the cumulative photon flux of the individual LEDs with the AP673L and G2 spectrum per wavelength range. For example, 12% of the total photon flux of the AP673L spectrum are photons in the wavelength range 400 - 500 $nm$. In an iterative process, the share of photons in this range for the four combined LEDs is matched with the AP673L spectrum by varying the forward current of each LED. This is done for every wavelength range each having a size of 100 $nm$. The comparison between the desired spectra and the recreated spectra are shown in figures 2.6 and 2.7 for the AP673L spectrum and the G2 spectrum, respectively. While the shares of photons are exactly the same in each wavelength range, the energy per wavelength range (the area under the graph) is almost the same for the AP673L spectrum and the recreated spectrum. This is because photons having a different wavelength, contain a different amount of energy, as can be concluded from equation 1.2. Since the spectral output of the AP673L spectrum and the recreated spectrum is not exactly overlapping, as visible in figures 2.6 and 2.7, there is a small difference in energy per wavelength range. This inaccuracy could be reduced by using a smaller wavelength range.

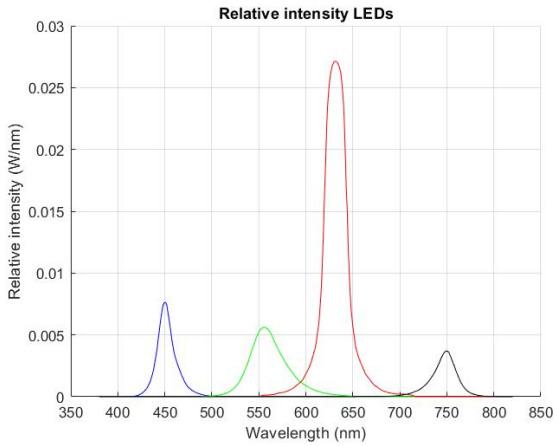


Figure 2.4: Adjusted relative spectral output of four single wavelength LEDs to recreate AP673L spectrum

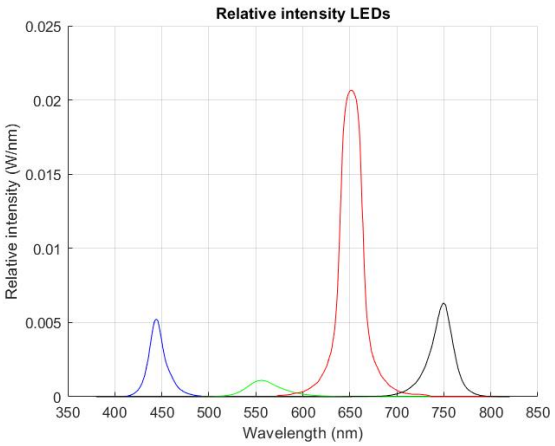


Figure 2.5: Adjusted relative spectral output of four single wavelength LEDs to recreate G2 spectrum

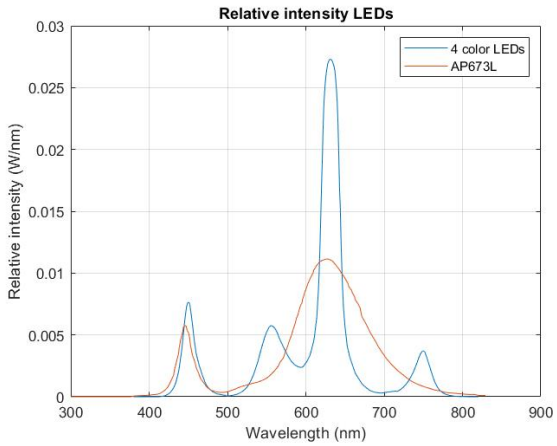


Figure 2.6: Comparison between AP673L spectrum and recreation with four LEDs

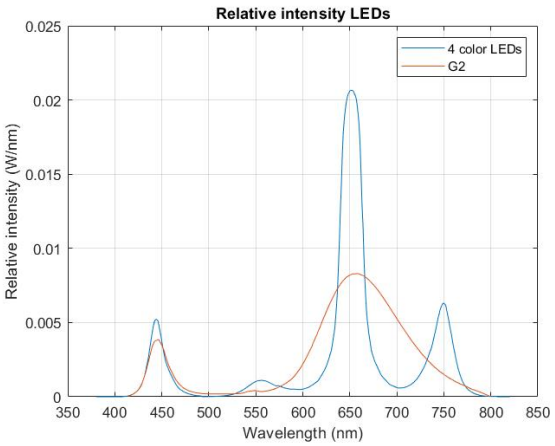


Figure 2.7: Comparison between G2 spectrum and recreation with four LEDs

### 2.4.3. Efficiency droop

LED efficiency is generally the highest at low currents - typically a few milli-amperes - and as the driving current increases, the efficiency decreases gradually. This process is called efficiency droop and its physical origin is not well understood [117]. The efficiency droop is displayed in figure 2.8 for a blue and green LED. Two of the most recognized causes to explain the origin of the efficiency droop are Auger recombination and carrier leakage [118]. Auger recombination is a non-radiative process in which the excess energy from electron-hole recombination is transferred to electrons or holes. Subsequently, instead of giving off photons, the electrons and holes are excited to higher energy states within the same band. Because the rate of Auger recombination is proportional to the cube of the carrier density, $n^3$, it may play an important role at high carrier/current density and leads to efficiency droop. Another explanation for efficiency droop could be carrier leakage. This is the escape of electrons from the active region and recombining with holes. The rate of carrier leakage is found to be enhanced with increasing current density.

The relation between the conversion efficiency and the forward current is wavelength dependent. The photon energy can be determined with equation 1.2 that has been introduced in the literature review. The conversion efficiency of LEDs can be determined by dividing the energy of the PAR photons emitted by the input energy. As discussed in section 1.1.2, the efficacy of LEDs is determined by dividing the PAR photons emitted by the input energy and has the unit $\mu mol/J$. The relation between the conversion efficiency and the efficacy of the LED is dependent on the wavelength and follows from equation 1.2.

$$\eta = E\frac{hcN_A}{\lambda}, \tag{2.4}$$

where $\eta$ is the conversion efficiency of the LED, $E$ is the efficacy in $\mu mol/J$, and $N_A$ is Avogadro constant in $mol^{-1}$. This constant is used to convert *electron Volts* ($eV$) to *Joule* ($J$). Figure 2.9 shows the efficacy of different LEDs over the forward current.

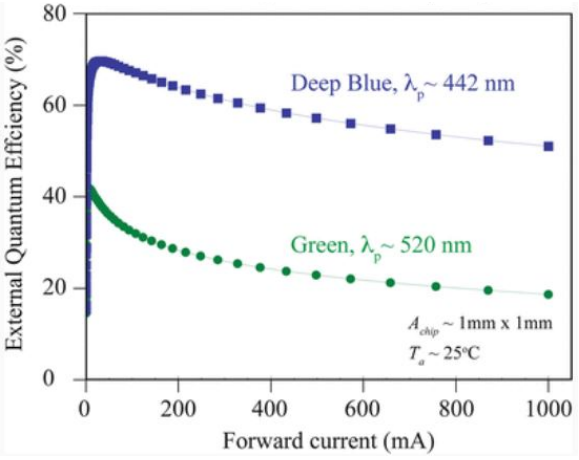


Figure 2.8: Plot of the external quantum efficiency (EQE) of blue and green LEDs over the forward current [119]

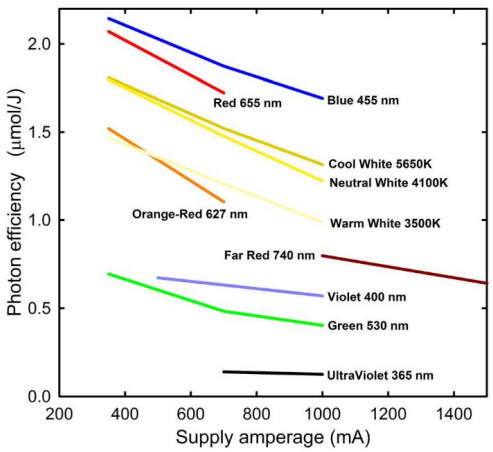


Figure 2.9: Efficacy of various LEDs at different wavelengths over an increasing forward current [80]

Since the LED model consists of multiple LEDs with single wavelength peaks, multiple trends of efficiency droop relations are needed. Each wavelength peak has an own relation between the efficiency droop and the forward current. The curve for blue and green LEDs is taken as displayed in figure 2.8. The efficiency droop curve for red and IR LEDs are determined using the data found in figures 2.8 and 2.9 in combination with equation 2.4. The forward current of 350 $mA$ is taken as the reference current. The corresponding efficacy (found in figure 2.9) for red and IR wavelengths is converted into the conversion efficiency, using equation 2.4. These efficiencies at 350 $mA$ are compared to the efficiency of blue LEDs at the same forward current. Subsequently, the efficiency droop curve for the blue wavelength peak is shifted down with the difference between the conversion efficiencies at 350 $mA$. The efficiency droop curves for each wavelength are noted in table 2.5 and shown in figure 2.10. It must be noted that the curves for the blue and green wavelengths are retrieved from figure 2.8 using curve fitting. This is why the curves are asymptotic close to 0 $mA$. At forward currents lower than 1.0 $mA$, the values become inaccurate. In this model, forwards currents lower than 1.0 $mA$ are not used to avoid this inaccuracy.

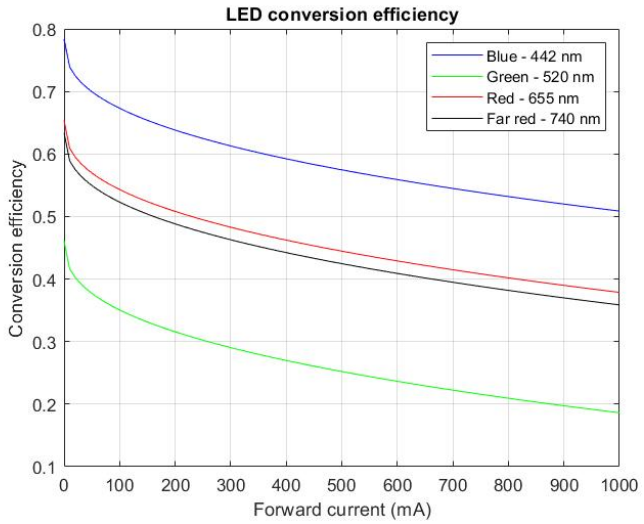


Figure 2.10: Efficiency droop over forward current

Table 2.5: Characteristics of LEDs used to recreate the AP673L spectrum

| Color | Wavelength Peak (nm) | Efficiency droop curve (-) | Low forward current (mA) | High forward current (mA) |
|---|---|---|---|---|
| Blue | 422 | $-0.01787 * I^{0.3957} + 0.7836$ | 20 | 350 |
| Green | 520 | $-0.4502 * I^{0.08169} + 0.9777$ | 20 | 350 |
| Red | 655 | $-0.01787 * I^{0.3957} + 0.0.6536$ | 50 | 1250 |
| IR | 740 | $-0.01787 * I^{0.3957} + 0.6336$ | 20 | 350 |

### 2.4.4. View factor

The distribution of the photons emitted by the LEDs is modelled using the view factor of radiation heat transfer between two surfaces. The view factor $F$ is defined as the fraction of the radiation leaving surface $A_1$ that is intercepted by surface $A_2$ [120]. In this situation, the two surfaces are the area of the LED ($A1$) and the illuminated surface with the lettuce ($A2$). The setup is displayed in figure 2.13. Since LEDs do not emit as much heat as conventional lamps, it is possible to place the LED relatively close to the plants. The shorter the distance between the LED fixture and the plants, the higher the light intensity is at the same LED output. This is because the light intensity of light varies over distance according to the inverse square law for a point source [121]:

$$I \propto \frac{1}{r^2}, \tag{2.5}$$

where $I$ is the light intensity at $r$, which is the distance from the point source. This relation is visualized in figure 2.11.

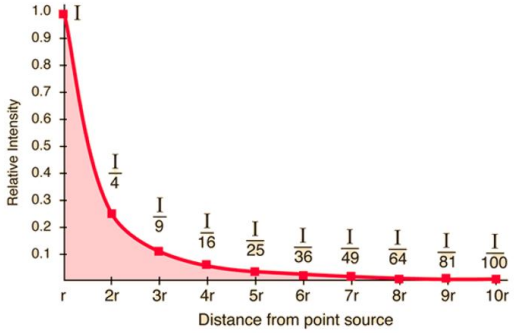


Figure 2.11: Relation between the distance and the light intensity at that distance from a point light source

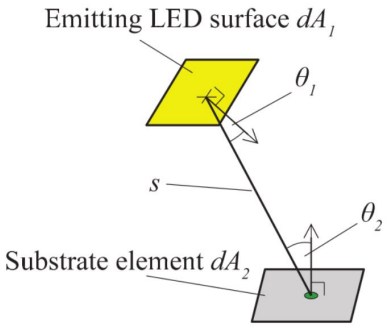


Figure 2.12: Geometry of view factor calculation [122]

This view factor is generally defined for an arbitrary configuration as [123]:

$$F_{1\to 2} = \frac{1}{A_1}\int_{A_1}\int_{A_2}\frac{cos\theta_1 cos\theta_2}{\pi s^2} dA_2 dA_1 \tag{2.6}$$

In this LED design, the receiving surface with the crops is 1 $m^2$ and is subdivided in 2500 elements with an area of 4 $cm^2$ each (shown in figure 2.14). The distance between the LED fixture and the crops, $h$, is assumed to be 0.3 $m$ (shown in figure 2.13) [124]. Since the LEDs emitting area $dA_1$ and the illuminated element area $dA_2$ are small compared to the distance $s$, for this situation, equation 2.6 can be simplified to [122]:

$$dF_{1\to 2} = \frac{cos\theta_1 cos\theta_2}{\pi s^2} dA_2 \tag{2.7}$$

The parameters listed in this equation are shown in figure 2.12. Because the surface of the LED lights and the crops surface are parallel to each other, $\theta_1$ and $\theta_2$ are always equal to each other, following the principle of *Z-angles*. The equation for the view factor can be simplified to:

$$dF_{1\to 2} = \frac{cos^2\theta}{\pi s^2} dA_2 \tag{2.8}$$

This equation is used in the matlab model to determine the light intensity from a single LED per element at the surface on which the plants are located.

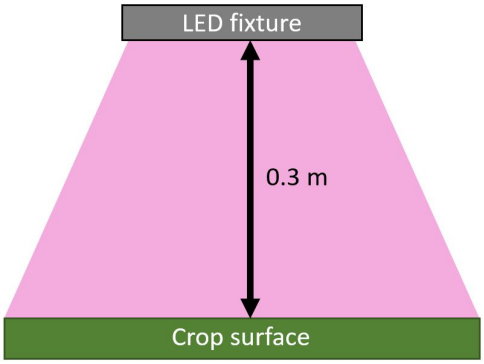


Figure 2.13: 2D view of orientation of the LED fixture with respect to the crops

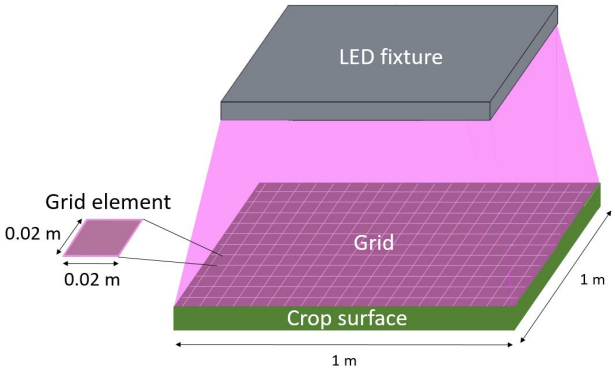


Figure 2.14: 3D view of orientation of the LED fixture with respect to the crops

Every LED has his own light distribution. The model determines the light distribution of each LED on the illuminated surface individually. Each LED present in a fixture has his own X- and Y-coordinates. The spacing between the LEDs is constant and is noted with quantity $C$. As mentioned above, the model assumes an illuminated area of 1 $m^2$, with a length and width of 1 $m$. The illuminated area is subdivided in 2500 elements with a length and width of 0.02 $m$, as can be seen in figure 2.14. The distance $S$ between an emitting LED and a certain element in the grid is determined with the following equation:

$$s_i = \sqrt{(X_{element_i} - X_{LED_i})^2 + (Y_{element_i} - Y_{LED_i})^2 + h^2} \tag{2.9}$$

The angle of the illumination, $\theta$, is determined with the following equation:

$$\theta_i = \cos^{-1}(h/s_i) \tag{2.10}$$

Finally, the photon flux density distribution is obtained by the summation of output photon fluxes of all LEDs:

$$\phi_{surface} = \sum_i^n \phi_{LED_i}\frac{cos^2\theta_i}{\pi s_i^2} \tag{2.11}$$

The parameter $A$ is removed from the equation in order to get the photon flux density ($\mu mol/m^2 s$).

### 2.4.5. Homogeneous distribution

In horticulture, an important requirement is the homogeneous spectral distribution of the light coming from the LED fixture. In the light simulation model, this equal distribution is created by using evenly distributed LEDs with an repeating color order. The configuration of LEDs in one module - with 4x4 LEDs - is shown in figure 2.15. 3x3 modules together form one LED panel. The exact distance between the LEDs and the dimensions of the panel are dependent on the application of the LED fixture. For lettuce and tomato, the optimal LED fixture configuration is discussed in section 2.5.

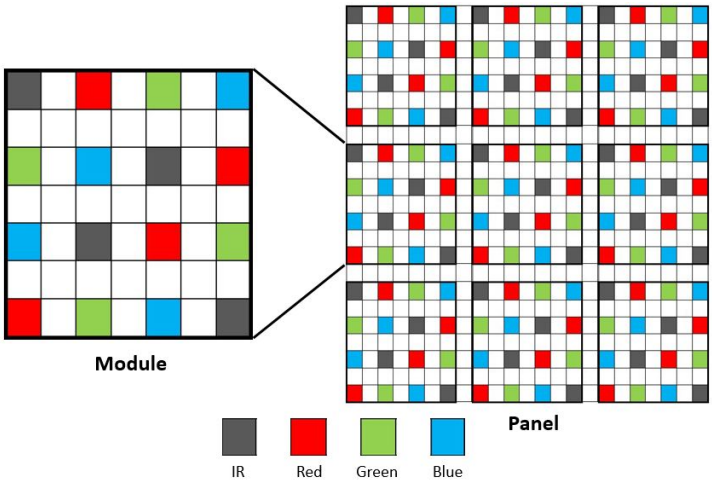


Figure 2.15: LED configuration in module (left) and module configuration in panel (right)

The number of LEDs of each type is the same in this configuration. If all LEDs would have the same photon flux, the spectral output would be similar to the spectrum presented in figure 2.3. However, since a certain ratio between the photon flux per colors is required for optimal plant growth, the photon flux per type of LED has to be adjusted. From equation 2.1, it can be concluded that the photon flux can be increased or decreased by changing the radiant power of the LED. The radiant power is proportional to the forward current (equation 2.2).

### 2.4.6. Trade-off high-low current LEDs

Commonly used values for the rated forward current are 20, 150, 350 and 700 *mA*. The low power LED with a low forward current (20 *mA*) is a DIP LED without heat-sink solution, whereas the high power LED with a high driving current (from 300 - 1000 *mA*) normally does have a heat-sink pad. In order to be able to make a choice between high current and low current LEDs, a trade-off analysis is done, taking into account the total electricity demand, the costs and lifetime of the LEDs, besides the spectral distribution and photon flux distribution. In this trade-off, the crop lettuce is used for the required lighting conditions.

**Energy consumption**

The total energy demand can be determined by calculating the total power input needed. The input power is calculated by multiplying the forward current with the voltage. By multiplying this power with the photoperiod a plant needs per day (i.e. the amount of operating hours of the lamp), the daily energy consumption can be determined. For two fixtures with the same photon flux output, but one consisting of low current LEDs and the other of high current LEDs, the system with the low current LEDs have a lower energy consumption. This is mainly because of the efficiency droop phenomena that is stronger at higher forward currents, as described above.

**Lifetime**

The two most important factors that accelerate the degradation of LEDs, and therefore the lifetime of the fixture, are the forward current used and junction temperature [125]. Both excessive current flow and high temperature cause long term modifications on the physical structure of the LED and on the packaging materials. The temperature within an LED and the current flowing through the device are closely related, which implies that an appropriate operating current cannot be chosen without an accurate thermal evaluation. A

high current can cause different types of long term modifications, such as the generation of lattice defects. These changes have important effects on the electrical behaviour of the LED, like the I-V characteristics. Furthermore, they degrade the optical efficiency. Also the high temperature levels, because of self-heating or imposed by the environment can have a significant effect on both the electrical characteristics and the mechanical/optical properties. High temperature levels cause different types of degradation mechanisms. For example, they concur in the defects generation activated by the carrier flow and trigger the degradation of the Ohmic contacts. In figure 2.17, the relation between the LED lifetime, forward current and junction temperature is shown. The relation between the lifetime and the forward current is used to determine lifetime of the specific LED, since the relation between the forward current and the junction temperature is close to linear [125, 126], as displayed in figure 2.16. The interactions of the junction temperature of LEDs within an array are not significant [127]. Therefore, module-level thermal interactions between LEDs may be neglected. Furthermore, it is assumed that the forward current is constant over the lifetime of the LED. The lifetime of the LED can be determined with the following equation [125]:

$$L_{90} = e^{2.221-0.698log(I)+\frac{2636}{T_{junction}}}, \tag{2.12}$$

where $L$ is the lifetime (in $hour$) of the LED when the light output is maintained at 90% of its initial value, $I$ is the forward current in $A$ and $T_{junction}$ the junction temperature in $K$.

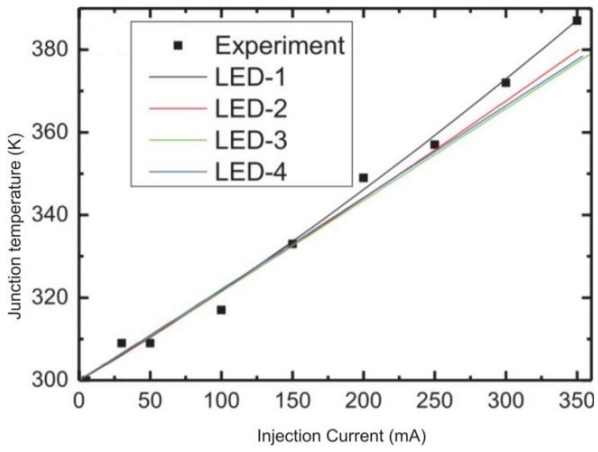


Figure 2.16: Relation between Junction temperature and forward current in multiple LEDs [126]

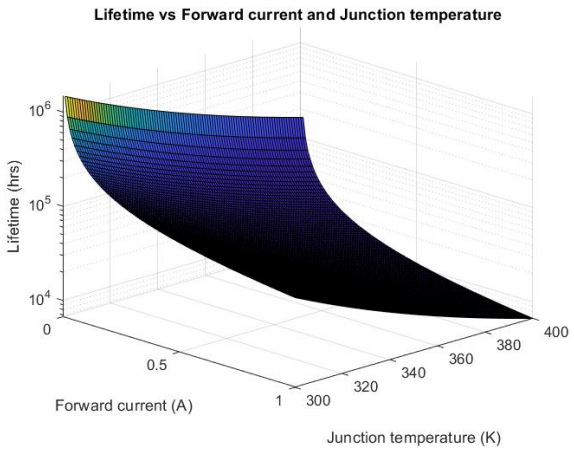


Figure 2.17: LED lifetime vs Forward current and Junction Temperature [128]

In this part of the analysis, it is assumed that the relation between the lifetime and the forward current is the same for all LEDs used.

**Costs**

The third characteristic used in the trade-off between low and high power LEDs is the costs. For this part of the analysis, the prize of commercially available LEDs is used. As mentioned before, the most common LEDs have an operating current of 20, 150, 350 and 700$mA$. Figure 2.18 gives an overview of the costs in euro's for LEDs with the aforementioned operating currents and different peak wavelengths (blue, green and red). From these graphs it can be concluded that the relative costs of the LED per $mA$ decrease as the rated forward current increases. With respect to the costs, the high current LEDs have an advantage.

The factors described in the previous sections have an effect on either the energy consumption or the costs over the lifetime of the LED. These parameters are integrated in the LED system to be able to choose the most beneficial fixture: a large amount of low current LEDs or a small amount of high current LEDs. The outcome of this trade-off is discusses in section 2.5.1.

### 2.4.7. Overview model

Before the results of the model are described, an overview of the simulation model is given. The overview is explained using the block diagram shown in figure 2.20. The input parameters are divided into three categories: the requirements of the crops, the LED characteristics and the geometry of the setup. For the requirements of the crops, the input that is needed by the model is an array with two columns that contains

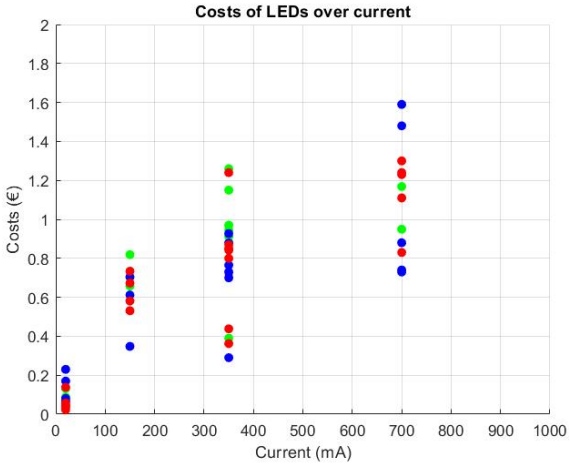


Figure 2.18: Costs of LEDs at different forward currents

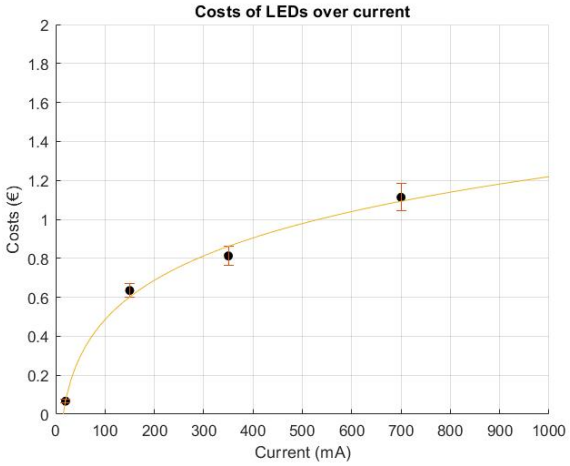


Figure 2.19: Average costs of LEDs plotted against the forward current

the optimal spectrum for the specific crop. The first column contains the wavelengths in $nm$ and the second column contains the corresponding spectral output in $W/nm$. The integral of the total spectrum has to be equal to 1 $W$. Furthermore, the desired PPFD is needed in $\mu mol/m^2s$ and the optimal photoperiod in $hour$. Besides the input parameters for the crop, a number of characteristics for the LEDs used are needed. First of all, the maximum forward current and the voltage of the LED has to be given in $mA$ and $V$ respectively. Also, the relative spectral output of each individual LED is needed. This can be a single wavelength spectrum, but also the spectrum of a white light LED, which spans the whole visible spectrum. The spectrum should be given in the same format as the desired spectrum for the crop. The last set of input parameters required is the geometry of the LED and crop setup. The distance between the light fixture and the bottom surface of the crops (height) as displayed in figure 2.13 needs to be specified in $m$. Also the spacing between the LEDs (in $m$) is given as an input. Then, the size of the illuminated surface has to be noted and the size of the elements (for both the width and length in $m$).

Subsequently, the model determines the output power (radiant power) per LED by taking into account the value of the efficiency droop based on the forward current. Then the radiant power is converted into a photon flux, using equation 2.3. After this conversion, the total photon flux of all types of LEDs that are given as input are tuned to create the desired spectrum and to obtain the right PPFD. This is an iterative process in which the forward current of the LEDs is changed until the right spectrum and PPFD is found. Regarding the right spectrum, this is the case when the shares of the photon fluxes of each wavelength range is equal to the shares as given in the input parameters of the optimal spectrum for the crop. When this iterative process is finished, the photon flux per LED is known and the number of LEDs per module is determined. Then, a panel is created, consisting of multiple modules. The number of modules is dependent on the size of the illuminated area. The photon flux per LED and the setup of a LED panel, containing the coordinates of each LED, are combined with the view factor and give the output parameters of the model. The results that are obtained from this calculation are the (operating) forward current per LED (in $mA$), the energy consumption per day of the whole fixture (in $kWh$), the photon flux distribution (in $\mu mol/m^2s$) and the spectral distribution of the LED fixture (in $\mu mol/(m^2snm)$). Based on the number of LEDs present in the panel and the equations for the costs and lifetime of the LEDs, the costs and lifetime of the fixture is determined and given as an output.

It is important to note that this model can also be used for lighting techniques, other than LEDs. The main difference with respect to LEDs is that other light source generally do not consist of individual colors. This results in that other techniques can be compared to a single LED, but with a relatively high power. The distance between the lamps is likely to be larger in such a setup, but the simulation of the light distribution works the same way. To use other lighting techniques, additional data is needed regarding the characteristics of the specific technique and small adjustments have to be made in the model. For example, the relations of the efficiency droop have to be replaced by another efficiency related trends applicable to the chosen lighting technique.

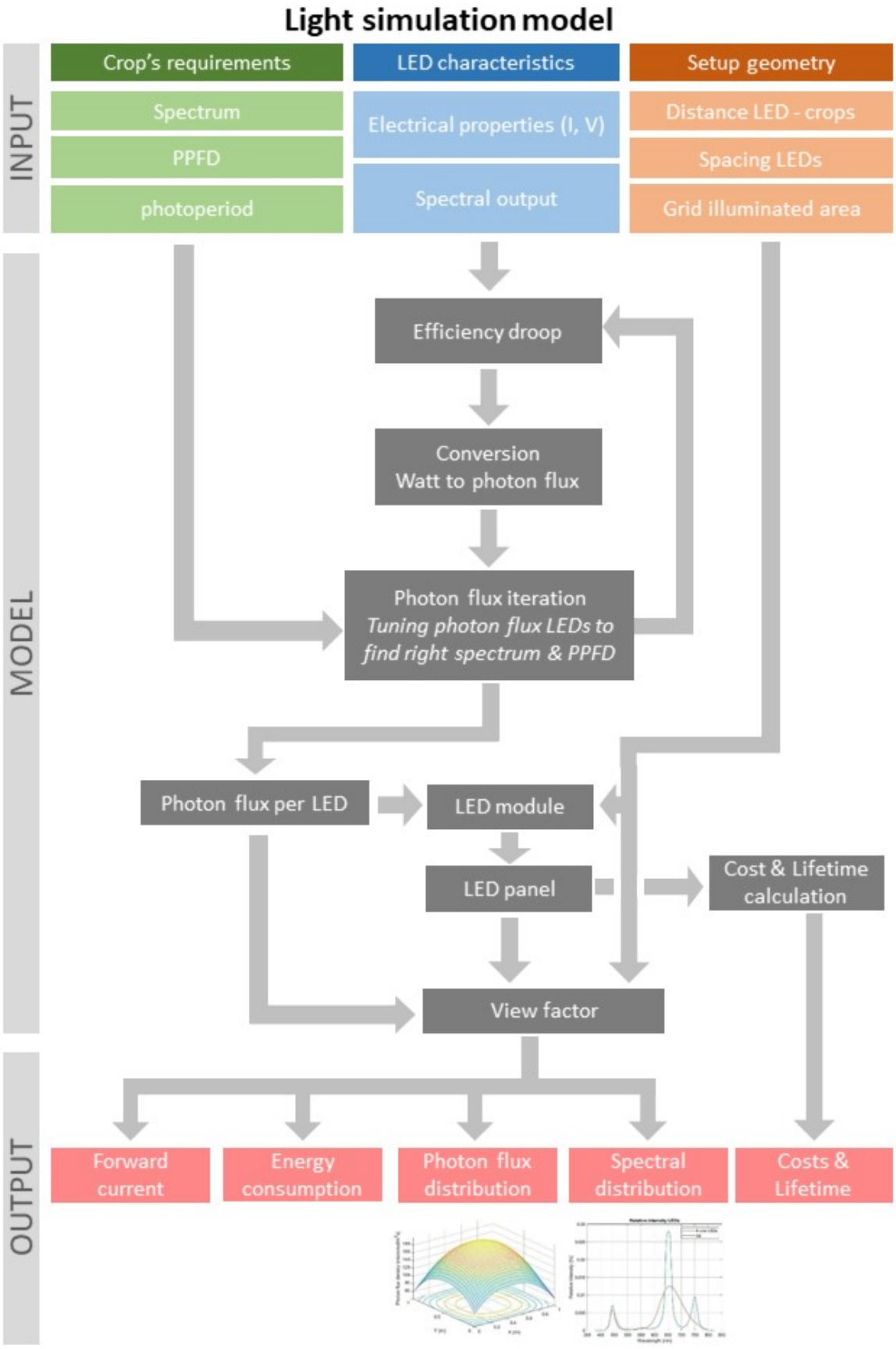


Figure 2.20: Block diagram of developed light simulation model

## 2.5. Results

In this section, the performance of the light simulation model is analysed. Firstly, the results of the trade-off between the high and low forward current is given. All simulation discussed in this section are based on the input parameters discussed in table 2.2 and it is assumed that the LEDs are the only source of light.

### 2.5.1. Trade-off

As mentioned before, the main parameters on which this trade-off is based are the energy demand, lifetime costs, photon flux distribution and spectral distribution. The two LED configurations are implemented in the simulation model and the results are compared. The characteristics of the LEDs important to the model are presented in tables 2.6 and 2.7, for the low power and high power configuration, respectively. For both tables, the column *Forward current* shows the rated current of the LED, while the column *Operating current* describes the actual current at which the specific LED operates within the configuration. The total photon flux is the sum of the photon fluxes of all LEDs of one color. The share of each photon flux in the total photon flux, corresponds with the color shares as presented in table 2.1. Figure 2.21 and 2.22 show the light distribution on the illuminated surface of the low and high LED configuration, respectively. In both figures, the left graph shows a 3D plot of the photon flux density and the right graph shows the photon flux density distribution seen from above. It can be seen that, for both configurations the distribution is symmetric without distortions.

Table 2.8 shows the comparison between the low power and high power configurations. First of all, the number of LEDs is significantly higher for the setup with low forward current LED. The low current setup needs sixteen times more LEDs to be able to generate the same photon flux density as the high current setup, which is approximately 196 $\mu mol/m^2 s$. Because of the higher number of LEDs, the distance between two single LEDs is smaller than for the high power situation. The first parameter that says something about the performance of the configurations is the daily energy consumption. The energy consumption of the low power setup is approximately 2/3 of the high power setup. This difference is mainly caused by the efficiency droop, which is stronger at high forward currents. The second important parameter is the lifetime of the configuration. To determine the lifetime, the LED with the lowest lifetime of the setup is taken as limiting lifetime. The lifetime for all LEDs is determined with equation 2.12. The temperature for the low power current LEDs is assumed to be 310 $K$, while the temperature for the high power LEDs is 380 $K$, according to figure 2.16. For the high power LEDs this junction temperature is a conservative assumption, since the junction temperature corresponding to the forward current of this LEDs is actually around 500 $K$. According to equation 2.12, the lifetime of the low current LEDs is significantly higher than the high current LEDs. However, it must be noted that the calculated lifetime of 420,000 $hours$ is questionable. In reality, the LEDs might still be emitting light after this amount of time, but the output would be just a small part of the initial output. In figure 2.17, it can be seen that at low currents, the lifetime becomes more asymptotic with the Z-axis, meaning that the lifetime goes to infinite. This is the reason for the lifetime having this order of magnitude. A lifetime with an order of magnitude of 60,000 $h$ is more realistic [129]. Still, when combining the lifetime with the costs of all the LEDs in the fixture (which is higher for the low power LEDs), the costs per 1000 $hours$ of lifetime would be in advantage of the low power LEDs with a lifetime of 60,000 $hours$. When taking into account the electricity costs that are saved over time when using the low power LED setup, this setup would be even more beneficial to use with respect to the high power configuration.

Another difference between the two setups is visualized in figure 2.23. The two graphs in this figure show a side view of the photon flux density at the edge of the illuminated square meter. The photon flux density of the low power LED configuration at the edge is lower than that of the high power LED configuration at the same location. A higher photon flux density at the edge means that a higher number of photons fall outside the desired square meter and can be explained as an inefficiency. However, when multiple LED configurations are placed next to each other and a larger surface with crops needs to be illuminated, this edge effect does not necessarily have to be a disadvantage. Also, light reflecting walls can be used to prevent this potential loss of light. The reason for this photon flux density being higher is the different the power density distribution in the LED configurations. As mentioned before, the low power setup has 16 times as many LEDs as the high power setup. If these 16 LED had to be replaced by one substitution LED with power output equivalent to the 16 LEDs, it would be located in the center point of the area as shown in figure 2.24 in red. On the other hand, in the high power configuration, the LEDs are place at the outer edge of the array. This difference in distance to the edge of the array, causes the difference in photon flux density at the edge.

Table 2.6: Data of low power LEDs used in simulation model

| Color | Peak wavelength (nm) | Forward current (mA) | Operating current (mA) | Forward Voltage (V) | Number of LEDs | Total Photon Flux (µmol/s) |
|---|---|---|---|---|---|---|
| Blue | 450 | 20.0 | 4.1 | 3.30 | 576 | 22.2 |
| Green | 545 | 20.0 | 11 | 3.40 | 576 | 42.0 |
| Red | 630 | 50.0 | 42.2 | 2.10 | 576 | 155 |
| IR | 750 | 20.0 | 5.4 | 1.70 | 576 | 24.4 |

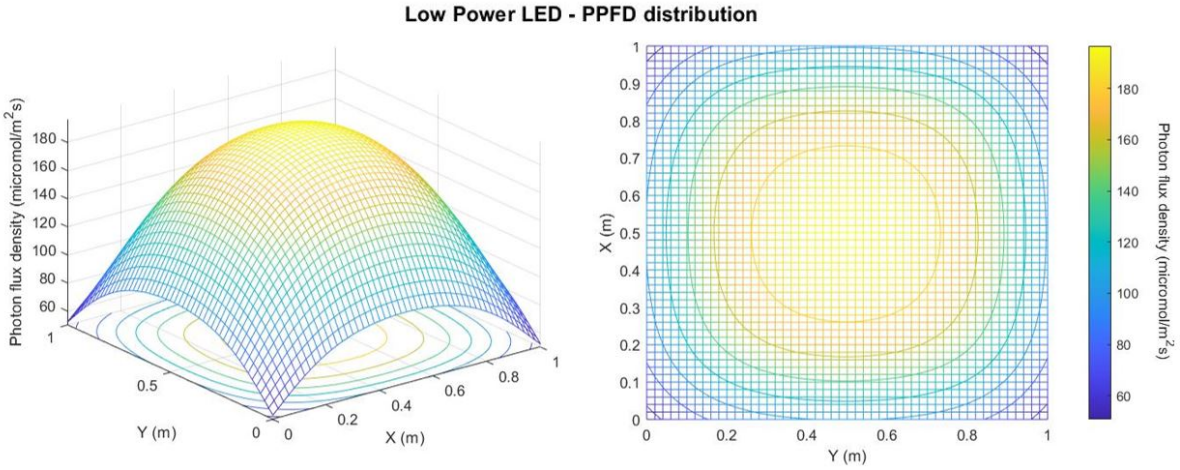


Figure 2.21: Output of LED simulation model: photon flux distribution of low power LEDs on 1 $m^2$ surface

Table 2.7: Data of high power LEDs used in simulation model

| Color | Peak wavelength (nm) | Forward current (mA) | Operating current (mA) | Forward Voltage (V) | Number of LEDs | Total Photon Flux (µmol/s) |
|---|---|---|---|---|---|---|
| Blue | 450 | 350 | 100.0 | 3.3 | 36 | 30.2 |
| Green | 545 | 350 | 283.0 | 3.4 | 36 | 47.9 |
| Red | 630 | 1250 | 1039 | 2.1 | 36 | 155 |
| IR | 750 | 350 | 80.00 | 1.7 | 36 | 20.0 |

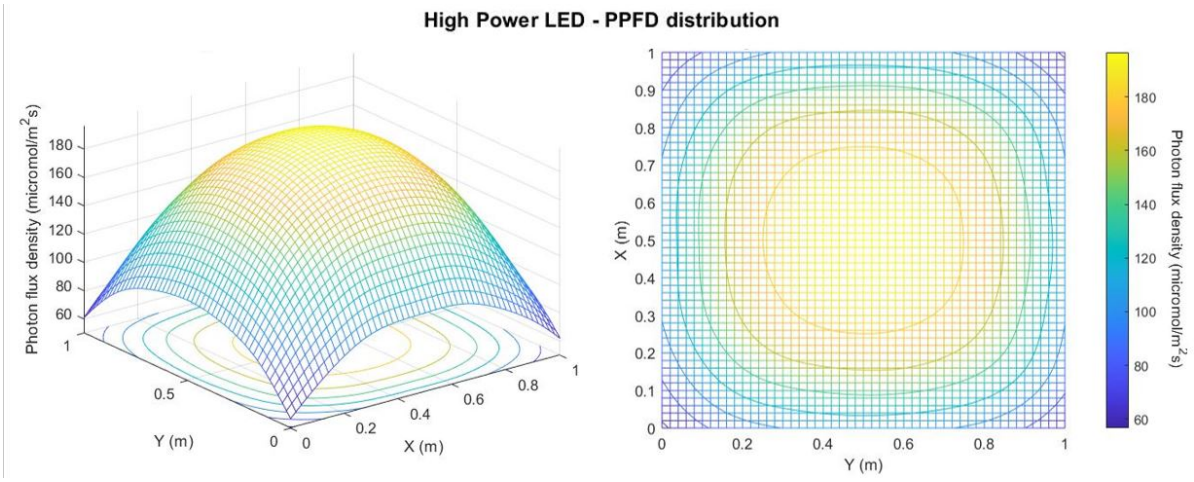


Figure 2.22: Output of LED simulation model: photon flux distribution of high power LEDs on 1 $m^2$ surface

Furthermore, in figure 2.23 it can be seen that the bottom edge of the high power LED setup is not perfectly symmetric. This is probably because the LED distribution is less homogeneous. As displayed in figure 2.15, a module consists of rows of four different colored LEDs. Since the output power of the different LEDs is not the same, the distribution of the photon flux is not perfectly homogeneous and the spectral distribution varies slightly. These effects becomes stronger when the distance between the LEDs becomes higher. In other words, the spectral distribution and the homogeneity of the photon flux distribution is better for the low power LED setup.

To conclude the trade-off, based on the energy demand, lifetime costs, photon flux distribution and spectral distribution, the LED configuration with the low power LEDs, scores best on all parameters.

Table 2.8: Trade-off between high and low power LED configuration

| LED fixture | Number of LEDs | PPFD (µmol/m$^2$s) | Distance LEDs (m) | Daily energy consumption (kWh) | Lifetime (hour) | Total costs (euro) | Costs per 1000 hours (euro/1000 hours) |
|---|---|---|---|---|---|---|---|
| Low current | 2304 | 196.4 | 0.020 | 2.03 | $4.2 \times 10^5$ | 295 | 0.7 |
| High current | 144 | 196.5 | 0.083 | 3.12 | $1.4 \times 10^3$ | 137 | 95.1 |

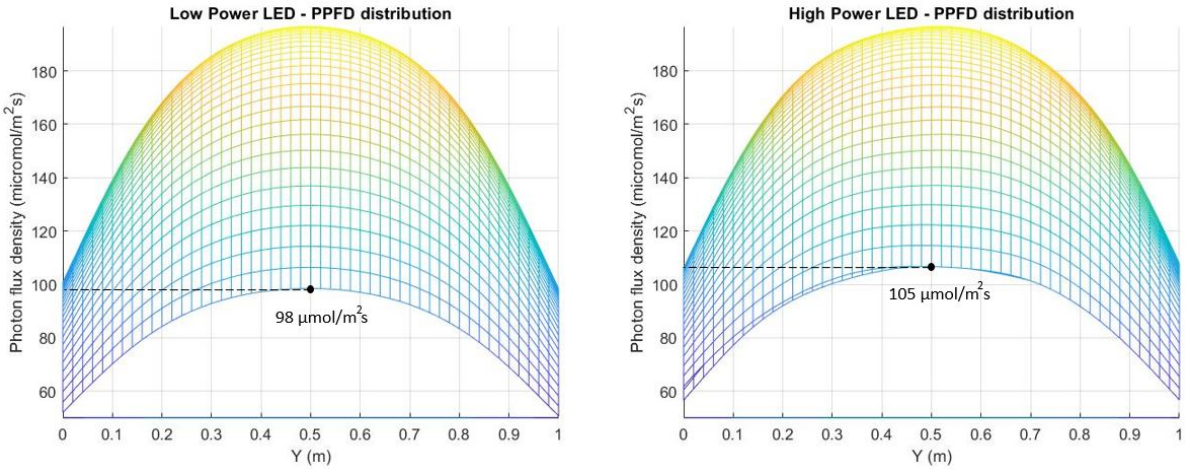


Figure 2.23: Side view of photon flux distribution of the low power LED setup (left) and the high power LED setup (right) showing the flux on the edge of the illuminated square meter

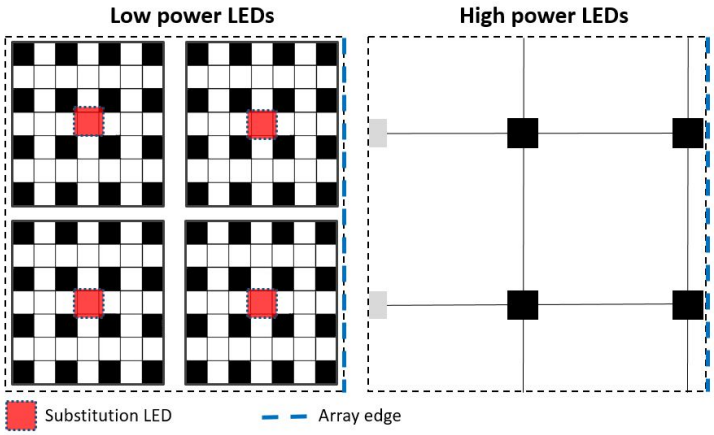


Figure 2.24: LED distribution for low power setup (left) and high power setup (right) showing difference of center point of light intensity

### 2.5.2. Tomato

The results of the simulation model for lettuce are presented in the previous subsection. This paragraph with elaborate on the outcomes of the model for the tomato plant. As presented in table 2.1, the PPFD for tomato is higher than for lettuce, namely 381 $\mu mol/m^2s$. The photon flux distribution is displayed in figure 2.25. Also the result of this simulation is a symmetric photon flux distribution. Table 2.9 shows the results of the simulation for both lettuce and tomato. It can be concluded that the tomato plant requires more lighting energy to grow, which is in line with the higher optimal DLI of tomato.

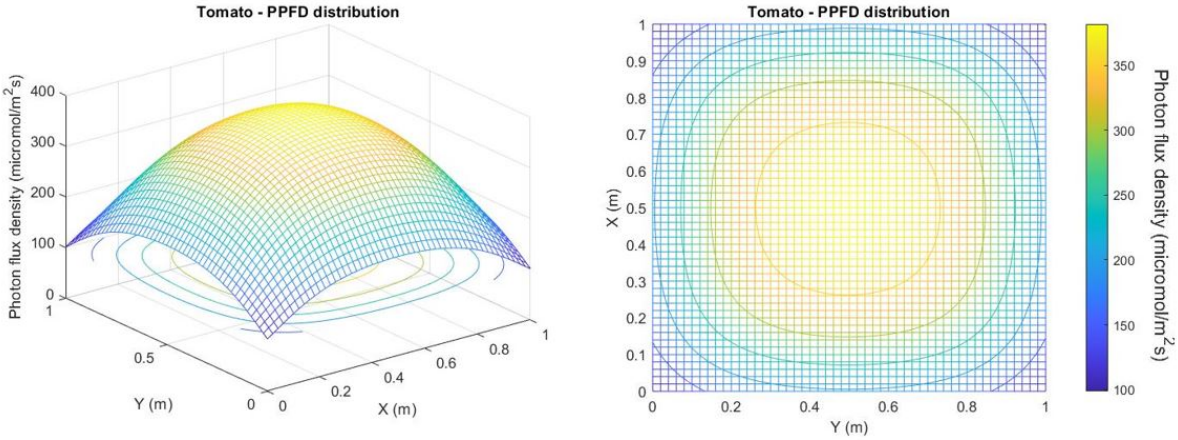


Figure 2.25: Light distribution for tomato plant

Table 2.9: Comparison of simulation results of lettuce and tomato

| Crop | Spectrum | PPFD (µmol/m$^2$s) | Daily energy consumption (kWh) | Power input (W) | Number of LEDs |
|---|---|---|---|---|---|
| Lettuce | AP673L | 196.4 | 2.03 | 84.6 | 2304 |
| Tomato | G2 | 381.8 | 2.42 | 152 | 2304 |

The results discussed above show that the model functions for multiple crops requiring various lighting conditions. One of the main advantages of this model with respect to the light planning tool by Valoya is that in this model, one is able to give their own optimal desired spectrum as an input. While in the tool by Valoya, only a selected number of light spectra are available. Since this is a first version of a light simulation model, there is still room for improvement. Section 2.7 discusses the shortcomings of this model and elaborates on several possible improvements and further applications.

## 2.6. Practical measurements

In order to verify the results of the model with the performance of a real LED fixture, practical measurements are done with a Valoya C65 lamp.

### 2.6.1. Valoya LED bar

The C65 bar of Valoya is a bar with a length of 1.2 meter and contains multiple LEDs installed in one line over the length of the bar. This bar is shown in figure 2.26. The bar uses two types of LEDs: LEDs that emit purple light and LEDs that emit white light. The sequence of these LEDs is displayd in figure 2.26. For every 3 white LEDs, there are 27 purple LEDs. In otherwords, for every single LED, there are 9 purple LEDs.

### 2.6.2. Measurement setup

The spectral output of the LED bar is the AP673L spectrum. In order to measure the spectral output of the C65 lamp, an Avantes spectrometer is used [130]. A spectrometer is an instrument used to measure certain properties of light over a specific part of the electromagnetic spectrum. For these measurements, a fiber-optic spectrometer is used, which has the focus on UV radiation, the visible spectrum and near-infrared radiation.

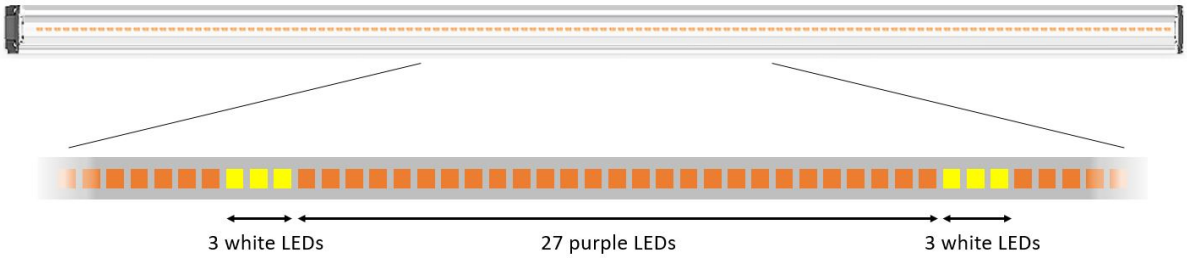


Figure 2.26: Valoya C65 LED bar and sequence of white and purple LEDs

Light coming from the light source passes through a slit, which is where the light enters the spectrometer via a fiber-optic cable. The light reflects from a collimating mirror as a collimated beam, towards the grating. A collimated beam has parallel rays and therefore spreads minimally as it propagates. A grating is a refractive element, which has a working mechanism comparable to a prism. The grating splits and diffracts light into several beams travelling in different directions. Since the diffraction angle is dependent on the photon wavelength, each wavelength head in another direction. The diffraction grating then spreads light across the focusing mirror, which directs light at each wavelength onto the detector. This detector translates each wavelength captured into a certain spectrum with the AvaSoft 8 software.

The spectral measurements were done in a dark room, to prevent other light from disturbing the measurements. The LED bar was placed 30 $cm$ above the fiber-optic spectrometer, as shown in figure 2.27. Since the LED bar consists of two types of LEDs, the spectral output of both types of LEDs was tested. This was done by blocking the light of one LED type and measuring the spectrum of the other type. The setup of this experiment is shown in figure 2.33. Case $a$ shows the setup in which the purple light were blocked and only light from the white LEDs could reach the spectrometer. In the top of the pictures, the LED bar is displayed with the (un)blocked LEDs. In case $b$, the white LEDs were covered and only the purple LEDs illuminated the spectrometer. In case $c$, no LED are covered and a combination of the white and purple light reached the spectrometer.

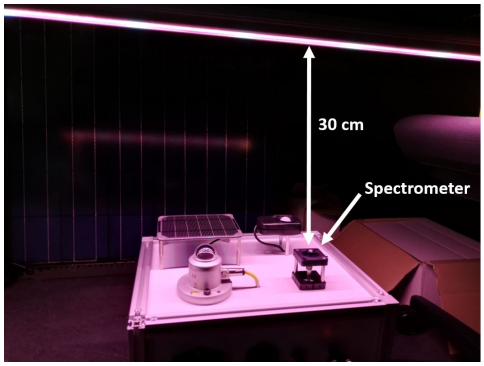


Figure 2.27: Valoya C65 LED bar placed 30 $cm$ above the Avantes spectrometer

Besides the spectral measurements, the relation between the forward current and the power output (radiant power) of the LED bar was analyzed. In order to determine this relation, the input current was changed using a potentiometer. By varying the resistance, the forward current was controlled with the potentiometer. The current was measured at the AC side of the LED driver. The LED driver is the device that regulates the power to the string of LEDs and converts the AC to DC. To measure the current, the ST 07 AC Load Connection was used to split the conducting cables within the power cable of the LED bar. Two multimeters were used in the setup. One multimeter was connected in series with the single phase conducting cable to measure the current, while the other multimeter was connected in parallel to measure the voltage over the single conducting cable and the neutral cable. With the potentiometer, the current was increased in steps of approximately 20 $mA$. Since the measurements were taken at the AC side of the LED driver, it is assumed that the efficiency of the LED driver is constant over the forward current. The output of the LED bar was measured using the Avantes Spectrometer combined with the AvaSoft 8 software. The integrated radiant power output was mea-

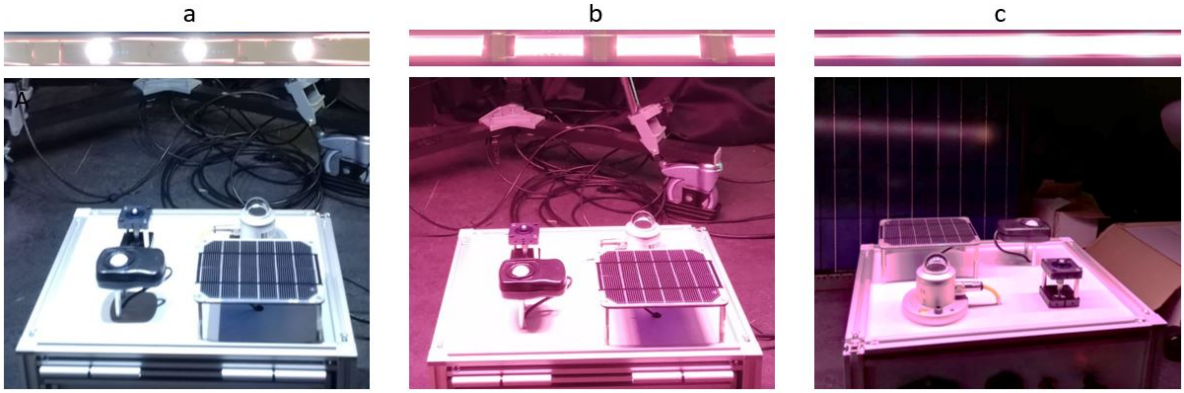


Figure 2.28: Different measurement setups, a: white LEDs, b: purple LEDs, c: white and purple LEDs combined

sured in $\mu W/cm^2$. To determine the relation between the forward current and the output of the lamp, it was sufficient to use the power output in $W$ instead of the photon flux in $mol/s$, since the relation between these quantities is linear when the relative spectral output stays the same.

### 2.6.3. Results

The output of the spectrometer was analysed in the AvaSoft 8 software and the results are plotted in figures 2.29-2.32. Figure 2.29 shows the spectral distribution of the purple LEDs. This graph explains the color output of the LEDs: it is a combination of blue and red light. Being more precise: the peaks of the spectrum range from 420-480 $nm$ and from 540-800 $nm$, the blue and red-infrared region respectively. The combination of blue and red light gives the purple color and this is why further in this analysis this spectrum is called purple. The integral of the spectrum gives the total power per square centimeter, being 507 $\mu W/cm^2$ for the purple LEDs. Figure 2.30, shows the spectral output of the white LEDs. It can be seen that this spectrum covers the whole visible spectrum, which causes the white appearance. The highest peak of this spectrum lies at 450 $nm$ and has a value of 0.43 $(\mu W/cm^2)/nm$. The integral of the white spectrum is 54 $\mu W/cm^2$. Figure 2.31 shows the output of both LED types and the sum of both types (the full spectrum). The integral of the combined spectrum equals 562 $\mu W/cm^2$.

Equation 2.1 is used to determine the total photon flux of the LED bar. The radiant power in $\mu W/cm^2$ per wavelength is shown in the figures discussed above and used in this equation. Figure 2.32 shows the spectral output as radiant power and the photon flux.

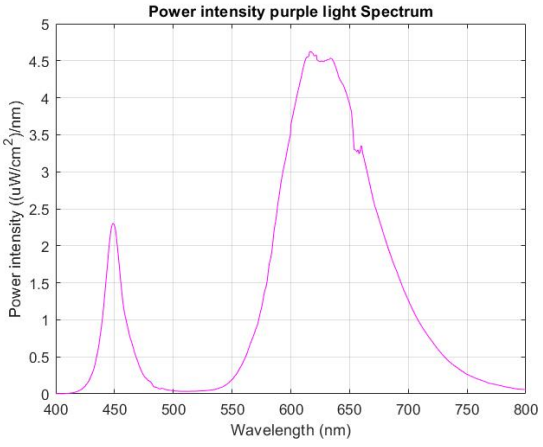


Figure 2.29: Spectral output of purple LEDs

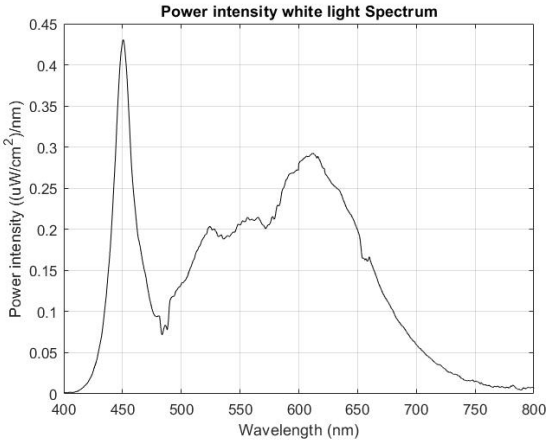


Figure 2.30: Spectral output of purple LEDs

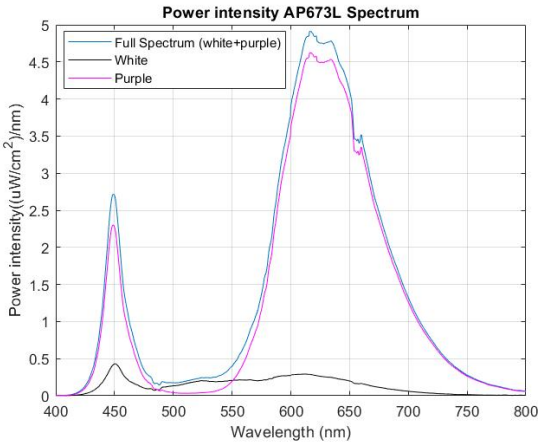


Figure 2.31: Spectral output of white LED, purple LED and the combination of both

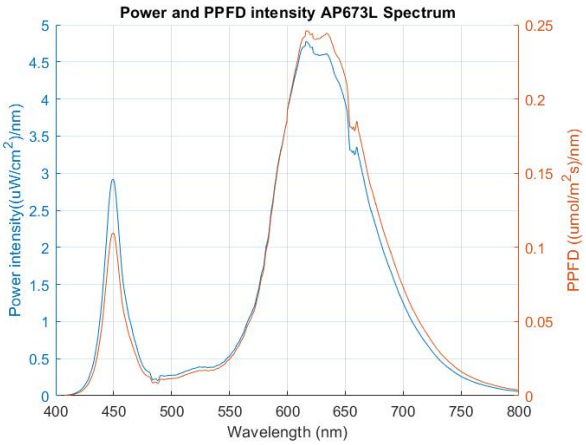


Figure 2.32: Power intensity and Photon flux intensity of AP673L spectrum

Besides the spectral output of the C65 LED bar, the light intensity distribution was measured at the illuminated area. This was done by placing the spectrometer at different locations of the area. The total width over which the intensity was measured was 120 $cm$ (x) and the LED bar was located in the center (at x=60 $cm$) at a height of 30 $cm$ from the spectrometer. The total length of the area measured was 70 $cm$ (y). For every 10 $cm$ in both the x and y direction, the power intensity was measured with the spectrometer and converted into the PPFD using equation 2.1. The flux density is given in $\mu mol/m2s$. The LED bar used maximum power and therefore its light output was maximum as well. The spectral distribution of the LED bar at the surface with a distance of 30 $cm$ from the LED is shown in figure 2.33. The magnitude of the photon flux is lower than the photon flux in the model and relatively far off the optimal PPFD for lettuce. This is probably caused by a deviant input parameter. However, the relative distribution is still relevant to analyze. It can be seen that the highest photon flux density is in the center of the area. The further away from the center, the lower the photon flux density is. At approximately 0.6 meter from where the light bar is located, the photon flux is close to zero. The distribution is approximately symmetric along the line x=0.6$m$.

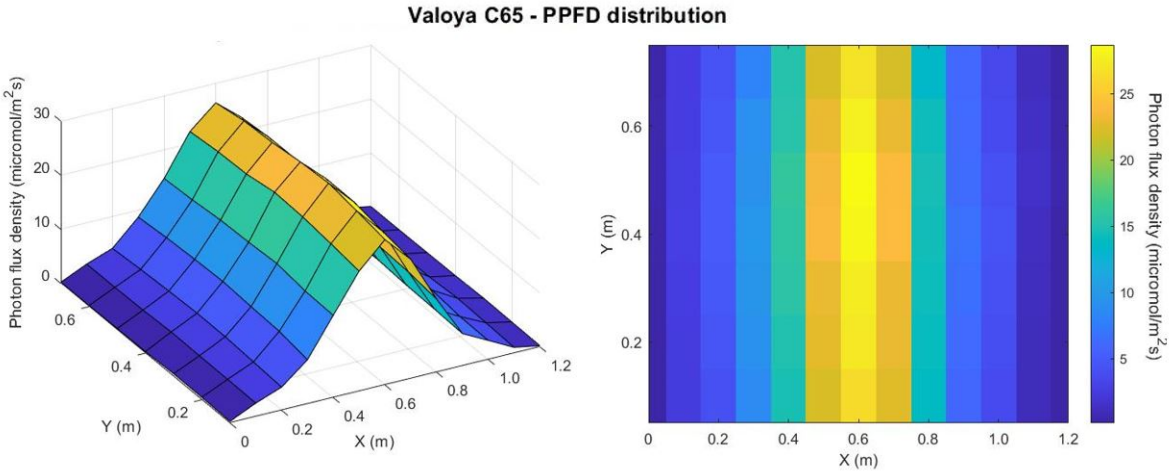


Figure 2.33: PPFD distribution on illuminated surface in $\mu mol/m^2 s$

The results for the relation between the forward current and the output of the LED bar are shown in figure 2.34. As discussed in the literature review, increasing the input current allows more electrons and holes to recombine in the p-n junction and therefore more photons are generated. In this figure, it can be seen that the relation seems to be proportional ($I_{forward} \propto P_{out}$) This is in line with was is stated in equation 2.2. For all measurements, the AC Voltage was constant at 233 $V$. The maximum forward current that is measured is 281.2 $mA$, which results in a power of 65.24 $W$, which is in line with the rated power noted on the installation

manual [131].

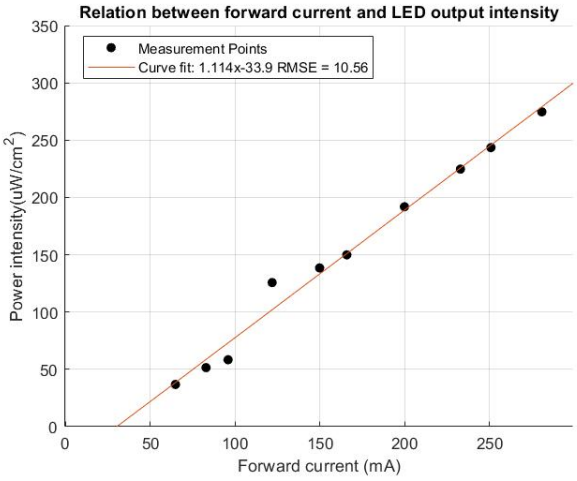


Figure 2.34: Relation between forward current and the output power of the C65 Valoya LED bar

### 2.6.4. Comparison model with practice

The main difference between the LED fixture of the light simulation model and the C65 bar of Valoya is the physical dimensions of the fixtures and the resulting light intensity distribution. On the one hand, in the LED configuration that is found using the model, the LEDs are distributed over an area of 1 $m^2$, which results in a circular symmetric distribution. At the edges of the illuminated surface ($1m^2$), the PPFD is still significant and approximately half of the PPFD in the center of the area. On the other hand, the C65 LED bar consists of LEDs installed over one axis. This results in a light distribution that has a high intensity over one axis. As can be seen in figure 2.33, at a distance of $0.6cm$ from the center (x=0$m$ and x=1.2$m$), the PPFD is almost zero. In practice, the LED bars are placed further away from the crops and placed in combination with other LED bars to ensure a homogeneous distribution. The C65 bar can be used as supplemental lighting source. The LED fixture that is found with the model, has the purpose of sole light source for the crops. However, the model also has the potential to place LEDs in one line instead of a matrix configuration and thereby it is able to simulate a bar placed further away from the crops as well.

Another difference is that the LED bar uses high power LEDs, while for the model the use of low power LEDs was found to be more beneficial in the trade-off analysis. The use of high power LEDs is a more practically feasible solution. Also, it can be argued that the determination of the lifetime of the LED fixture in the model is not accurate. First of all, as already discussed before, the relation between the forward current and the lifetime of an LED is symptotic at low forward currents. This leads to unrealistic high lifetime expectancies. According to the installation guide of the C65 bar, the use life (L90) is 36.000 hours [131], while for the low current fixture, a lifetime of 420.000 hours was determined. Also, the LED fixture in the model has a large amount of LEDs. when using a significant amount of low power LEDs and therefore the amount of components in a system is high, the chance that components or the complete system fail is higher.

As concluded before, the four individual LED colors used as an initial input in the model does not accurately recreate the desired AP673L spectrum. Since the spectral output of the two types of LEDs used in the C65 light bar are measured with the spectrometer, the spectra of the white and purple spectrum, as shown in figures 2.29 and 2.30 are used as an input in the light simulation model. In contrast with the C65 bar, the light simulation model uses low power LEDs. Also, the ratio between white and purple LEDs present in the fixture in the model is 1:1, while in the C65 bar this ratio is 1:9. By varying the forward current per LED, this ratio is created for the fixture in the model. Figure 2.35 shows the relative spectral distribution of the white and the purple LED. In figure 2.36, the output of the model is shown. In this graph, the desired AP673L spectrum is compared with the spectrum created by the white and purple LEDs together. The share of the number of photons per wavelength range in the total photon output, is the same for both spectra. In general, it can be concluded that by using the spectra of the white and purple LEDs, the output spectrum of the model is close to the desired spectrum. Figure 2.37 shows the photon flux distribution of the LED fixture with the white and

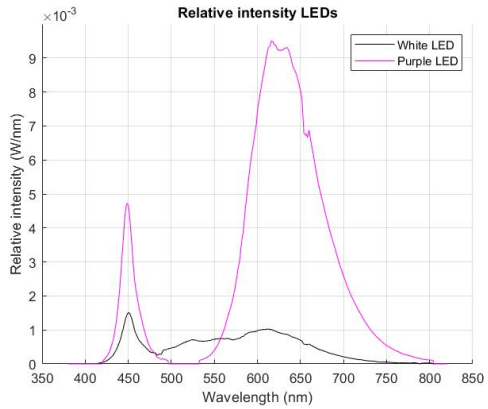


Figure 2.35: Spectral output of white and purple LED

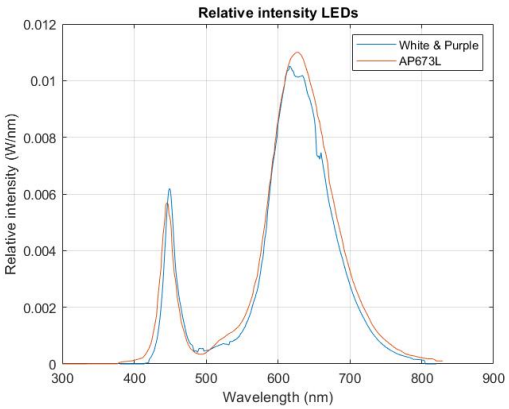


Figure 2.36: Spectral output of model using the white and purple LEDs and the desired AP673L spectrum

purple LEDs as found with the simulation model. The maximum photon flux is 196 $\mu mol/m^2s$ which is optimal for lettuce. According to the model output, the total power needed for the fixture to ensure this photon flux distribution is 80 $W$. This power is able to deliver a total flux of 237 $\mu mol/s$, which results in an efficacy of 2.9 $\mu mol/J$. According to the installation guide of Valoya's C65 light bar [131], the total power is 65$W$ and the maximum light output is 117 $\mu mol/s$. This is an efficacy of 1.8 $\mu mol/J$.

It can be concluded that the efficacy found with the model is significantly higher than the efficacy of the C65 according to the installation guide. The high efficacy is a result of the low power LEDs used in the model. The lower the forward current of an LED, the lower the efficiency droop and the higher the efficacy is. However, the efficacy of 2.9 $\mu mol/J$ for the whole LED fixture might be an overestimation.

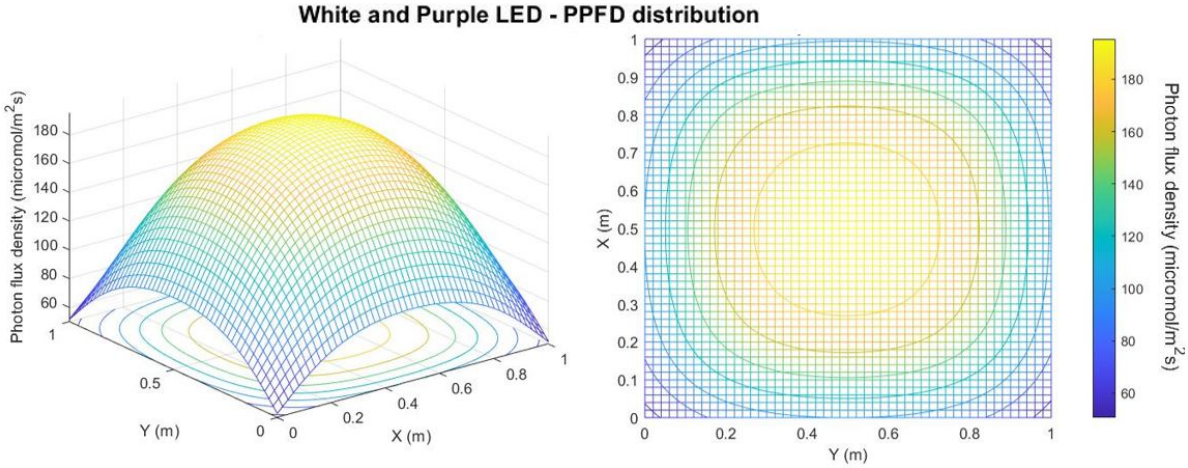


Figure 2.37: Output of LED simulation model: photon flux distribution of fixture using Valoya's white and purple LEDs on 1 $m^2$ surface

## 2.7. Conclusion

The sub-question that has been discussed in this chapter is: What are the requirements for an artificial lighting system for optimal crop cultivation? This question is worked out by means of the design of a light simulation model. It has been discussed in this chapter that the requirements for a lighting system used for the cultivation of crops is dependent on the needs of plants. The plants lighting requirements can be subdivided into the quality and the quantity of light or the spectral distribution and the amount of photons reaching the crops per time period. These parameters are crop dependent and therefore each crop has its own optimal values. Besides these two characteristics, the homogeneity of the lamps output is important for equal crop development on a specified surface. Also, it has been concluded that LED lighting is the most suitable lighting

technology for this application.

The light simulation tool developed in this study is able to design LED configurations that satisfy these requirements. LED configurations for multiple crop species, with different light quality and quantity requirements, can be created. By giving the desired spectrum, photoperiod and optimal daily lighting integral as input parameters, one can determine the characteristics of the required LED fixture. The results found with the model are close to the results of practical measurements and therefore it can be concluded that the model has the potential to be used for the design of lighting systems for crop cultivation. At the moment, the model is semi-automated and needs little manual action to simulate the output. Also, more accurate data regarding LED characteristics is needed to further improve the model. The further shortcomings and possible improvements for the light simulation model are discussed in the following section.

## Shortcomings and improvements

At the moment, a limited amount spectral data of LEDs is present in the model and therefore not every desired spectrum that is input in the model, can be accurately replicated. More spectra of different LEDs should be included in the model to ensure this more accurate replication of any desired spectrum. By having a broader choice of spectral outputs, the model itself could combine various LEDs having specific spectra in an iterative process to create a cumulative spectrum that is as close to the desired spectrum as possible.

In the light simulation model, no walls are integrated. It would be an improvement to give boundaries to the geometry with the addition of (reflecting) walls. In this way, the path of the light that falls outside the illuminated square meter and is partly reflected can be determined as well. Another improvement of the model would be to be able to determine the spectral distribution per element of the illuminated surface. In this way, the number of LEDs can be limited to an amount that is just able to assure the right spectral output. Also, at the moment, the model does not have an option to take into account narrowing reflectors in the LED lamps, which limit the spread of the light beam. Furthermore, the LED configuration in the model has a constant light output. This light output can be varied dependent on the DLI and the optimal photoperiod of the crops. The light output is constant over time because in this model, it is assumed that the LED configuration is the only source of light. An improvement of the model would be to integrate the possibility to simulate the LED configuration as supplemental lighting source. A control system would be needed that determines the amount of supplemental light that is needed based on the available sunlight.

The model can also be improved regarding the electrical characteristics of the LEDs. A more accurate relation between the forward current and the efficiency droop can be used. Besides that, at the moment, the model does assume a constant forward current and does not assume degradation of the LEDs over time. Adding degradation parameters that are dependent on both the forward current and junction temperature, could improve the determination of the lifetime of the fixture. It would also give a prediction for required maintenance. Furthermore, the model does not take into account other dynamics of the electronics of the LED fixture, like the effect of the heat transfer in the LED, the thermal conductivity of typical materials used in LED systems and for example other power losses in the system.

In general, the model could be made more automatized. At the moment, the iteration process to determine the optimal ratio between the different LED colors happens manually. If this manual operation are made automatic, the model can become an actual tool, which solely needs input parameters and gives the desired results as output without the need of manual operations. Furthermore, the tool can be implemented in 3D design software to design a complete greenhouse and be able to estimate the amount and properties of the lighting systems needed for optimal crop cultivation.

# 3

# Greenhouse scenarios

The previous chapter described a light simulation model, focusing on the dynamics of light and its effects on crops. This chapter zooms out one step further and looks at a complete greenhouse system. The sub-question that is discussed in this chapter is: how can LED and PV technology be arranged in a greenhouse system? To answer this question, multiple greenhouse scenarios are described in which LED technology and/or PV technology are integrated: the concepts of agrivoltaics and LED technology are combined. First of all, a reference greenhouse is created which has the characteristics of a greenhouse that is commonly used in agriculture nowadays. Subsequently, three other greenhouse scenarios are designed, each using different combinations of the technologies mentioned above. Then, a model that analyses the performance of each greenhouse scenario is explained in detail and the main performance indicators are discussed. Lastly, the approach for an economic analysis is described to determine the most economical scenario for future farming.

## 3.1. Greenhouse structure

This section discusses the main characteristics of the greenhouse structure that is used in this research. As discussed in the literature review, many types of greenhouse geometries have been used over time worldwide. For this study, the commonly used Venlokas is taken as the basic structure. Figure 3.1 shows the dimensions of the Venlo-type greenhouse that are used in this study. The angle of the roofs is 26º. This angle is found to be optimal because it has the highest average light transmission value in the Netherlands [132]. The complete greenhouse that forms the core of this study is displayed in figure 3.2. This greenhouse is build from three times the greenhouse unit shown in figure 3.1 and has a depth of 40 $m$. Besides the steel structure, the main covering material is glass. An average glass transmission for solar radiation of 70% is assumed [133]. In reality, the transmittance is dependent on the angle of incidence [66] and on the spectrum of the incoming light. However, for simplicity, it is assumed to be constant and able to transmit the whole PAR range at the same rate.

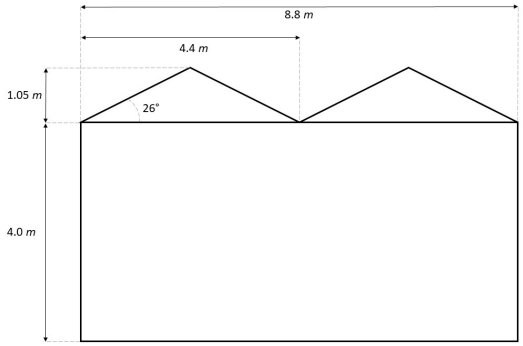


Figure 3.1: Dimensions of single unit Venlo-type greenhouse

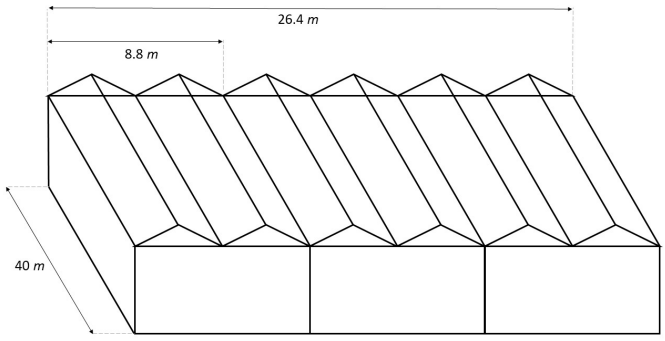


Figure 3.2: Dimensions of reference greenhouse

Besides this structure of the greenhouse, also the dimensions of the cultivation area within the greenhouse are important. It is assumed that 85% of the greenhouse area is actually used for crop cultivation. With a total greenhouse area of 1058 $m^2$ (40x26.4$m$), the area that is used for crops is 899 $m^2$. Per greenhouse block, this is a surface of approximately 300 $m^2$. This is displayed in figure 3.3 and is used to determine the part of the light that does not reach the crops and is therefore wasted. In a greenhouse the space inbetween the crop fields is needed to be able to reach the crops.

Furthermore, it is assumed that the ventilation windows are mounted on just one side of the roof of the greenhouse, as displayed in figure 3.4 and that the windows do not have an effect on the transmission rate. Because the windows should be able to be opened, nothing can be placed on top of the windows.

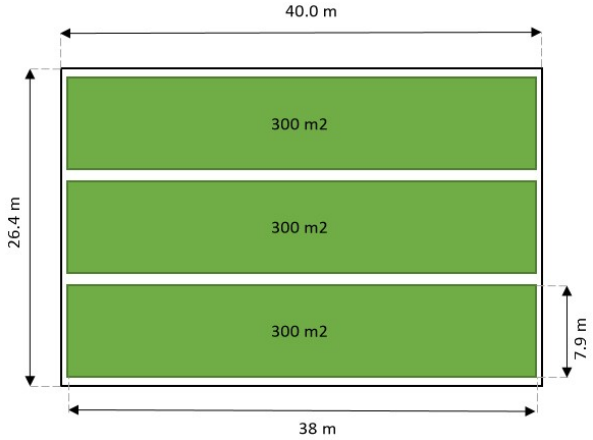


Figure 3.3: Dimensions of the crop area inside the greenhouse

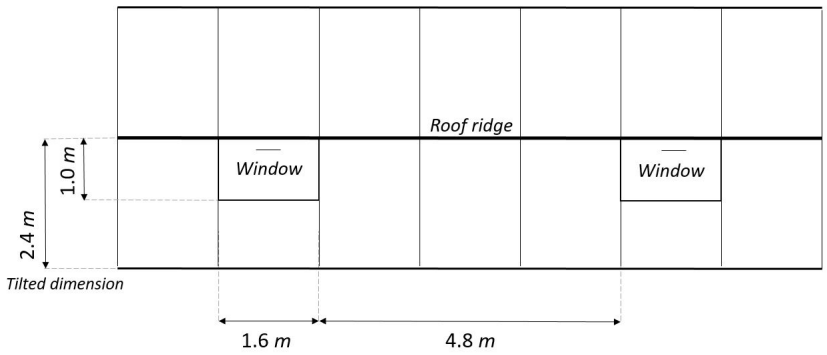


Figure 3.4: Dimensions of greenhouse roof including the dimensions of the ventilation windows present in the roof

## 3.2. Greenhouse PV system

Before the details of the various PV systems on the greenhouses are described, the PV technology used in this research is discussed. In this study, a trade-off is made between conventional mono-crystalline silicon (c-Si) PV modules and flexible thin film silicon modules to find the suitable PV technology to integrate in the greenhouse.

### 3.2.1. Mono-crystalline Silicon

This type of PV modules are the most commonly used PV modules at the moment and therefore widely available. The conventional c-Si modules can be both integrated (as replacement of the greenhouse glass) or placed on top of the greenhouse glass. The integration of modules as a replacement of glass (shown in figure 3.5) is generally more complex in case the greenhouse has already been build, since the modules have to make a perfect fit with the structure of the greenhouse. An easier option is to place the modules on top of

the glass with an assembly system, as shown in figure 3.6. These systems are widely available for the placement of c-Si modules on a greenhouse roof and therefore the installation is relatively easy. Also, because the modules are placed on an assembly rack, there is a free space between the greenhouse and the module. The greenhouse temperature is found to have little effect on the modules temperature when there is a spacing between the glass and the modules. Because of this spacing, air can flow through this spacing and the effect of possible high temperatures inside the greenhouse on the performance of the modules is found to be little. On the other hand, the PV modules have an insulation effect preventing solar energy from entering the greenhouse. In summer, they can (partly) replace energy screens (as shown in figure 1.7 in the literature review). Furthermore, because of the high availability of the technology, the price for these modules is relatively low, namely 64.15 $euro/m^2$ [134]. This has a positive effect on the economical feasibility of the integration of c-Si modules. Also, they have a high energy conversion efficiency.

The downside of the usage of c-Si modules on greenhouses is that they are relatively heavy and therefore a significant extra static load is added to the greenhouse structure. Also, the dynamic load due to wind increases and is it not possible to melt snow which is an extra load on the greenhouse structure. Furthermore, this type of PV modules has limited sizes available, which might cause problems when a more uncommon greenhouse structure is used.

Figure 3.5: c-Si modules integrated in greenhouse roof by replacing glass [135]

Figure 3.6: c-Si modules installed on assembly rack on top of greenhouse roof [136]

### 3.2.2. Thin film

The installation of thin film modules is relatively easy and no extra assembly system is needed: they are installed directly on the greenhouse glass. Furthermore, this technology is light weight (0.6 $kg/m^2$ [134]) and therefore no significant static load is added to the greenhouse structure. Another important advantage of thin film modules is that the size of the modules is highly adjustable and therefore can be custom made for a certain greenhouse. Because of this, also the light transmittance can be controlled better than the fixed size c-Si modules. The costs of the technology is 82.13 $euro/m^2$ according to HyEt Solar [134]. A disadvantage of the thin film modules compared to the c-Si modules is that the efficiency of commercial thin film modules is significantly lower at the moment. Furthermore, the placement of the thin film modules directly on the greenhouse glass, might result in the possible high temperature in the greenhouse ridge having a negative effect on the module performance. Also, compared to the conventional c-Si modules, the thin film modules are less commonly used at the moment. However, it is expected that this technology will acquire a higher market share in the short term future [137].

Based on the broad availability, the relatively low price, the high conversion efficiency and the common utilization in practice on greenhouse roofs, the c-Si modules are further used in this study. In this research, the characteristics as presented in table 3.1 are used. The module has a total of 60 cells (6x10). The modules has three bypass diodes which divide the module into three strings, as shown in figure 3.7.

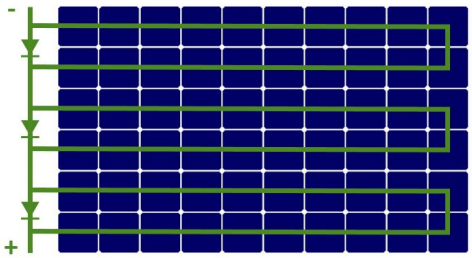


Figure 3.7: Strings connecting the cells in PV module

Table 3.1: Characteristics of mono c-Si module used in this study

| PV technology | Module efficiency (%) | Length (m) | Width (m) | Number of cells | Number of bypass diodes |
|---|---|---|---|---|---|
| Mono c-Si | 20 | 1.6 | 1.0 | 60 | 3 |

### 3.2.3. Solar radiation simulation

In order to analyse the electricity generation of the PV modules present on the greenhouses for the different scenarios, solar radiation simulations have to be done. Commonly used software for solar radiation simulations include Ecotect & Geco, DIVA, Ladybug and OpenStudio. The first three software are all plug-ins for the 3D design program Rhinoceros. They are used within the visual programming language and environment Grasshopper that runs within the Rhinoceros application. OpenStudio is used as a plug-in for Sketchup. In 2019, Han et al [138] compared the performance of a solar energy simulation with Ecotect & Geco, Diva and Ladybug. They found that Ecotect & Geco had a disadvantage in terms of visualization and climate analysis compared to DIVA and Ladybug. Also the accuracy of the outcome was worse for Ecotect & Geco compared to the other two. DIVA and Ladybug had an equal performance. Comparing DIVA (Rhinoceros) and OpenStudio (Sketchup), it was concluded that daylight quantities predicted by DIVA are closer to the measured experimental data collected from monitoring a physical model [139]. To achieve accurate and efficient solar radiation simulations, the simulations were done with the DIVA plug-in in Rhinoceros.

In Rhinoceros, a 3D geometry is designed having the dimensions as displayed in figures 3.1 and 3.2, forming the greenhouse strucutre. With DIVA it is possible to perform a sunlight analysis on this greenhouse via the integration with Radiance and DAYSIM [140]. In this study, the functions *Daylight simulation* and *Radiation Map* are used to determine the shadow length of certain objects and the amount of radiation falling on objects respectively. Both Radiance and DAYSIM use a backward ray-tracing method to perform all lighting calculations [141]. This means that light rays are traced in the opposite direction to that which they naturally follow. The process of backward ray-tracing starts from the viewpoint and subsequently traces the rays up to the light sources present in the model, while taking into account all physical interactions (refraction, reflection) with the surfaces of the objects present in the 3D scene in Rhinoceros.

**Module orientation**

To find the optimal orientation (portrait or landscape) of the c-Si PV modules on the greenhouse rooftop, firstly a simulation is done to determine the orientation with the highest annual yield. PV modules with the characteristics discussed in the previous section are placed on the greenhouse roof as shown in figure 3.8. Four modules have the landscape orientation and four modules have the portrait orientation. These placements are tested for a greenhouse with a north-south (N-S) orientation as well as for a greenhouse with an east-west (E-W) orientation. In this analysis, the yield of the individual cells of each module are determined to take into account the strings in the module. The current in the string is limited by the cell in the string with the lowest current.

The Radiation Mapping tool in DIVA is used to determine the energy yield on each cell of each module. This data is exported and analysed in Matlab. The radiation mapping of the modules is shown in figure 3.9 and is done for both the N-S and the E-W orientated greenhouse. The weather data that is used as input in the simulation is retrieved from Meteonorm. Radiation data for Delft (the Netherlands) from the period 1991-2010 with a time resolution of *hours* is used.

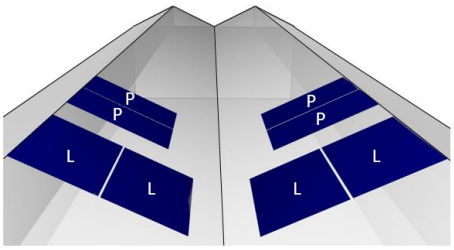


Figure 3.8: Module placement on greenhouse roof: 4 modules in landscape (L) and 4 modules in portrait (P)

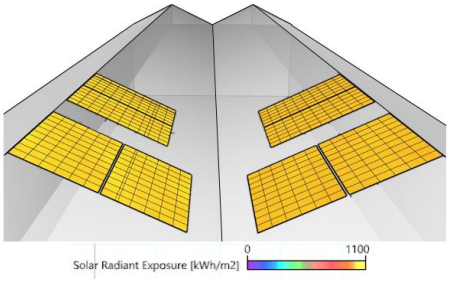


Figure 3.9: PV modules radiation simulation for the different module orientations

The simulations show that the landscape PV module configuration has the highest annual energy yield. The annual energy yield for every setup is displayed in table 3.2. Also, the N-S greenhouse orientation was found to have the highest energy yield, but the results do not differ significantly. Besides the energy yield of the PV modules, the light distribution within the greenhouse is important. In 2018, Cossu et al. concluded that a N-S orientation of the greenhouse increased the average cumulative global radiation on the greenhouse floor by 24%, compared to the E-W orientation [142] for greenhouses in southern Europe. Besides that, the N-S orientation allowed to improve the uniformity of light distribution, also with the integration of PV modules. Also in the Netherlands, a N-S orientation has a higher amount of radiation reaching the greenhouse floor annually compared to an E-W orientation [143]. It can be concluded that for both the PV production as for the crops, a N-S orientation is optimal. Therefore, in this study, c-Si modules in a landscape orientation and a greenhouse with a N-S orientation are used for further simulations.

Table 3.2: Results of simulation of different PV module and greenhouse orientations

| Module orientation | Greenhouse orientation | Number of modules | Annual energy yield (kWh) |
|---|---|---|---|
| Portrait | N-S | 4 | 1106 |
| | E-W | 4 | 1102 |
| Landscape | N-S | 4 | 1135 |
| | E-W | 4 | 1117 |

## 3.3. Greenhouse light sources

This paragraph describes the characteristics of the three light sources that are used in this study: sunlight, HPS lamps and LED lamps. In case the amount of sunlight is not sufficient, the artificial lamps can be used as supplemental light. In this section, the parameters of these light sources important for the analysis of the greenhouses are discussed.

**Sunlight**

In order to determine the amount of sunlight that reaches the crops, solar radiation data is retrieved from Meteonorm. This data has the unit $W/(m^2)$, which is not a suitable unit for crop performance analysis. As discussed in the literature review, the most common parameter to quantify the light intensity for crops is the photosynthetic photon flux density (PPFD) in $\mu mol/(m^2 s)$. In order to be able to use the light intensity data retrieved from Meteonorm, the irradiance in $W/(m^2)$ is converted into the PPFD in $\mu mol/(m^2 s)$. To determine the relation between these two quantities, SMARTS (Simple Model of the Atmospheric Radiative Transfer of Sunshine Version 2.9.5) [144] is used. With SMARTS, one is able to compute clear sky spectral irradiances for specified atmospheric conditions. Delft, the Netherlands is used as the location and the calculations are done for both the 1st of January and the 1st of July of the year 2010. The other input parameters are taken as default. As output, both the photon flux and the irradiance are selected for each hour between 9h and 17h of those days. The output data is given for a wavelength range from 300 to 2000 $nm$ and is given in $\mu mol/(m^2 s.nm)$ for the photon flux and $W/(m^2 nm)$ for the irradiance. The spectral irradiance data in

the PAR region for multiple hours of the day is shown in figure 3.10. At this day, at 12h the irradiance is the highest. Furthermore, it can be seen that the wavelengths of the peaks and drops of the irradiance are time independent.

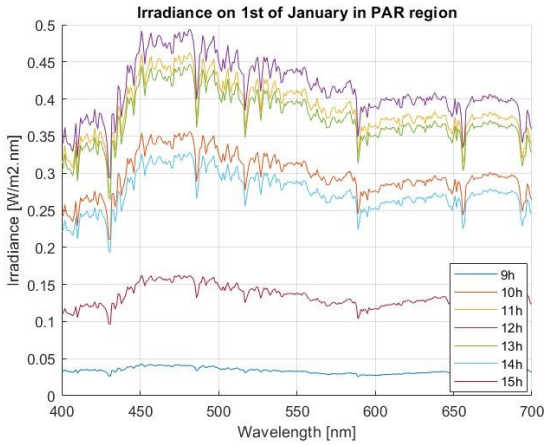


Figure 3.10: Spectrum of the PPFD and the irradiance at the 1st of January 2010 in Delft

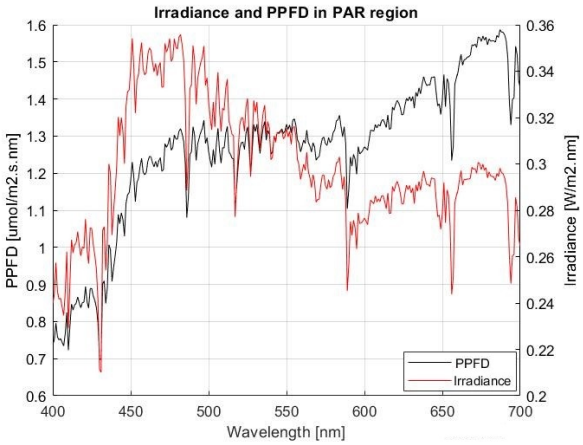


Figure 3.11: Spectrum of the PPFD and the irradiance at the 1st of January 2010 in Delft

Figure 3.11 shows both the irradiance and the PPFD at 12h in the PAR region. The integral of both quantities over the PAR wavelengths are taken to find the relation. The integral for the irradiance is as follows:

$$I_{PAR} = \int_{400nm}^{700nm} I(\lambda) \quad d\lambda, \tag{3.1}$$

with the integral of the irradiance ($I_{PAR}$) in $W/(m^2)$ and the irradiance per wavelength ($I$) in $W/(m^2 nm)$. The integral for the PPFD is determined as follows:

$$PPFD_{PAR} = \int_{400nm}^{700nm} PPFD(\lambda) \quad d\lambda, \tag{3.2}$$

with the integral of the PPFD in the PAR range ($PPFD_{PAR}$) in $\mu mol/(m^2 s)$ and the PPFD per wavelength ($PPFD$) in $\mu mol/(m^2 s.nm)$. Subsequently, the PPFD is divided by the irradiance to find the conversion factor $\gamma$:

$$\gamma = \frac{PPFD_{PAR}}{I_{PAR}}, \tag{3.3}$$

where $\gamma$ is the conversion factor between the PPFD and the irradiance in the PAR range in $\mu mol/J$. The conversion factors for the multiple hours of the day for both the 1st of January and the 1st of July, 2010, are listed in table 3.3. It can be seen that the values for all different moments are close to each other. In this study the mean value of 4.57 $\mu mol/J$ is used to convert the solar irradiance into the PPFD. This value is exactly the conversion value as presented in literature [145]. As discussed in the literature review, the part of the sunlight spectrum that is in the PAR region is 48.7%. In order to determine the PPFD that falls on the crops, this share is multiplied with the conversion factor giving a final conversion factor of 2.23 $\mu mol/J$.

Table 3.3: Conversion factor between irradiance and PPFD of multiple hours during January and July 1st of 2010 and mean value

| | **9h** | **10h** | **11h** | **12h** | **13h** | **14h** | **15h** | **16h** | **17h** | **Mean** |
|---|---|---|---|---|---|---|---|---|---|---|
| $\gamma$(µmol/J) (Jan 1, 2010) | 4.56 | 4.59 | 4.59 | 4.58 | 4.58 | 4.58 | 4.59 | 4.58 | 4.61 | 4.58 |
| $\gamma$(µmol/J) (Jul 1, 2010) | 4.57 | 4.56 | 4.56 | 4.56 | 4.56 | 4.56 | 4.56 | 4.56 | 4.56 | 4.56 |
| | | | | | | | | | $\gamma(\mu mol/J)$ | **4.57** |

**HPS lighting**
It is assumed that HPS lamps are used as supplemental light source in case the amount of sunlight is not sufficient. A commonly used HPS lamp in greenhouses is Philips' SON-T lamp. The SON-T lamps is assumed to have an efficacy of 1.7 $\mu mol/J$ [80, 146, 147]. Also, the lamps are able to ensure a PPFD of 200 and 381 $\mu mol/m^2s$ for lettuce and tomato, respectively.

**LED lighting**
The technology behind the LEDs and the application for the cultivation of crops is extensively discussed in both the literature review and chapter 3. In the scenarios discussed later in this chapter, LED lamps are used as supplemental lighting source or as the sole source of light. As supplemental lighting source, the LED fixture is placed at a relatively large distance of 3 meters above the crops. By having this setup, sunlight can still reach the crops. In case no sunlight is able to reach the crops and LED lamps are the only source of light to grow crops, the LED fixtures can be placed close to the plants. As discussed in the previous chapter, this distance is assumed to be 30 $cm$ from the top of the plant. By doing this, less light is wasted to the environment without crops, like the walking paths in between the crop fields, as shown in figure 3.3. As discussed before, the part of the greenhouse area that is covered by crops is 85%. This means that 15% of the light coming from the LED fixtures that are used as supplemental lighting source, is lost to the walking paths as displayed in figure 3.12. Because in reality probably a larger share of the light falls on walls and other structural objects instead of the plants, this value is a conservative value. For the situation where the LEDs are placed at a short distance from the crops, this factor is not taken into account.

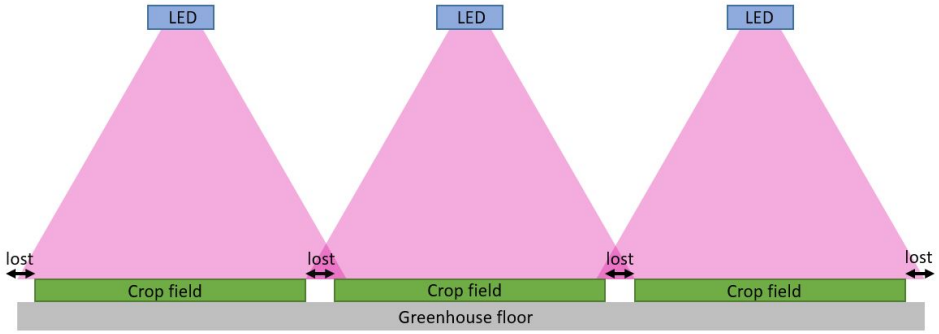


Figure 3.12: The setup of the LED lamps used as supplemental lighting source and the part of the light that is lost, because does not reach the crops

Other characteristics of the LED lamps is that they have a spectral output that matches the needs of the specific crops. As mentioned in the literature review, gradual advancements in diode fabrication techniques have resulted in a significant increase in the LED efficacy. This increase over the last years and the expected future increase in efficacy is shown in figure 3.13. The projected future saturation at approximately 3.1 $\mu mol/J$ is related to the phosphor conversion efficiency [82]. For this study, an efficacy of 2.5 $\mu mol/J$ is assumed [79–82]. A further characteristic of the LEDs fixtures is that they are able to ensure a PPFD of 200 and 381 $\mu mol/m^2s$ for the lamps used for lettuce and tomato, respectively.

## 3.4. Greenhouse scenarios

In this section, four greenhouse scenarios are created and the characteristics relevant for this study are discussed. The structure of each greenhouse is the same and equal to the one discussed in section 3.1. In two of the four designs, there is no PV system integrated, while in the other two a PV system is present. Three of the four scenarios make use of an LED lighting system and one scenario makes use of HPS lighting. The following paragraphs discuss the most important characteristics of the different designs.

**Scenario 1: Reference Greenhouse**
The reference greenhouse is created in order to be able to make a comparison between the performance of the new greenhouse designs that are discussed in the following paragraphs and the current process of crop cultivation. This greenhouse has the characteristics and makes use of technologies of a commonly used greenhouse in the Netherlands. SON-T HPS lamps are used as the supplemental lighting source in the greenhouse.

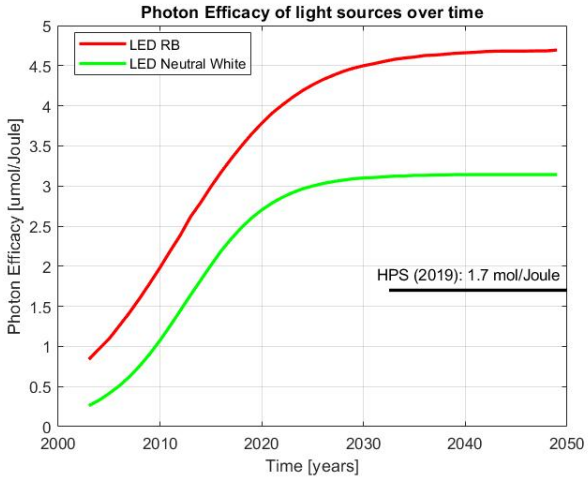


Figure 3.13: (Expected) Efficacy trends of Neutral white and Red/Blue (4:1 power ratio) LEDs over time and reference line of HPS efficacy [82]

**Scenario 2: LED lighting**
The second scenario is comparable with the first scenario, but instead of HPS lighting, this greenhouse uses LED lighting as supplemental light source. This scenario is also used to be able to make a fair comparison between the following scenarios which also integrate PV modules.

**Scenario 3: LED lighting - Checkerboard PV**
This greenhouse scenario uses LED lighting as the supplemental lighting technology. Besides that, this design has PV modules. The PV modules form an array on the roof of the greenhouse. The modules in this array are installed in a checkerboard configuration, as shown in figure 3.14. The checkerboard configuration is used because it ensures the most homogeneous sunlight distribution within the greenhouse, as discussed in the literature review. Furthermore, the modules follow the shapes of the greenhouse roof. This means that the modules are placed with a tilt angle of 26 degrees. The modules are placed in landscape mode and the spacing between two modules is equal to the length of one module. The modules are placed as close to the rooftop ridge as possible. The total amount of PV modules per titled roof sruface is 24. Each greenhouse unit has four titled roofs, and the whole greenhouse consists of three units. This gives a total of $24 \times 4 \times 3 = 288$ PV modules. In this greenhouse scenario, it is assumed that the PV electricity production is directly dumped on the grid and not directly used by the lamps.

**Scenario 4: LED - Full PV**
In the fourth scenario the greenhouse is fully covered with PV modules, except for the windows in the roof in order to ensure the possibility of ventilation, as shown in figure 3.14. The PV modules follow the tilt angle of the roof of the greenhouse. The modules are placed in landscape orientation and two modules fit on a titled roof glass. Each tilted side of the roof has 48 modules installed on it. For the titled roof part with windows, this amount is 42 modules. Per greenhouse unit, the are two roof sides with windows and two without windows. The whole greenhouse consists of three units, which is results in a total amount of PV modules of $(48+42) \times 2 \times 3 = 540$. In this setup, LED lighting is the only source of light for the crops. As discussed above, this means that the LED fixtures can be placed close to the crops. In this greenhouse scenario, it is assumed that the PV electricity production is directly dumped on the grid and not directly used by the lamps.

### 3.4.1. Performance indicators
In order to analyse the performance of the different scenarios, five main performance indicators are listed and explained in this section.

**Energy consumption**
The first indicator is the annual energy consumption of a greenhouse system. This is the sum of the total energy needed for the artificial lighting system and the other relevant energy demanding processes within

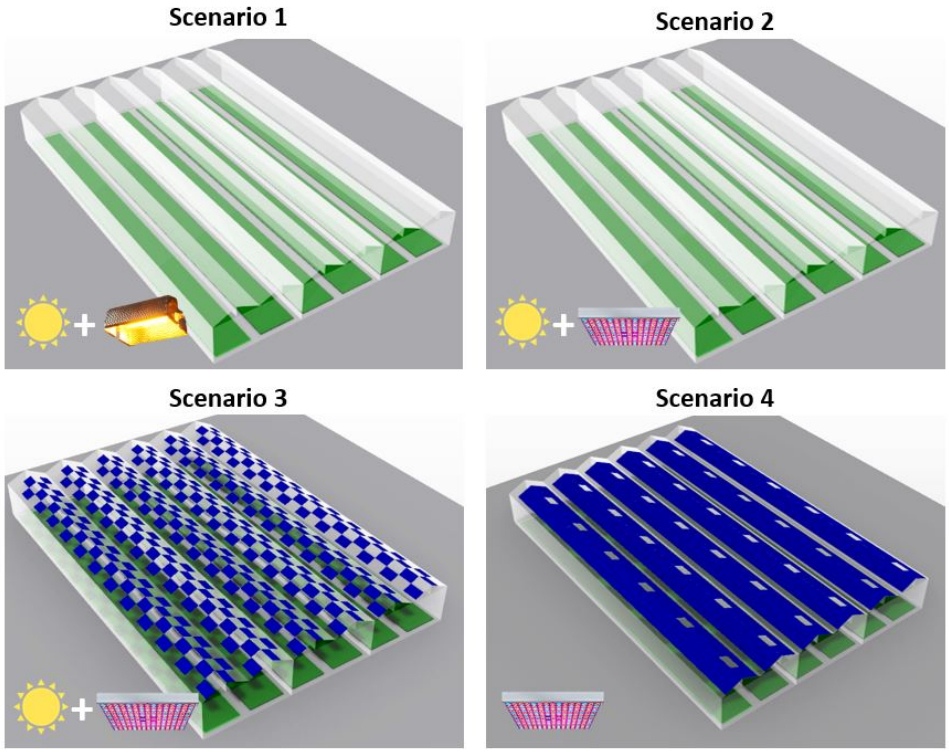


Figure 3.14: Greenhouse scenarios. Scenario 1: Reference greenhouse with HPS lighting system. Scenario 2: Greenhouse with LED lighting system. Scenario 3: Greenhouse with checkerboard PV array and LED lighting. Scenario 4: Greenhouse completely covered by PV modules and LED lighting as sole lighting source

a greenhouse. These most important energy demanding processes besides lighting are discussed later. The annual energy use is given in $kWh/m^2$.

**Crop Production**

Another indicator is the crop production. In this study, the effect of light on plant growth is researched. Since plant growth is dependent on many different parameters, it is assumed that all required external resources are optimal for each scenario and that the only variable affecting plant growth is light. As discussed in the literature review, light is the driving energy source for photosynthesis. The photosynthetic rate, being the rate at which photons are utilized in the photosynthetic apparatus [148], is used as a measure for crop growth and therefore the crop production. In 2019, Weaver and van Wiersel [13] stated that photosynthetic rates can be taken as indicator for plant growth. This assumption can be made because increases in photosynthesis invariably increases plant growth [149]. Increased photosynthesis increases carbon availability for plants. To what extent this translates into increased growth is dependent on co-limiting factors, especially nutrient availability. As mentioned before, it is assumed that these co-limiting factors are not dependent on the lighting conditions applied and that light is the limiting factor. The performance indicator *crop production* is the integral of the photosynthetic rate over a year and is given in $mol/m^2$. Since commonly used measures for crop production (like the fresh or dry weight of a crop) are dependent on a lot of variables, which are beyond the scope of this study, the photosynthetic rate is taken as the performance indicator to compare the relative production of the different scenarios.

**Efficacy**

The efficacy is a measure that uses the number of photons used for photosynthesis per $kWh$ of energy that has to be added to the system annually. It is determined by dividing the crop production by the energy needed per square meter. The energy that has to be added to the greenhouse system is determined by summing the energy demand of all significant energy demanding processes in the greenhouse and subtracting the annual energy produced by the PV modules in case a PV system is present in the system.

**Land Equivalent Ratio**
The Land Equivalent Ratio already has been discussed in the literature review. It is a measure for the productivity of a piece of land by combining the production of different goods, like electricity and crops. It is determined by using equation 1.6. For the sole production of PV power, the maximum potential PV power production of an area equal to the greenhouse area of 1058 $m^2$ (40x26.4$m$) is assumed. To determine the potential PV generation of this area only used to produce PV energy ($Y_{mono-electricity}$) , a radiation simulation is performed in Rhinoceros using the PV field as shown in figure 3.15. This field has a total of 572 PV modules and the modules face North and South with a tilt angle of 15 degrees. This angle is not the optimal angle of tilt for the different locations, but it is used to reduce the amount of wind loading on the PV modules, as commonly done in practice [150]. For this field filled with PV modules it is assumed that the PV modules can be placed directly next to each other. In other words, there is no spacing between the arrays. In this way, a situation is created which is comparable to the PV systems installed on the greenhouses: the modules are placed to next to each other, the (roof) area is filled as much as possible and reaching the modules for maintenance is relatively difficult. A more detailed description of the design of this PV system is given in section 5.2 of chapter 5.

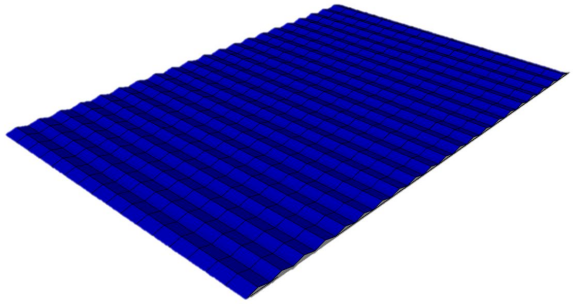

Figure 3.15: Area of 1058 $m^2$ (40x26.4$m$) with PV modules used to determine $Y_{mono-electricity}$

**Costs**
The last performance indicator is the costs of the system. The costs of the system are given in euro per mol photosynthetic photons used annually. It is a measure to get an idea about the economical differences between the different scenarios. In section 3.7, the parameters that are taken into account and the assumptions made to determine the investment and variable costs over time for the scenarios, is discussed.

### 3.4.2. Crops
The four greenhouse scenarios are tested for two types of crops: lettuce and tomato. As discussed before in the light simulation model, the optimal DLI for lettuce is 17 $mol/m^2day$ and for tomato it is 22 $mol/m^2day$. These values are assumed in the analysis of the scenarios. For both crops, it is assumed that the total crop area is 85% of the total greenhouse area and the crop fields have the dimensions as displayed in figure 3.3. It is assumed that the crops fill this entire area. It is also assumed that the crops are in the vegetative growth phase [151]. In practise, this would mean that crops that are not in their vegetative growth phase anymore, are replaced by crops that are at the beginning of this phase. Furthermore, the optimal temperature for lettuce is assumed to be 18°C [152] and for tomato a day temperature of 25°C and night temperature between 18°C and 25°C is optimal [153].

An important parameter that is used to compare the performance of the different scenarios is the photosynthetic efficiency of the crops at different lighting conditions. This quantity is elaborated on in the next paragraph.

**Photosynthetic rate**
Because in this analysis, each scenario uses different types of lighting, the light use efficiency of the crops for each light source is needed to determine the performance of each scenario. In order to determine the efficiency of the light utilization of the crops, the McCree curve as discussed in the literature review and displayed in figure 1.3 can be used. When the exact spectrum of the light source is known, McCree's photon weighted action spectrum curve is used to determine the photosynthetic efficiency of the plant receiving that

specific spectrum. To determine this efficiency, the weighted spectral output of the specific light source is weighted with the McCree curve:

$$P_{efficiency} = \frac{\int_{\lambda_1}^{\lambda_2} M_{curve}\, S_{light}\, d\lambda}{\int_{\lambda_1}^{\lambda_2} S_{light}\, d\lambda}, \tag{3.4}$$

where $P_{efficiency}$ is the photosynthetic efficiency of the plant illuminated with the spectrum $S_{light}$ of the light source. $M_{curve}$ is the photon weighted action spectrum curve by McCree (figure 3.16). In order to be able to multiply the photon weighted McCree curve with the spectral output of the light source, the output of the light source should be given with the unit of photons as well. To convert the power output of the light source to photons emitted ($mol/s$), equation 2.1 is used. Equation 3.4 is applied to the three light sources used in the different scenarios, being: Sunlight, HPS (SON-T) and LED (AP673L for lettuce). The results of this multiplication are shown in figures 3.17, 3.18 and 3.19. Applying equation 3.4, the total photosynthetic efficiencies of the solar spectrum, SON-T spectrum and the AP673L spectrum are determined to be 66%, 88% and 85%, respectively. This means that illuminating the plant with the HPS (SON-T) lamp results in the highest photosynthetic efficiency. This can be explained by the fact that the HPS spectrum mainly consists of light with wavelengths around 600 $nm$, the wavelengths that are most efficiently used by the crops according to McCree. Following this reasoning, light with a single peak at 600 $nm$ results in a plant's photosynthetic efficiency of 100%.

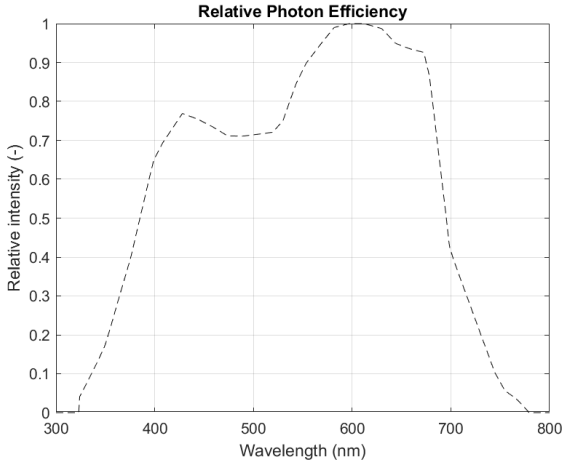


Figure 3.16: Quantum yield showing the photosynthetic efficiency at different wavelengths [30]

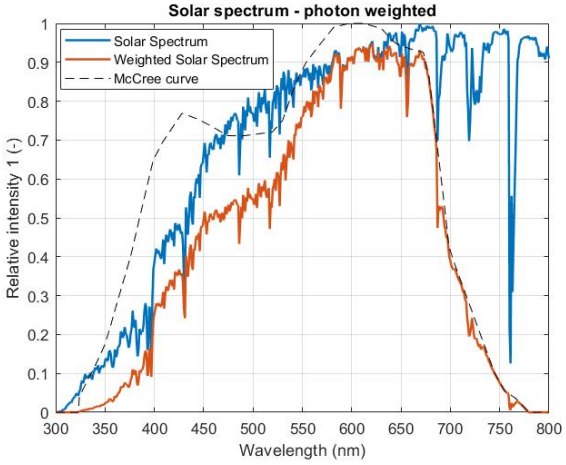


Figure 3.17: Solar spectrum and the solar spectrum weighted with the quantum yield curve

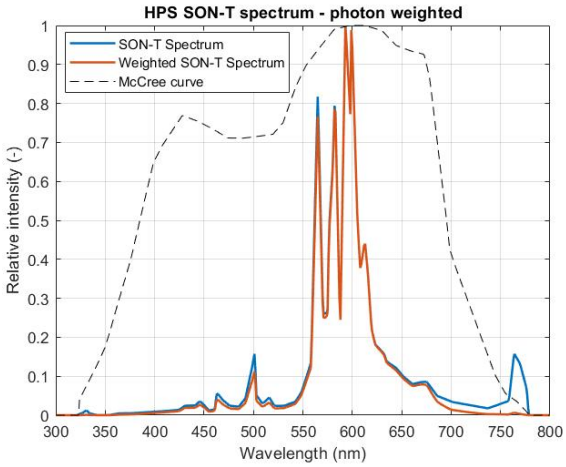


Figure 3.18: SON-T spectrum and the SON-T spectrum weighted with the quantum yield curve

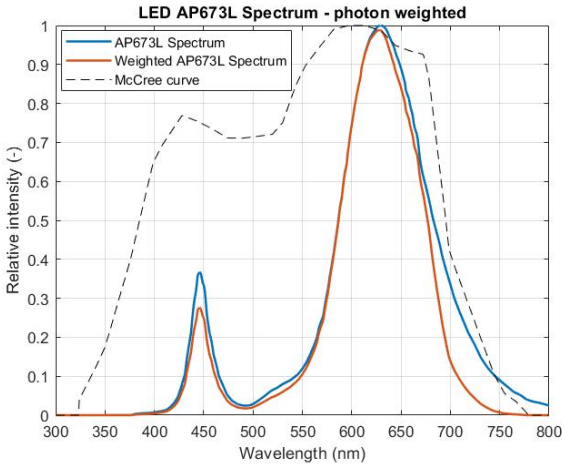


Figure 3.19: AP673L spectrum and the AP673L spectrum weighted with the quantum yield curve

However, practical measurements with different crop species have shown that plants grow better with a light spectrum containing wavelengths of the whole PAR range as discussed in the literature review in section 2.3. The main shortcoming of McCree curve is that it is based on single wavelength measurements. The effect of a combination of multiple wavelengths on the photosynthetic rate (Emerson effect [39]) is not taken into account. Because of this, for this research, the relation between the photosynthetic rate of the crops and the light sources is retrieved from practical measurements, as discussed below.

As discussed before, the production of crops is quantified with the number of photons that are used by the specific crop in the photosynthetic process annually per square meter. This quantity is determined using the rate of photosynthesis. The rate of photosynthesis is closely related to the Electron Transport Rate (ETR) as discussed in paragraph 1.1.1 and displayed in figure 1.5. The photosynthetic rate increases linearly with the ETR [154], which means that the higher the photon flux reaching the crops is, the less the photosynthetic rate increases. At a certain photon flux (dependent on the crop type), an additional increase in light does not increase the photosynthetic rate. This point is called the light saturation point. This can be seen in figures 3.20 and 3.21, that show the relation between the photosynthetic rate and the PPFD for lettuce and tomato, respectively. Besides light, the photosynthetic rate is also dependent on other factors, like the ambient temperature and the $CO_2$ concentration. The effect of light intensity, temperature and $CO_2$ concentration on the photosynthetic rate are interrelated. For example, when the concentration of $CO_2$ is low, the light saturation point is decreased [155]. In this study, it is assumed that the quantities that have an effect on the photosynthetic rate, besides light, are ideal in each scenario for each moment in time.

As discussed in the literature review, besides the amount of photons in the PAR region reaching the plants every second, also the spectral distribution has an effect on the amount of photons that are used in photosynthesis. This is why also the spectral output is taken into account to determine the photosynthetic rate. In figures 3.20 and 3.21, the rate of photosynthesis is shown for the three light sources present in the different scenarios. The photosynthetic rates for single leaves were determined by measuring the difference in $CO_2$ concentration over time. For the measurements of lettuce, the LED lamp consists of blue, green and red LEDs, with peak wavelengths at 440 $nm$, 530 $nm$ and 660 $nm$ [156]. To measure the photosynthetic rate of tomato under LED illumination, an LED with a broad blue peak at 430 $nm$ and red LED with a peak at 660 $nm$ is used [157]. It can be concluded that the spectral output of the LEDs used in these studies are not exactly the same as the spectra assumed to be optimal in this study. However, these results found in these studies are still a good measure and might be even considered as conservative, since for example far red light is not present. As discussed, the far red light in combination with wavelengths in the PAR region, are found to have a positive effect on plant growth [24]. The trendlines for the photosynthetic rates are a curve fit based on practical measurements taken. The function of these curves are presented in table 3.4.

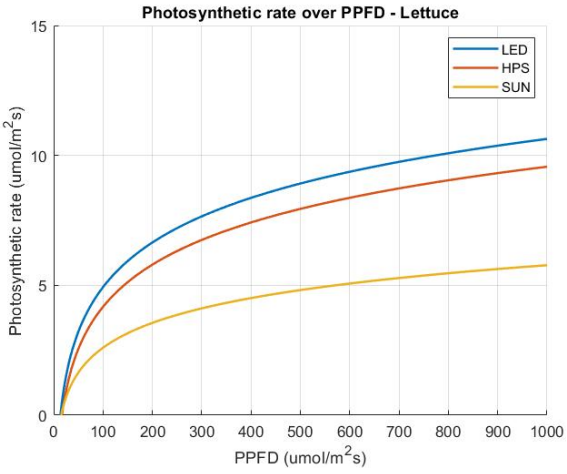


Figure 3.20: Photosynthetic rate of tomato at an increasing PPFD for three light sources: LED, HPS and Sunlight [156]

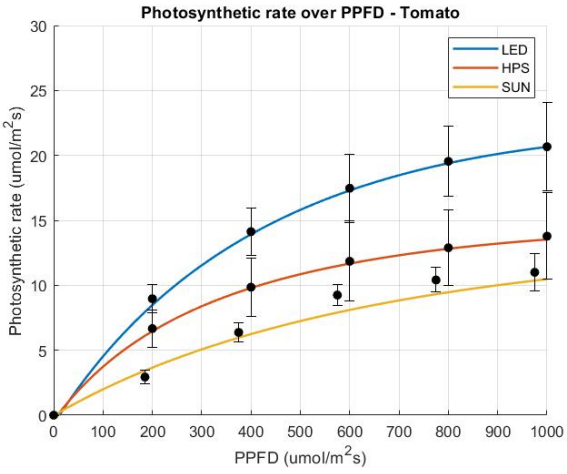


Figure 3.21: Photosynthetic rate of tomato at an increasing PPFD for three light sources: LED, HPS and Sunlight [157, 158]

Table 3.4: Trendlines of photosynthetic rate over the photon flux (x) for different light sources

| Light source | Trendlines Lettuce [156] | Trendlines Tomato [157, 158] |
|---|---|---|
| Sunlight | $1.3796ln(x)$–3.7577, $R^2 = 0.8881$ | $(-0.002669x^2 + 24.96x - 31.49)/(x + 1126)$, $RMSE = 0.04894$ |
| HPS | $2.3427ln(x) - 6.6181$, $R^2 = 0.8891$ | $(-0.0001851x^2 + 21.22x - 166.1)/(x + 419.7)$, $RMSE = 0.07446$ |
| LED | $2.4785ln(x)$–6.4855, $R^2 = 0.8974$ | $(-0.0079x^2 + 44.67x - 522.3)/(x + 755)$, $RMSE = 0.3207$ |

### 3.4.3. Locations

Besides the two different crops as analysis variables, the scenarios are also tested for three locations. The locations are Kiruna in Sweden (SWE: 67.8° N, 20.2°E), Delft in the Netherlands (NLD: 52.0° N, 4.36 °E) and Abu Dhabi in the United Arab Emirates (UAE: 24.5° N, 54.7 °E). These locations are selected because their climates differ significantly. Figure 3.22 displays the average monthly solar radiation and temperature for each location. The hourly radiation data for these locations used in the radiation analysis in Rhino is retrieved from Meteonorm.

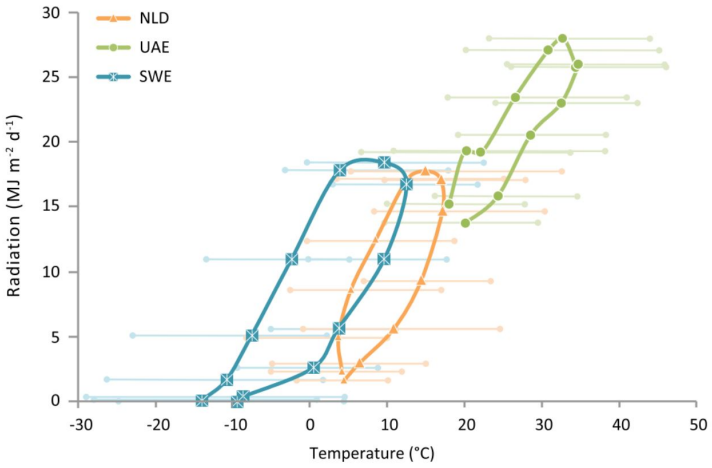


Figure 3.22: Monthly average temperatures and average daily radiation per month for Kiruna (SWE), Delft (NLD) and Abu Dhabi (UAE). January is lower left data point in cycles

## 3.5. Other energy requirements

Besides the energy needed for supplemental lighting, greenhouses need energy for other processes. Because this study focuses on the lighting dynamics within a greenhouse in combination with the power generation by PV modules, energy demanding processes besides lighting systems are retrieved from literature. In 2018, Graamans et al. [152] compared the resource use efficiency of greenhouses with plant factories. In this research, the main energy demanding processes are simulated for a greenhouse in which lettuce is cultivated for each of the three locations mentioned above. The relevant energy demanding processes, besides lighting, are forced ventilation, heating, light cooling and dehumidification. Unless stated otherwise, the values are retrieved from the study by Graamans et al. [152]. For tomato, only energy data for the scenarios in Delft is used. An overview of the quantities discussed in the following paragraphs is given in tables 3.5, 3.6 and 3.7, for Kiruna, Delft and Abu Dhabi, respectively.

**Forced ventilation**

When the temperature within the greenhouse becomes too high for the crops to grow optimally, ventilation of the greenhouse takes place. This can be done naturally, by opening the windows of the greenhouse. When natural ventilation is not sufficient, forced ventilation is often used to lower the air temperature within the greenhouse. This is normally done with fans. For lettuce in Delft, the energy needed to drive this ventilation is 183 $kWh/m^2$ annually. As discussed in the literature review, Fatnassi et al. [92] found that PV modules covering the greenhouse act as a passive cooling system during summer. By covering the greenhouse for 50% with PV modules, the internal air temperature decreased with 3°C. Also for scenarios 3 and 4, a required ventilation energy of 183 $kWh/m^2$ is assumed. However, as reasoned above, with the coverage of PV modules, this is likely to be lower in practice, making this a conservative assumption. Also for greenhouses with lettuce

in Kiruna and Abu Dhabi, the assumptions for the ventilation energy of scenario 3 and 4 are conservative, because of the extra cooling effect of the PV modules.

**Heating**
Greenhouses are a semi-closed environment and can lose a significant amount of heat when the outside temperature is lower than the inside temperature. In order to maintain the temperature that is optimal for the specific crop, heating is needed. As discussed before, lettuce has a lower optimal temperature than tomato and therefore the amount of energy needed to maintain the temperature for tomato is higher than for lettuce in Delft and Kiruna, as noted in tables 3.6 and 3.5, respectively. A normal greenhouse in Delft without supplemental lighting in which lettuce is grown, uses 143 $kWh/m^2$ for heating, by burning gas. In this study it is assumed that all scenarios in Delft need this amount of heating. For all scenarios this can be considered to be a conservative assumption, since all scenarios use supplemental lighting, which -at different rates- produce heat as well. Furthermore, the greenhouse in scenarios 3 and 4, where the greenhouse is (partly) covered with PV modules, can be better insulated (with energy screens as discusses in the literature review) than the greenhouses in scenarios 1 and 2. Therefore less energy is lost through the glass and less energy is needed to maintain the indoor temperature. The same reasoning can be used for the amount of heating that is needed for all greenhouse scenarios located in Kiruna. Because of the high temperature throughout the year in Abu Dhabi, no additional heating is required to maintain the optimal temperature inside the greenhouse.

The amount of gas used for heating for tomato annually in Delft is assumed to be 24.5 $m^3/m^2$ [159]. With an energy density of 8.8 $kWh/m^3$, this equals 216 $kWh/m^2$. Also for tomato, the conservative reasoning as discussed above for lettuce, can be used for the amount of heat needed in each scenario.

**Dehumidification**
The dehumidification of a greenhouse is an important part of the climate control. A high humidity enlarges the chance of crop diseases which reduce the quantity and quality of production. The amount of water vapor air can contain is dependent on the air temperature. Warm air can hold more water vapor than cold air [160]. This is the reason why greenhouses in which tomato is cultivated, which has a higher optimal growth temperature, needs to dehumidify the greenhouse climate actively. The most common method to dehumidify a greenhouse is by ventilation. For greenhouses in the Netherlands and Sweden in which lettuce is cultivated, the dehumidification of inner climate happens sufficiently by natural ventilation by opening the rooftop windows. This is why for lettuce in these locations, no additional energy is assumed for dehumidification. In Abu Dhabi on the other hand, because of the high air temperature, a significant amount of additional energy is needed for dehumidification, which is assumed to be 693 $kWh/m^2$ [152]. Since the possibility of ventilation is the same for every scenario, because all scenarios have the same amount of windows, the humidification is assumed to be the same for each scenario. This is a conservative assumption for scenarios 3 and 4, because the air temperature is lower for these scenarios at moments when sunlight heats up the greenhouse. When this is the case, the scenarios with PV modules, are heated less significantly than the uncovered scenarios and therefore the air temperature does increase less and the air can hold less water vapor. The energy needed to dehumidify the tomato greenhouse is 77.4 $kWh/m^2$ [161].

**Light cooling**
As discussed, a significant part of the input energy for lighting systems is converted into heat. For light fixtures that are placed high above the crops, as in scenarios 1, 2 and 3, cooling of the lamps takes place at macro-level [79]. This means that cooling of these lamps happens with natural or forced ventilation as described above. For these situations, the energy needed for the cooling of the lamps is already taken into account under *Forced ventilation*. For the LED fixture that is placed close to the crops, as in scenario 4, ventilation alone is not sufficient. It is assumed that these LEDs are cooled with liquid cooling. This cooling is done to maintain the lifetime and efficiency of the LEDs [79], because as discussed in the previous chapter, the lifetime of an LED decreases faster at a high junction temperature.

Table 3.5: Relevant energy demanding processes for the cultivation of lettuce in Kiruna, Sweden

**Kiruna**

| Crop | Energy process | Scenario 1: HPS | Scenario 2: LED | Scenario 3: LED - Checkerboard PV | Scenario 4: LED - Full PV |
|---|---|---|---|---|---|
| Lettuce | Forced Ventilation (kWh/m$^2$) | 103 | 103 | 103 | 103 |
| | Heating (kWh/m$^2$) | 308 | 308 | 308 | 308 |
| | Dehumidification (kWh/m$^2$) | 0 | 0 | 0 | 0 |
| | Light cooling (kWh/m$^2$) | 0 | 0 | 0 | 214 |

Table 3.6: Relevant energy demanding processes for the cultivation of lettuce and tomato in Delft, the Netherlands

**Delft**

| Crop | Energy process | Scenario 1: HPS | Scenario 2: LED | Scenario 3: LED - Checkerboard PV | Scenario 4: LED - Full PV |
|---|---|---|---|---|---|
| Lettuce | Forced Ventilation (kWh/m$^2$) | 183 | 183 | 183 | 183 |
| | Heating (kWh/m$^2$) | 143 | 143 | 143 | 143 |
| | Dehumidification (kWh/m$^2$) | 0 | 0 | 0 | 0 |
| | Light cooling (kWh/m$^2$) | 0 | 0 | 0 | 214 |
| Tomato | Forced Ventilation (kWh/m$^2$) | 9.0 | 9.0 | 9.0 | 9.0 |
| | Heating (kWh/m$^2$) | 216 | 216 | 216 | 216 |
| | Dehumidification (kWh/m$^2$) | 77.4 | 77.4 | 77.4 | 77.4 |
| | Light cooling (kWh/m$^2$) | 0 | 0 | 0 | 214 |

Table 3.7: Relevant energy demanding processes for the cultivation of lettuce in Abu Dhabi, UAE

**Abu Dhabi**

| Crop | Energy process | Scenario 1: HPS | Scenario 2: LED | Scenario 3: LED - Checkerboard PV | Scenario 4: LED - Full PV |
|---|---|---|---|---|---|
| Lettuce | Forced Ventilation (kWh/m$^2$) | 840 | 840 | 840 | 840 |
| | Heating (kWh/m$^2$) | 0 | 0 | 0 | 0 |
| | Dehumidification (kWh/m$^2$) | 693 | 693 | 693 | 693 |
| | Light cooling (kWh/m$^2$) | 0 | 0 | 0 | 214 |

## 3.6. Greenhouse simulation model

In this section, the calculations used to determine the optimal greenhouse scenario are explained. The main goal of this simulation is to find the amount of supplemental light that is needed from the artificial light sources throughout the year.

### 3.6.1. Sunlight

The conversion factor $\gamma$ to determine the PPFD that reaches the crops was found to be 4.57 $\mu mol/J$. Furthermore, it was stated that 48.7% of the sunlight lies within the PAR region. Hourly irradiance data (in $MJ/m^2$) is retrieved from Meteonorm for each location. This irradiance per hour is converted into mol photons per hour with the following equation:

$$PPFD_{hour} = 0.487 \times 4.57 \times 3600 \times 10^{-4} \times I \tag{3.5}$$

In this equation, the multiplication with $3600 \times 10^{-4}$ is done to convert the PPFD ($I \times 0.487 \times 4.57$) from $\mu mol/m^2 s$ to $mol/m^2 h$. By doing this, the total PPFD for one hour that falls on the greenhouse is found. To determine the PPFD that reaches the crops, the transmission of the greenhouse glass is taken into account. It is assumed that 70% of the light that reaches the greenhouse is transmitted through the glass. Furthermore, it is assumed that 10% of the light is blocked by the greenhouse supporting structure and the artificial light fixtures. The PPFD that reaches the crops becomes:

$$PPFD_{hour\,crops} = 0.7 \times 0.9 \times PPFD_{hour} \tag{3.6}$$

### Available sunlight scenario 3

For scenario 3, with the checkerboard PV configuration on the roof of the greenhouse, an extra sun blocking factor is taken into account. A radiation simulation with the 3D model in Rhinoceros is done to determine the amount of light that reaches the crops despite the presence of the PV modules. For this simulation, the glass structure of the greenhouse is removed and only the PV modules are located at a height of four meters above the crops as shown in figure 3.23. The annual radiation simulation (diplayed in figure 3.24) shows that the PV modules block a significant part of the radiation compared to the uncovered area on the sides. The lowest value on the radiated surface is found to be 670 $kWh/m^2$. Comparing this reduced radiation with the average radiation falling on the uncovered surface, the share of radiation that actually reaches the floor annually is determined as follows:

$$\frac{670}{1030} = 0.65 \tag{3.7}$$

According to this analysis, the extra factor to take into account the blocking of sunlight by the PV modules in scenario 3 is 0.65.

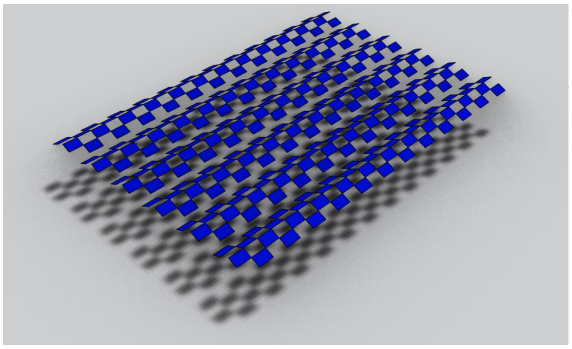

Figure 3.23: Checkerboard PV module configuration without greenhouse structure

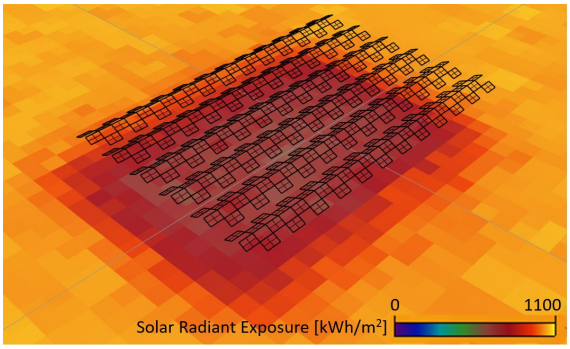


Figure 3.24: Radiation distribution under checkerboard PV module configuration

However, since this calculation only takes into account the radiation reaching the surface integrated over a year, the result does not take into account a potential non homogeneous distribution of shading of a shorter period of time. As shown in figure 3.23, the shading on the greenhouse floor is not homogeneous at a specific moment in time. To check the available sunlight for 1 $m^2$ for a shorter time interval, the hourly global radiation data for the three locations is used. Figure 3.25 shows the global radiation trends for three consecutive days for two types of horizontal surfaces in Delft: a surface that is partly shaded by a checkerboard PV module configuration at a vertical distance of $4m$ (blue line) and an uncovered surface (orange line). The effect of the shading due to the checkerboard PV array is clearly visible in the hourly trend. At the higher peaks of the blue line, the surface receives more direct radiation than at the lower peaks. To determine the reduced radiation more accurately, the integral of the reduced radiation for the each day of the year is taken. This integral is divided by the integral of the radiation for the same days for the non covered surface. In other words, for each day, the surface under the blue graph is divided by the surface of the orange graph for a period of 24 hours. By doing this, the factor found is a measure for the reduced radiation. For Delft this factor is 0.62, for Kiruna 0.65 and for Abu Dhabi 0.60. In figure 3.24, these factors for the first day of each month for the three locations are shown. It can be seen that the factors are close to the previously determine value of 0.65. The reduction factor for Kiruna in February is significantly higher then the other factors. However, because the amount of radiation at days of this month is negligible (it is only 2% of the radiation on the same day in July) the value of 0.65 is still assumed.

To determine the total amount of sunlight reaching the crops in a day, the $PPFD_{hour\,crops}$ is integrated over 24 hours and $PPFD_{day\,crops}$ is found. This is done for each day of the year. In order to determine the amount of photons that are actually used by the crops for photosynthesis, the relation between the PPFD and the photosynthetic rate as presented in table 3.4 for sunlight is used. In these curves, $PPFD_{hour\,crops}$ is filled in for $x$. The integral of the photosynthetic rate over the year gives the total amount of photons used for photosynthesis ($Photons_{sun}$) in $mol/m^2$.

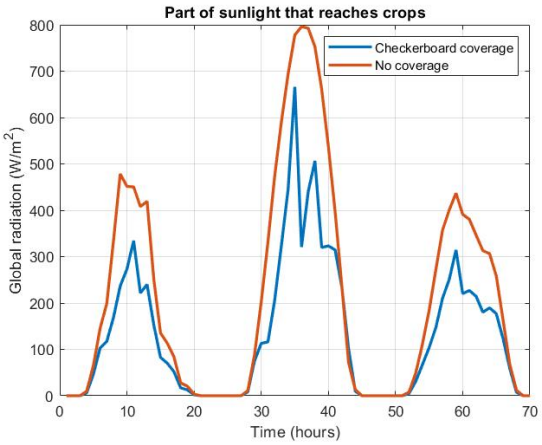


Figure 3.25: Global radiation on horizontal surface in Delft with Checkerboard PV array coverage and without coverage for 3 consecutive days

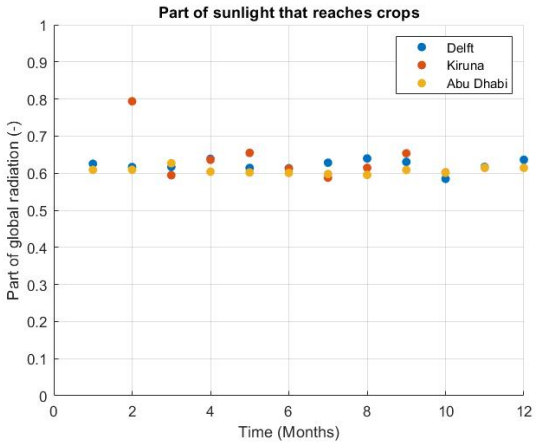


Figure 3.26: Global radiation reduction factors for the first day of each month for Delft, Kiruna and Abu Dhabi

### 3.6.2. Supplemental lighting

The amount of supplemental lighting that is needed per day is dependent on the amount of sunlight that reaches the crops and the specified optimal DLI. The amount of photons needed per day from the supplemental lighting source is found with the following equation:

$$S_{light} = DLI - PPFD_{daycrops}, \tag{3.8}$$

where $S_{light}$ is the amount of photons that the lamps need to deliver to the crops in a day in $mol/m^2$. When $S_{light}$ is equal or lower than zero, no supplemental lighting is needed. For the supplemental lighting source, the average PPFD per hour is determined to calculate the amount of photons that are used for photosynthesis, $Photons_{lamp}$. This is done with the formula for the specific artificial light source as displayed in table 3.4.

The energy use of the artificial lamps is determined by using the efficacy of the artificial light source, which is 1.7 and 2.5 $\mu mol/J$ for the HPS and LED lamp, respectively. The following integral is used to find the energy consumption of the lamp for a whole year:

$$E_{suppl} = \int_1^{365} \frac{S_{light}(t)}{3.6\eta} dt, \tag{3.9}$$

where $E_{suppl}$ is the annual energy demand that is needed for supplemental lighting per square meter of crops in $kWh/m^2$ and $\eta$ is the efficacy of the supplemental lighting in $\mu mol/J$. The total amount of photons used for photosynthesis per scenario is determine with the following equation:

$$Photons_{year} = 0.85(Photons_{sun} + Photons_{lamp}), \tag{3.10}$$

where $Photons_{year}$ is the amount of photons used annually in $mol/m^2$. It is assumed that the crops cover 85% of the total area of the greenhouse, as displayed in figure 3.3. Therefore, the total amount of photons used is multiplied with a plant coverage factor of 0.85 to account for the unused greenhouse area.

### 3.6.3. PV production

To determine the annual PV production of scenario 3 and 4, radiation data with a resolution of hours is used. The amount of DC PV power generated each hour is calculated with the DIVA Archsim plugin which converts the surfaces, as for example shown in figure 3.23, into PV modules. The efficiency of the modules is set to be 20% and the effective area of the modules is 95%. Furthermore, an inverter efficiency of 95% is assumed [162] to convert the DC power to AC power. For this model, it is assumed that the energy produced by the PV modules goes to the grid. The annual electricity generation is determine by taking the integral of the PV power over a year (8760 $hours$). As discussed, the greenhouse structure consists of three greenhouse units. Each unit has four PV arrays on top, one on each titled roof surface.

For the scenario that is fully covered by PV modules, these arrays are shown in figure 3.27 and labelled with A1, A2, A3 and A4. The whole greenhouse has 12 arrays mounted on top. In the calculation of the electricity production, only the generation on one greenhouse unit is assumed, for each of the four arrays (A1, A2, A3, A4). The two greenhouse units on the sides are taken away, to remove the shadowing effect of these structures. Array A1 and array A4 are the arrays on the side and array A2 and A3 are in between and are expected to have a lower electricity generation because they have a lower skyview factor. To determine the electricity production of a greenhouse consisting of $N$ units, the following general calculation is used:

$$E_{PV\,year}(N) = E_{A1} + (2N-1) \times (E_{A2} + E_{A3}) + E_{A4}, \tag{3.11}$$

where $N$ is the amount of greenhouse units and $E_{PV\,year}$ the annual electricity production in $kWh$. In the greenhouse structure as discussed above, $N$ is 3. To determine the production per $m^2$, this $E_{PV\,year}$ is divided by the total area of the greenhouse:

$$E_{PV\,area}(N) = \frac{E_{PV\,year}(N)}{N \times 40 \times 8.8}, \tag{3.12}$$

where $E_{PV\,area}$ is the total PV energy production of the greenhouse in $kWh/m^2$. The numbers 40 and 8.8 are the dimensions of a single greenhouse unit in $m$ as displayed in figure 3.2. The same method can be applied to the checkerboard PV module configuration.

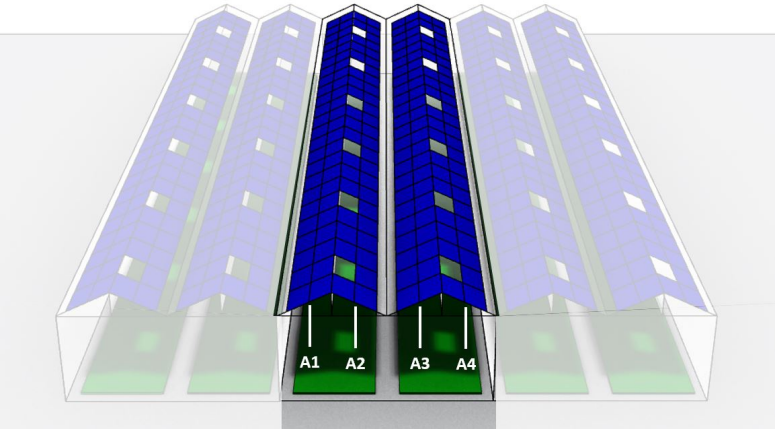


Figure 3.27: PV module arrays (A1, A2, A3, A4) on greenhouse unit

### 3.6.4. Efficacy

The efficacy is determined by dividing the amount of photons used by the amount of energy that is needed. The amount of photons used is given with $Photons_{year}$. The energy needed is determined with the following equation:

$$E_{total} = E_{suppl} + E_{Ventilation} + E_{Heating} + E_{Dehumidification} + E_{Lightcooling} - E_{PV\,year} \tag{3.13}$$

In this equation, all quantities are given in $kWh/m^2$. Subsequently, the efficacy is determined with:

$$Efficacy = \frac{Photons_{year}}{E_{total}} \tag{3.14}$$

The efficacy is given in $mol/kWh$.

## 3.7. Economic analysis

This section describes the approach for an economic analysis for the different scenarios. For this analysis, the system is divided into three main systems: the PV installation, the LED fixture and the crops. Firstly, the important factors per component are discussed. Subsequently, these factors are combined in a final analysis. The economic analysis gives as a result the costs of the total system per mol photons used for photosynthesis. The analysis is done for a time period of twenty years.

### 3.7.1. Crop production

Firstly, the production of crops per square meter is important for the different scenarios. This production can be calculated in kilogram crop produced per square meter, but because this price is fluctuative over time and as discussed in the previous sections the amount of kilograms produced is dependent on many factors, the crop production is expressed as the number of photons that are used for photosynthesis annually. It is assumed that this amount is the same for every year in the analysis and only takes into account the energy demand and production of the lighting system and the PV system, respectively.

### 3.7.2. Lighting system

In 2014, Nelson and Bugbee [80] presented an economic analysis in which they compared different lighting technologies for greenhouses. They analysed the costs of various lighting techniques over a period of five years. In the analysis done in this study, a period of twenty years is assumed to be able to also include the PV system in this analysis, which generally has a lifetime of around 25 years [163].

**Life expectancy**

The life expectancy is used to determine at which interval it is expected that the lamps need to be replaced. HPS lamps have a life expectancy of 10.000 hours to 90% survival [79, 80]. LED lights have a longer life expectancy than HPS lamps. When operated at the right conditions, LEDs have a predicted lifetime of up to 50.000 hours [79]. It depends on the scenario how intensively the lamps are used. For example, scenario 3 and 4 are covered with PV modules and are more dependent on LED lighting and therefore the LEDs are generally turned on for more hours per day. The life expectancy of the lighting system used in each scenario is determined by dividing the light expectancy of the lamp to 90% survival by the amount of hours the lamp is used per year. The result gives the number of years after which the lamps has to be replaced and therefore a new investment is needed. The amount of operating hours per year for the lamps are determined by dividing the total electricity demand for the lamps by the installed power.

**Lighting costs**

Furthermore, the investment costs of both lighting technologies are used in this analysis. The investment costs of LED fixtures are twice as high as HPS fixtures [164, 165]. In their analysis, Nelson and Bugbee (2014) used the costs per $Wp$, being 0.45 $euro/Wp$ for HPS and 1.31 $euro/Wp$ for LEDs. Eaves et al (2017) found comparable values for the LED lamps [166]. By using the maximum PPFD of the specific lamp and the efficacy of the light source, the installed power per square meter is found. Subsequently this rated power is multiplied with the costs per watt and the investment costs per square meter are found. In equation form, this looks like:

$$Cost_{Investment} = \frac{PPFD_{max}}{\eta} \times C, \tag{3.15}$$

where $Cost_{Investment}$ is the investment costs in $euro/m^2$, $PPFD_{max}$ the maximum photon flux the lamps need to deliver per square meter in $\mu mol/m^2 s$, $\eta$ the efficacy in $\mu mol/J$ and C the costs of the lamps per watt installed in $euro/Wp$.

Regarding the costs of electricity, an electricity price of 10 $cents/kWh$ is assumed [164]. This value is assumed to be constant over the years. Other variable costs are the maintenance costs. Nelson and Bugbee [80] show that the maintenance costs for both the HPS lamps as the LED fixtures are small. The yearly maintenance costs are small compared to the costs of electricity and can be better combined with the life expectancy of the lamps. It is assumed that the maintenance costs are comparable for both technologies in the different scenarios and for simplicity they are not taken into account in this analysis. To determine the annual costs for electricity, all energy consuming processes (as presented in tables 3.6,3.5 and 3.7) are taken into account. For heating, generally natural gas is used. Since the price per $kWh$ is lower for gas, the costs for heating is considered separately. The gas price for non-domestic consumers in the Netherlands in the first half of 2019 is taken, being 0.04 $euro/kWh$ [167].

### 3.7.3. PV system

The investment costs of a PV system can be divided into many parts. The PV modules are responsible for the highest share in the total costs. The other costs come from the balance of system and developer overhead. In 2018, NREL determined the costs of a PV system with an installed power between 100 and 200 kW to be 1.83 USD per Wattpeak [168]. Converting this to euro with the conversion rate in 2018, this is equal to 1.6 $euro/Wp$. It is assumed that scenario 3 and 4 use 327 Wp modules.

Besides the investment costs of the PV system, the system generates electricity. As discussed before, the electricity price is assumed to be 10 $ct/kWh$.

## 3.8. Conclusion

In this chapter, the following sub-question has been discussed: how can LED and PV technology arranged in a greenhouse system? In this chapter, four greenhouse scenarios have been designed to show how these technologies can be added to a greenhouse structure. The first scenario is a reference greenhouse that uses HPS lighting in addition to sunlight. The second scenario is comparable to the reference greenhouse, but uses LED lighting instead of HPS lighting. The third scenario is a greenhouse that uses LED lighting and also has a checkerboard PV array configuration installed on the roof. In this greenhouse, the amount of sunlight reaching the crops is reduced, but the LED lamps ensure a sufficient amount of light reaches the crops. Literature has shown that a checkerboard PV module configuration leads to the best homogeneous light distribution on the greenhouse floor. The fourth scenario is a greenhouse that is fully covered with PV modules and therefore no sunlight is able to enter the greenhouse. LED lamps are the source of light for the crops. In the third and fourth scenarios, c-Si PV modules are installed on the tilted roof of the greenhouse. It is assumed that the electricity produced by the PV systems is dumped on the grid. Besides that, the electricity needed for the systems driven by electricity, is drawn from the grid. There is no storage system present in these systems.

This chapter has also discussed the most relevant measures to quantify the performance of the different scenarios. The first measure is the energy consumption of the whole system, including the main energy demanding processes besides energy needed for lighting. The second measure is the crop production. This quantity is given in the number of photons used for photosynthesis by the crops annually. The third measure is the efficacy. This is the ratio between the production and energy consumption of a scenario. The fourth measure is the Land Equivalent Ratio, which say something about the cumulative productivity of a piece of land. The last measure is the costs of a scenario over time and gives an idea about what the expected costs are of a scenario over a period of twenty years. Both investment and variable costs are taken into account.

# 4

# Optimal greenhouse scenario

In this chapter, the results of the analysis for the different scenarios as described in the previous chapter is elaborated on. The sub-question that is discussed in this chapter is: what is the optimal LED-based agrivoltaic greenhouse design for different climates? Firstly, the results of the basic results of the analysis are given, being the PV production, the total energy consumption and amount of photons used for photosynthesis per scenario. The outcomes of the simulations are further analyzed and discussed using the performance indicators per location for the two crops, lettuce and tomato. Subsequently, the results of the economic analysis for both scenarios are discussed in detail.

## 4.1. Key findings

In this section, the main output parameters of the scenario simulations is presented. Firstly the PV energy production is described. Subsequently the energy use of each scenario is discussed and lastly the number of photons used in every scenario are elaborated on.

### 4.1.1. PV production

As discussed in the previous chapter, the greenhouse structure of each scenario consists of three units. By using equations 3.11 and 3.12, with N (greenhouse units) is equal to three, the annual PV production per $m2$ is found. In table 4.1, the energy produced by the PV modules for scenario 3 and 4 for Kiruna, Delft and Abu Dhabi is displayed.

Table 4.1: Annual PV production for scenario 3 and 4 in Kiruna, Delft and Abu Dhabi

| | **Annual PV production (kWh/m$^2$)** | | |
|---|---|---|---|
| | **Kiruna** | **Delft** | **Abu Dhabi** |
| **Scenario 3** | 64.3 | 82.4 | 156 |
| **Scenario 4** | 123 | 156 | 296 |

From this table, it can be concluded that for each location, the annual PV production for scenario 4 is approximately twice as high as the production of scenario 3. This is as expected since scenario 4 has approximately twice the number of PV modules compared to scenario 3. Furthermore, the energy production in Abu Dhabi for both scenarios is approximately twice as high as the production in Delft and 2.4 times as high as the production in Kiruna. The PV production is independent from the cultivated crop.

### 4.1.2. Energy consumption

In contrast with the PV production, the total energy consumption per scenario is dependent on the type of crop that is cultivated within the greenhouse. First, the energy demand for lettuce is discussed, followed by the energy needed for tomato.

**Lettuce**

Figures 4.1, 4.1 and 4.3 give the energy demand for the four scenarios in Kiruna, Delft and Abu Dhabi, respectively. The three bar charts each have two bars per scenarios. The left bar stands for the electricity needed

for supplemental lighting, while the right, lighter colored bar stands for the energy consumption of all energy demanding processes summed. It must be noted that the energy demand includes the production of PV energy (for scenario 3 and 4), which has a negative sign in the summation.

Comparing the three locations first, it can be concluded that for Kiruna and Delft, the energy needed for supplemental lighting is a significant part of the total energy use of the greenhouse for each scenario. In contrast to that, for Abu Dhabi, the lighting energy is responsible for only a small share in the total energy demand. This is because of two reasons. On the one hand, the amount of radiation throughout the whole year is high. In this way, the DLI is reached because of the amount of sunlight and little supplemental light is needed. On the other hand, since lettuce has a relatively low air temperature to grow optimally and the temperature in Abu Dhabi is generally significantly higher than this value, a significant amount of energy is needed for forced ventilation and dehumidification.

For Kiruna (figure 4.1), the energy demand for supplemental lighting is the highest for scenario 1 (the reference greenhouse). This can be explained by the fact that over the year, the amount of sunlight reaching the crops is low, because of the high latitude of Kiruna. This results in a high demand for supplemental lighting in order to reach the optimal DLI for lettuce. Because the HPS lamps used in scenario 1 have a lower efficacy than LEDs, the energy demand for lighting is higher for the reference greenhouse. Taking into account all energy consuming processes, one can see that the energy demand for the fully covered greenhouse has the highest energy demand. This is because for this scenario, the dehumidification of the internal climate is taken into account as well.

Comparing the greenhouse scenarios for lettuce in Delft (figure 4.2), the energy demand for lighting only is lowest for scenario 2 (LED) and 3 (LED and checkerboard PV configuration). This is because the LED lamps are more energy efficient than the HPS lamps (scenario 1) and as supplemental lighting source for sunlight, it has less running hours compared to the closed system in scenario 4. Adding the other energy sources as well, the same trend is visible: scenario 2 and 3 have the lowest energy consumption. The energy demand for scenario 2, that has more available sunlight and therefore needs less supplemental lighting, is in balance with the energy demand for scenario 3, which has less available sunlight (because of the PV modules), needs more energy for supplemental lighting, but also has PV energy production.

Shifting the focus to the greenhouse scenarios for lettuce in Abu Dhabi (figure 4.3), one can see that scenario 3 has a negative energy demand, when only taking into account the energy needed for lighting. On the one hand, this is because of the low amount of supplemental lighting needed due to the available sunlight, as in scenarios 1 and 2. On the other hand, scenario 3 also produces electricity with the integration of PV modules. Zooming out, also the total energy use of scenario 3 is the lowest of all. It can be concluded that scenario 4, that is fully covered with PV modules, by not making use of the abundantly available sunlight for crops, has the highest energy demand.

**Tomato**

This paragraph discusses the energy demand needed for the cultivation of tomato in greenhouses located in all three location. Figure 4.4, 4.5 and 4.6 show the results for Kiruna, Delft and Abu Dhabi, respectively. Since for the locations Kiruna and Abu Dhabi, no information was available for the energy demanding processes besides lighting, only the supplemental lighting energy needed is presented and discussed. In line with the results of lettuce, the amount of energy needed for supplemental lighting is highest for greenhouses in Kiruna.

In figure 4.4, it can be seen that scenario 1, with the HPS lighting, has the highest energy demand. This is because the HPS lamps have a lower efficacy than the LED lamps used in the other three scenarios. Furthermore, scenario 2 has a lower energy demand than scenario 3, while for lettuce the two scenarios where more in balance. This is because tomato has a higher DLI than lettuce, which means that tomato needs more light throughout the day than lettuce. For scenario 3, less sunlight reaches the crops because a part is blocked by the PV modules. The ratio between the electricity that is needed for supplemental lighting and the PV energy produced, is lower at higher DLI's.

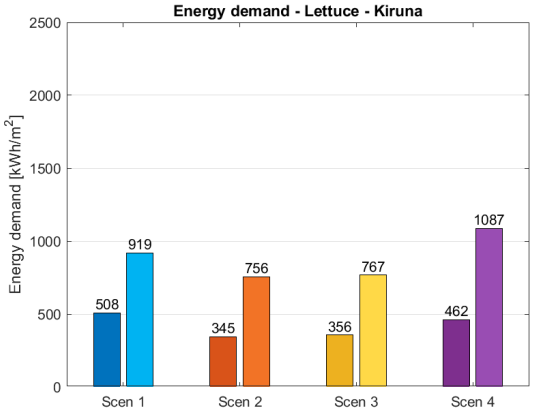


Figure 4.1: Annual energy demand of supplemental light (dark colored bars - left) and all energy demanding processes (light colored bars - right) for cultivation of lettuce in Kiruna

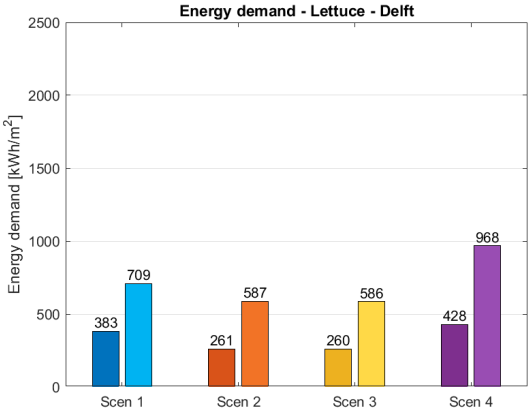


Figure 4.2: Annual energy demand of supplemental light (dark colored bar - left) and all energy demanding processes (light colored bars - right) for cultivation of lettuce in Delft

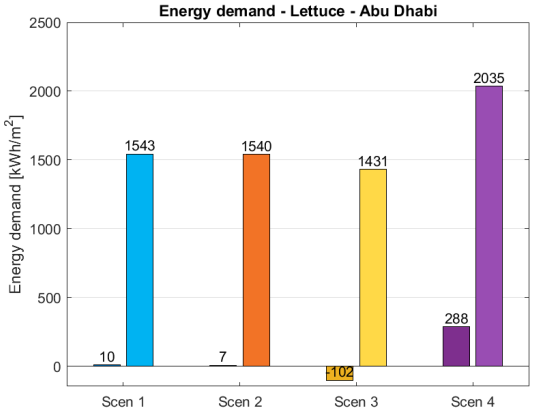


Figure 4.3: Annual energy demand of supplemental light (dark colored bars - left) and all energy demanding processes (light colored bars - right) for cultivation of lettuce in Abu Dhabi

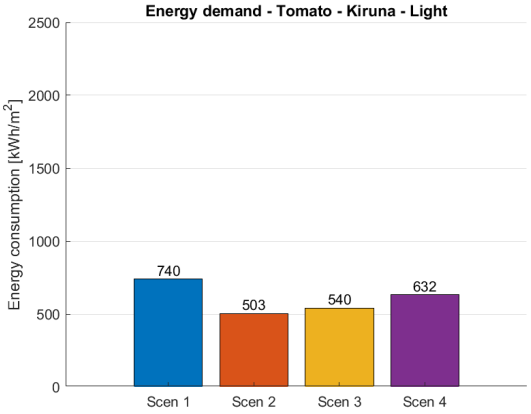


Figure 4.4: Annual energy demand of supplemental light for cultivation of tomato in Kiruna

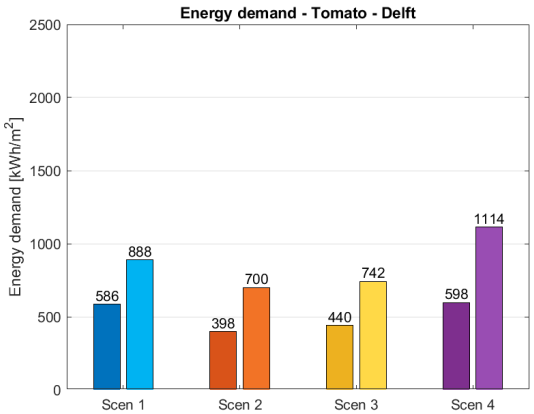


Figure 4.5: Annual energy demand of supplemental light (dark colored bars) and all energy demanding processes (light colored bars) for cultivation of Tomato in Delft

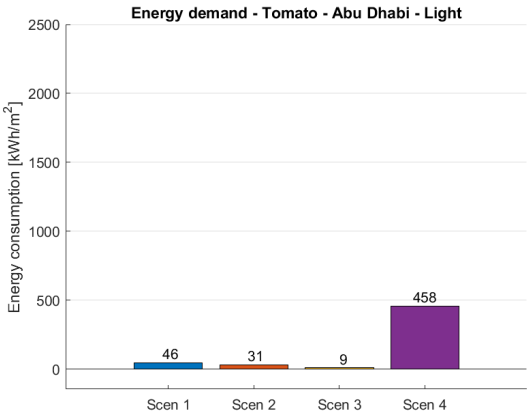


Figure 4.6: Annual energy demand of supplemental light for cultivation of Tomato in Abu Dhabi

For the cultivation of tomato in Delft (figure 4.5), scenario 1 and 4 have a comparable energy demand for supplemental lighting and the total energy demand. For scenarios 2 and 3, that both use as combination of sunlight and LED lighting, the total energy demand is lowest. In general, for the cultivation of tomato in Delft goes that the ratio between the energy demand for supplemental lighting are comparable to the ratio between the total energy demand for the different scenarios.

Focusing on the cultivation for tomato in Abu Dhabi, comparable to the cultivation of lettuce in Abu Dhabi, the energy needed for supplemental lighting for scenario 1, 2 and 3 is low compared to scenario 4. This is because the first three scenarios make optimal use of the available sunlight, while in scenario 4 the only source of light is LED lighting.

### 4.1.3. Crop production

Besides the amount of energy needed per scenario per location, the amount of crops produced in each scenario is an important measure. As discussed in the previous chapter, the amount of photons used for photosynthesis by the crop is used as a measure for the amount of crop production over a year. This section elaborates on the production per $m^2$ for both lettuce and tomato for the four greenhouse scenarios located in three different locations. First, the production for lettuce is discussed, followed by tomato.

**Lettuce**

In figures 4.7, 4.8 and 4.9, the amount of photons used for photosynthesis per $m^2$ for the four scenarios in the three locations are presented. Comparing the results of the three locations, it can be seen that the number of photons is the same for scenario 4 in all three locations. This can be explained by the fact that in this scenario, LED light is the only source of lighting. Furthermore, on average, the amount of photons used is highest for the scenarios in Kiruna and lowest for the scenarios in Abu Dhabi. This is because less sunlight is available for the greenhouses in Kiruna and therefore more supplemental lighting is needed. As shown in figure 3.20 in the previous chapter, the spectral output of the supplemental lighting is used more efficiently by the crops than sunlight. In contrast to Kiruna, for the scenarios in Abu Dhabi, sunlight is the main source of light for scenarios 1, 2 and 3 and therefore the photon utilization is relatively low.

When focusing on the differences between the scenarios of one location, it becomes clear that the more a greenhouse makes use of artificial lighting, the higher the amount of photons used per $m^2$ per year. To be more concrete, the increase of the production of scenario 4 compared to the reference greenhouse is 48% in Kiruna. For Delft this percentage increase is 59%. The most significant increase in crop production is found for Abu Dhabi, namely 176%.

**Tomato**

Figures 4.10, 4.11 and 4.6, show the amount of photons used for photosynthesis per $m^2$ for Kiruna, Delft and Abu Dhabi, respectively. Compared to lettuce, the photons used for photosynthesis is generally higher for tomato. This is because the DLI of tomato is higher and therefore the total amount of light reaching the crops over a day. The trends as seen in the results for lettuce are also visible here. Again, the number of photons used in scenario 4 for each location is the same. Besides that, the higher the share of sunlight is compared to artificial lighting, the less photons are used per $m^2$. The percentage increase between the reference greenhouse and scenario 4 is 63%, 72% and 153% for Kiruna, Delft and Abu Dhabi, respectively.

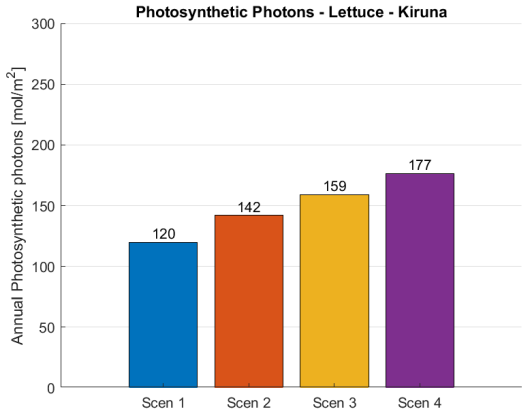


Figure 4.7: The amount of photons used for photosynthesis annually for lettuce in Kiruna

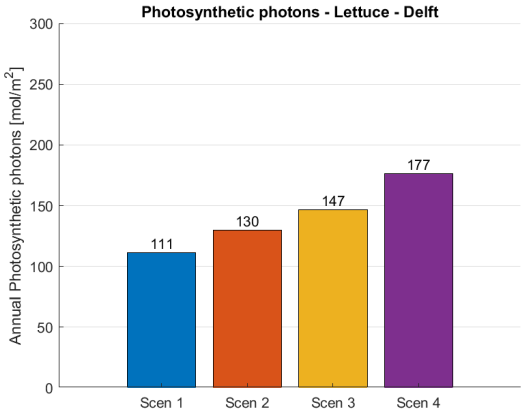


Figure 4.8: The amount of photons used for photosynthesis annually for lettuce in Delft

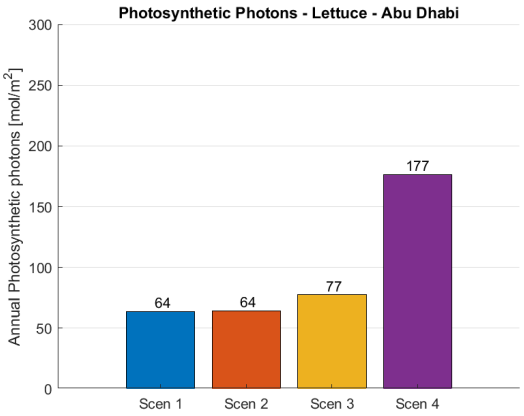


Figure 4.9: The amount of photons used for photosynthesis annually for lettuce in Abu Dhabi

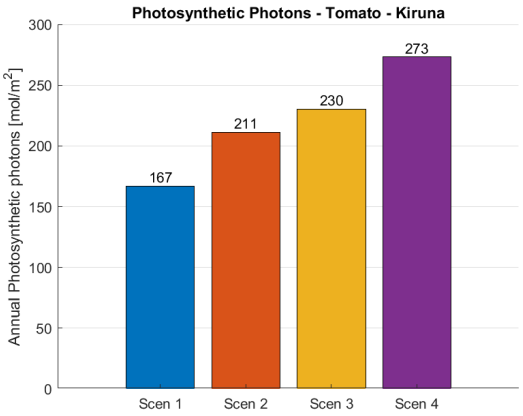


Figure 4.10: The amount of photons used for photosynthesis annually for tomato in Kiruna

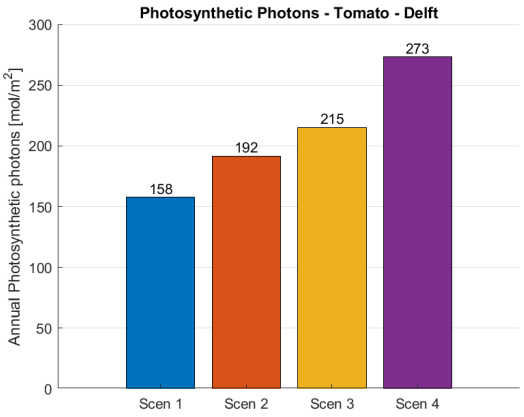


Figure 4.11: The amount of photons used for photosynthesis annually for tomato in Delft

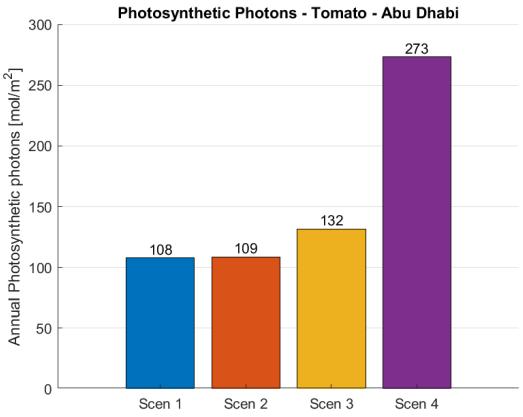


Figure 4.12: The amount of photons used for photosynthesis annually for tomato in Abu Dhabi

## 4.2. Performance indicators

In this section, the results discussed in the previous paragraphs, the *energy demand* and the *crop production*, are used to determine the *efficacy* and the *Land Equivalent Ratio* for each scenario in each location.

### 4.2.1. Efficacy

The efficacy of a greenhouse system is determined by dividing the amount of photons used for photosynthesis by the energy use of the system. Also the efficacy is subdivided in the efficacy with the energy needed for supplemental light and the efficacy with the total energy needed for the system. First the results for lettuce are discussed and subsequently the results for tomato.

**Lettuce**

The efficacy results for Kiruna, Delft and Abu Dhabi are shown in figures 4.13, 4.14 and 4.15. The dark bars (left bar of each duo of bars) show the efficacy for each scenario only taking into account the energy needed for supplemental lighting. The light colored bars (right bar of each duo of bars) shows the efficacy of the systems by taking into account all energy demanding processes.

In figure 4.13, the efficacy for the four scenarios in Kiruna is shown. For both types of efficacies, the ratio between the scenarios is the same and scenario 3 (checkerboard PV) has the highest efficacy. A relatively low energy consumption and a relatively high number of photons used results in the highest efficacy of the system. Furthermore, it can be concluded that the reference greenhouse has the lowest efficacy of all scenarios. The efficacy of scenario 3 is 1.62 times higher than that of the reference greenhouse. The fact that HPS lamps have a lower conversion efficiency and that the spectrum of light is used less efficiently than the spectrum of LEDs, the system has a high energy demand and lower photon usage, respectively.

Comparable results are found for the scenarios in Delft, as shown in figure 4.14. Again the system with the highest efficacy is scenario 3, with the checkerboard PV module setup installed on the roof. The efficacy of this scenario is 1.56 times higher than the efficacy of the reference greenhouse. When comparing the efficacy of Delft with Kiruna, it can be seen that the efficacy of each scenario is higher in Delft than the efficacy of the same scenario in Kiruna. While the amount of photons used for photosynthesis is higher in Kiruna than in Delft, the energy use is also higher. The difference in energy use is higher than the difference in amount of photons used, resulting in an efficacy that is -on average- higher in Delft.

Regarding the efficacy for the cultivation of lettuce in Abu Dhabi, the results are not comparable to the locations Kiruna and Delft, as can be seen in figure 4.15. Regarding the efficacy that only takes into account the energy needed for supplemental lighting, the results are significantly different for the scenarios. Firstly, the efficacy for scenario 1 and 2 is high. This is mainly caused by the low amount of energy needed by the lamps annually. Besides that, for scenario 3 the efficacy is negative. This is because the energy needed for supplemental lighting is negative, as shown in figure 4.3 because of the PV energy production. Based on these efficacies, it can be concluded that for this location, the efficacy that only takes into account the energy needed for the supplemental light, is not a good measure. The efficacy that takes into account all energy demanding processes, however, gives more comparable results. The effect of the low energy need for supplemental light is less strong because of the high energy demand of the other processes. In Abu Dhabi, the efficacy of scenario 4 is the highest of the four scenarios and is 2.12 times higher than the efficacy of the reference greenhouse.

**Tomato**
The efficacy for tomato for the different locations and scenarios is shown figures 4.16, 4.17 and 4.13. Because the data for other energy demanding processes for the cultivation of tomato in Kiruna and Abu Dhabi, only the efficacy taken into account the energy needed for supplemental lighting is shown. As visible in figure 4.16, the efficacy for scenario 2, 3 and 4 is comparable. Compared to the reference greenhouse, these three scenarios perform significantly better when it comes to efficacy. While the photons used and the energy needed for supplemental lighting for the three scenarios vary significantly, as visible in figures 4.4 and 4.10, the efficacies are approximately the same.

Furthermore, the ratio of the efficacy of the scenarios taking into account only the supplemental lighting and the ratio of the efficacy of the scenarios including all energy demanding processes for the cultivation of tomato in the different systems are comparable. However, for the efficacy with the supplemental light energy, scenario 3 is most efficient, while taking into account the other energy processes as well, scenario 2 has the highest efficacy. Besides that, the efficacies taking into account all energy demanding processes, are closer to each other for all scenarios than the efficacies with only the supplemental lighting. Assuming this trend is comparable for the scenarios in Kiruna, the difference between scenarios 1, 2, 3 and 4 becomes less significant.

Finally, the efficacy of the scenarios for the cultivation in Abu Dhabi. The efficacy for scenario 3 is significantly higher than the other scenarios. This is mainly caused by the low energy demand, as a results of the low amount of supplemental light needed and the PV energy that is produced. Besides that, the efficacy for scenario 4 is relatively low compared to the other three scenarios. This is caused by the relatively high amount of energy needed for supplemental lighting in this scenario, compared to the other scenarios.

Overall, it can be concluded for the cases that the amount of energy needed for supplemental lighting is almost negligible compared to the energy needed for the other processes, the efficacy that only takes into account the energy for supplemental lighting, does not give results that are representative for the total system. This is mainly the case for the scenarios in Abu Dhabi, where the amount of supplemental lighting needed is low.

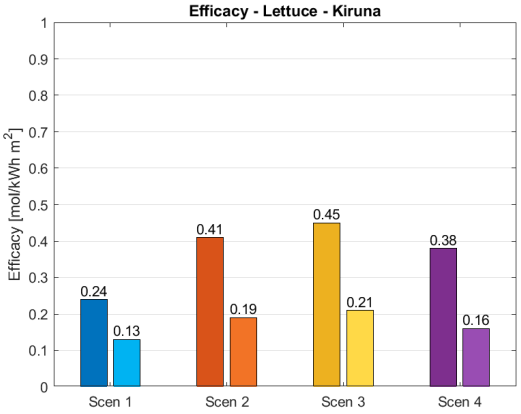


Figure 4.13: The efficacy including only the supplemental lighting energy (dark colored bar) and the efficacy including the total energy demand (light colored bar) for lettuce in Kiruna

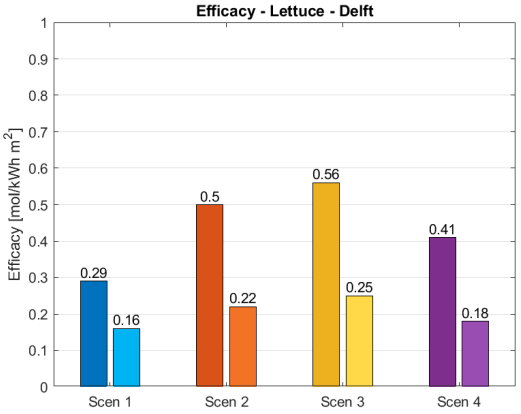


Figure 4.14: The efficacy including only the supplemental lighting energy (dark colored bar) and the efficacy including the total energy demand (light colored bar) for lettuce in Delft

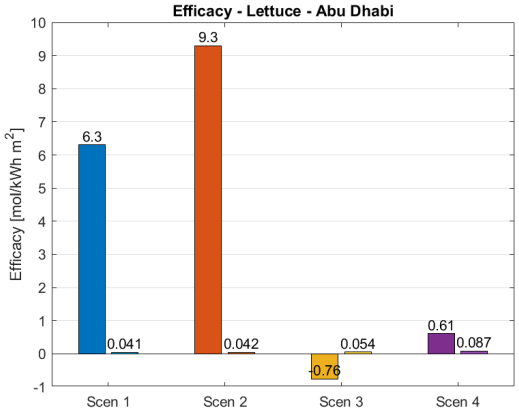


Figure 4.15: The efficacy including only the supplemental lighting energy (dark colored bar - left) and the efficacy including the total energy demand (light colored bar - right) for lettuce in Abu Dhabi

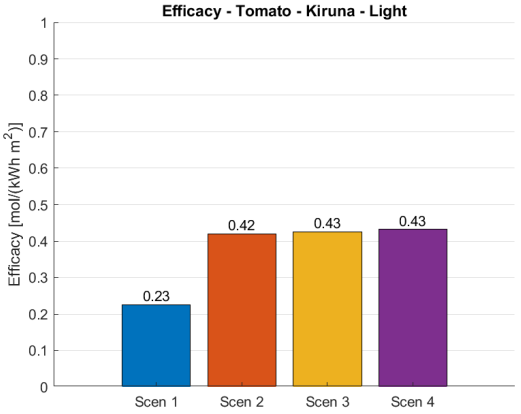


Figure 4.16: The efficacy including only the supplemental lighting energy for tomato in Kiruna

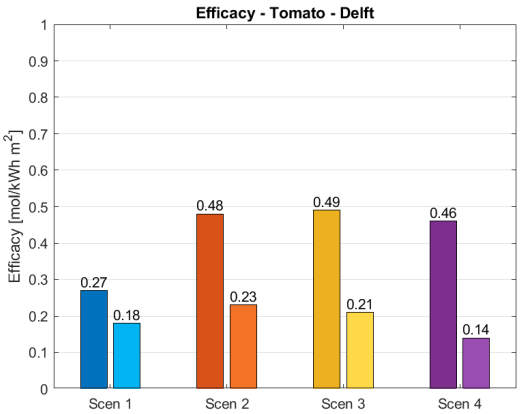


Figure 4.17: The efficacy including only the supplemental lighting energy (dark colored bar - left) and the efficacy including the total energy demand (light colored bar - right) for tomato in Delft

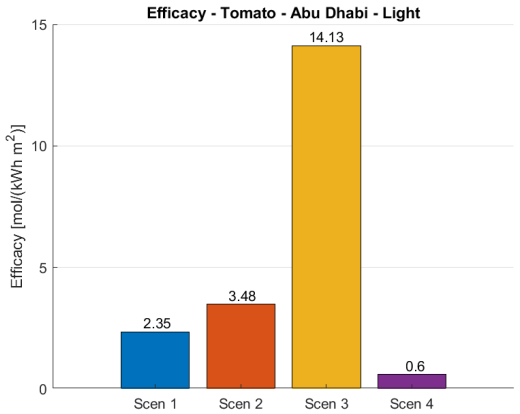


Figure 4.18: The efficacy including only the supplemental lighting energy for tomato in Abu Dhabi

### 4.2.2. Land Equivalent Ratio

The Land Equivalent Ratio (LER) is, in contrast with the measures discussed before, not dependent on the crop cultivated. As discussed in equation 1.6 in the literature review, to determine the LER, four quantities are important, namely: the crop production in an agrivoltaic system ($Y_{AV-crop}$), the crop production of an area only used to harvest crops ($Y_{mono-crop}$), the electricity production in an agrivoltaic system ($Y_{AV-electricity}$) and the electricity production of an area only used to produce electricity with PV modules ($Y_{mono-electricity}$). The ratio between $Y_{AV-crop}$ and $Y_{mono-crop}$ is assumed to equal one for each scenario, since for each scenario makes use of supplemental lighting. Because of this, the optimal DLI for each crop is assured, resulting in the maximum possible production for the specific system. The electricity production by the PV systems present in scenario 3 and 4, the results of the simulation is used as a value for ($Y_{AV-electricity}$). As discussed in the previous chapter, ($Y_{mono-electricity}$) is determined using a radiation simulation applied on an area equal to the area of a greenhouse fully covered with PV modules.

As can be concluded, the LER value of the scenarios is only changed by the implementation of a PV system. Figures 4.19, 4.20 and 4.21 show the LER for the scenarios in Kiruna, Delft and Abu Dhabi, respectively. The LER values for the scenarios for the different locations are almost equal. Scenario 4 has a higher LER than scenario 3 because for the same area, scenario 4 has more PV modules. The small difference between the value for both scenario 3 and 4 for the different locations, is caused by the different amount of global radiation for each location.

In general, it can be concluded that the LER for scenario 3 and 4 is significantly higher than the reference scenario 1 and scenario 2. With a LER higher than 1.8, it means that the overall productivity for a specific piece of land is the highest for scenario 4 in all locations.

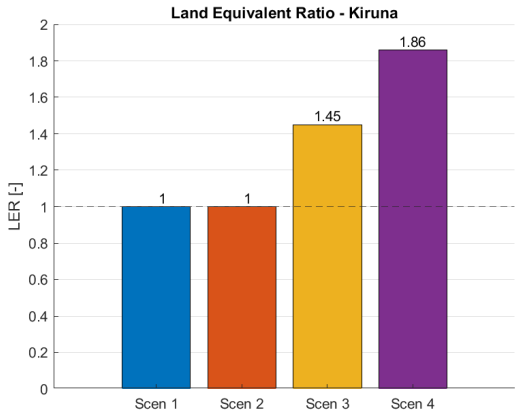


Figure 4.19: Land Equivalent Ratio for the scenarios in Kiruna

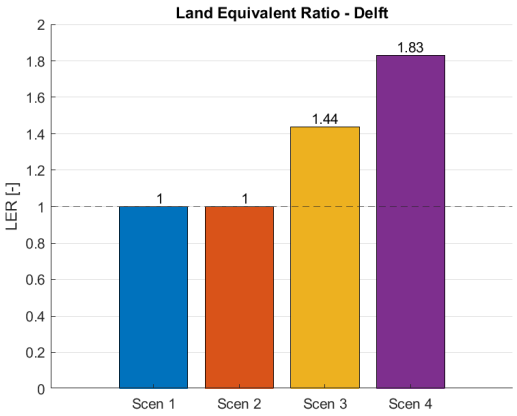


Figure 4.20: Land Equivalent Ratio for the scenarios in Delft

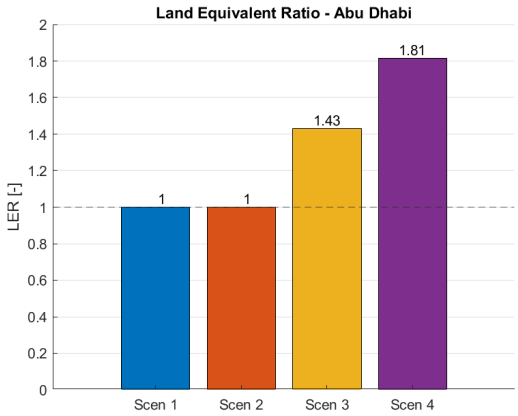


Figure 4.21: Land Equivalent Ratio for the scenarios in Abu Dhabi

## 4.3. Economic analysis

This section describes the results of the economic analysis. Tables 4.2 and 4.3 show the costs of the lighting fixture per $m^2$ for lettuce and tomato, respectively. It can be seen that for both crops, the costs are approximately twice as high per $m^2$ for the LED fixture compared to HPS fixtures, which is in line with the results found in literature [164, 165].

Table 4.2: Costs per light system for the different scenarios for the cultivation of lettuce

| Scenario | Installed Power (W/m$^2$) | Costs technology (euro/Wp) | Light fixture costs (euro/m$^2$) |
|---|---|---|---|
| **1** | 117 | 0.45 | 52.94 |
| **2** | 80 | 1.31 | 104.8 |
| **3** | 80 | 1.31 | 104.8 |
| **4** | 80 | 1.31 | 104.8 |

Table 4.3: Costs per light system for the different scenarios for the cultivation of tomato

| Scenario | Installed Power (W/m$^2$) | Costs technology (euro/Wp) | Light fixture costs (euro/m$^2$) |
|---|---|---|---|
| **1** | 224 | 0.45 | 101 |
| **2** | 152 | 1.31 | 200 |
| **3** | 152 | 1.31 | 200 |
| **4** | 152 | 1.31 | 200 |

The analysis is done for both crops, lettuce and tomato. For tomato, this analysis is only done for Delft, since the data for the energy demanding processes besides energy needed for lighting is not available. The results for lettuce are shown in figures 4.22, 4.23, 4.24, for Kiruna, Delft and Abu Dhabi, respectively. The trends for the four scenarios are in $euro$ per $mol$ photons used for photosynthesis. In all figures, the starting point of each scenario is the investment costs for the light fixture and PV system (for scenarios 3 and 4). The gradient of the line is determine by costs for electricity and heating energy per scenario. The stairs in each line are the costs needed to replace the lighting fixture. The interval at which this replacement needs to happen is dependent on the expected lifetime of the light fixture and the amount of operating hours per year.

Figure 4.22 shows that for the cultivation of lettuce in Kiruna, the relative investments costs are the lowest for the reference greenhouse. However, after eight years approximately, the cumulative costs for each of the other three scenarios is lower than that of the reference greenhouse. This is mainly caused by the relatively high energy consumption and low amount of photons used for photosynthesis annually for the reference greenhouse. The greenhouse scenario with LED lighting (red line) and the scenario with LED lighting and checkerboard PV module configuration (yellow line) have the lowest cumulative costs after 20 years for lettuce in Kiruna. The same conclusions can be drawn for the cultivation of lettuce in Delft, as shown in figure 4.23. However, the total costs after twenty years is slightly lower for each scenario compared to the scenarios in Kiruna. This is because there is less sunlight throughout the year in Kiruna and therefore there is more supplemental lighting needed.

For the greenhouses in which lettuce is cultivated in Abu Dhabi, the trends are different, as visible in figure 4.24. The investment costs are still the lowest for the reference greenhouse and it takes approximately 3.5 years for scenario 2 (red line) and 3 (yellow line) to become more economically beneficial than the reference case (blue line). Because of the low amount of supplemental lighting that is needed in Abu Dhabi to reach the optimal DLI for lettuce, the lighting fixtures do not reach the end of life and therefore do not have to be replaced within the 20 years for scenario 1, 2 and 3. Scenario 3 (yellow line), with the checkerboard PV module configuration on the roof, performs better economically seen, mainly because of the extra energy it produces with the PV modules. The effect of the PV modules on the economical trend is even higher for scenario 4 (purple line), which has a roof fully covered with PV moduels. The combination of a high number of photons used (because of the LED lamps) and the high PV energy production, results in this system having the lowest cumulative costs per photon used after 20 years, despite that the LED fixture has to be replaced twice during the 20 years.

For the cultivation of tomato in Delft, the trends are comparable to the cultivation of lettuce in Delft. However, the relative cumulative costs for scenario 3 (yellow line) stay higher than those for scenario 2 (red line) for the total period of 20 years. This is mainly because tomato has a higher DLI than lettuce and therefore in scenario 3, with the checkerboard PV module configuration, the effect of the reduced amount of sunlight weights stronger.

In general, this economic analysis shows that the reference greenhouse is economically the worst system over a period of 20 years in Delft and Kiruna. In these locations, where the sunlight throughout the year is not sufficient for the crops, the lighting technique used makes a significant economic difference on the long term. The cumulative costs over 20 years for the LED fixture that have a higher efficacy and better spectrum for the crops, are significantly lower than the HPS lights, despite the higher investment costs. On the other hand, at a location where there is a lot of sunlight available and therefore an almost negligible amount of supplemental light needed, as in Abu Dhabi, the economic difference for the different lighting techniques disappears. In locations like this, however, the electricity cost savings because of the PV modules present, is significant. So for Abu Dhabi, it is economically more beneficial to integrate PV modules in the design.

In case one is considering the refurbishment of a reference greenhouse to a greenhouse with LED lighting and possibly PV modules on the roof, it can be concluded that the change to LED lighting (and PV modules) is economically a better investment after a couple of years, depending on the system. Even if the investment costs for the reference greenhouse are removed at 0 years, the other three scenarios are a better economical solution over 20 years (for scenarios 2 and 3 the economic crossing point is even earlier).

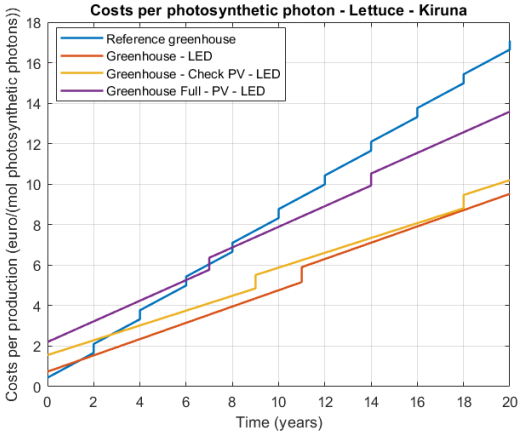


Figure 4.22: Cost per amount of photons used for photosynthesis for lettuce in Kiruna

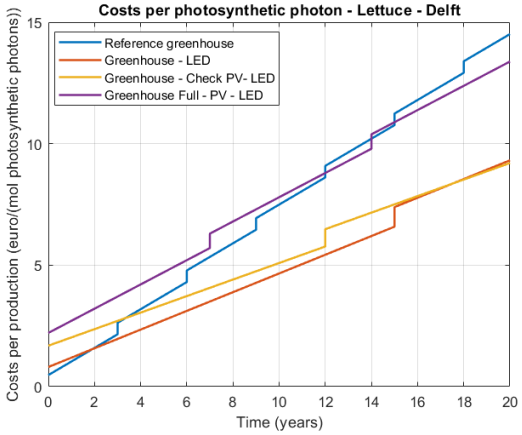


Figure 4.23: Cost per amount of photons used for photosynthesis for lettuce in Delft

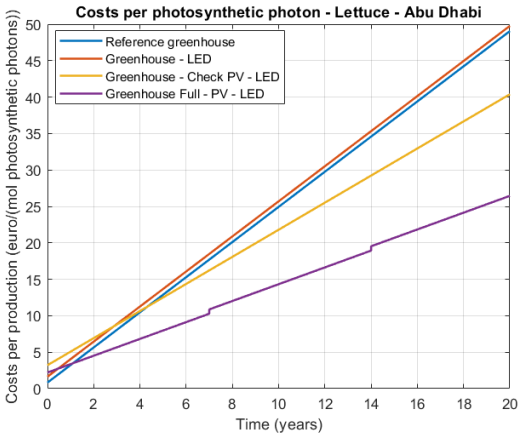


Figure 4.24: Cost per amount of photons used for photosynthesis for lettuce in Abu Dhabi

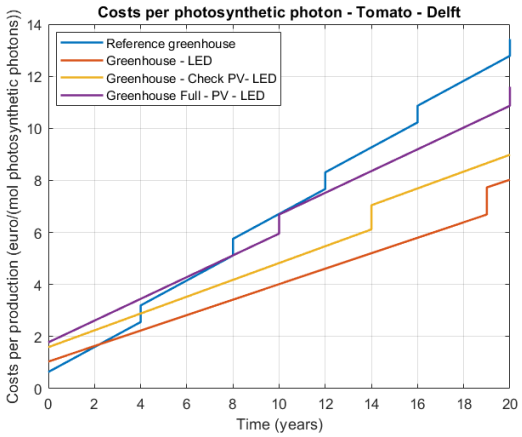


Figure 4.25: Cost per amount of photons used for photosynthesis for tomato in Delft

## 4.4. Conclusion

The question that has been discussed in this chapter was: what is the optimal LED-based agrivoltaic greenhouse design for different climates? To answer this question, the performance of the four scenarios has been analyzed for the locations Kiruna, Delft and Abu Dhabi and for the crops lettuce and tomato. The main conclusion that can be drawn from the results discussed in this chapter is that it is dependent on the location, which greenhouse scenario is the optimal design. But first of all, the purpose of the greenhouse at a specific location is of importance. When the purpose of a greenhouse is to make productivity per square meter as high as possible, the optimal scenario is different than for the case both productivity and energy consumption are important. The optimal scenarios for the various purposes are described in the following subsections.

### 4.4.1. Productivity

When the purpose of a greenhouse is to have the highest productivity per specific piece of land and the energy consumption is of less importance, the greenhouses which use LED technology and have PV modules (scenario 3 and 4) are the best systems for each location. Important measures for the productivity are the amount of photons used for photosynthesis per year and the Land Equivalent Ratio (LER) of a design. For all locations and both crops, scenario 4, that has a roof fully covered with PV modules and the only source of light is the LED lighting system, is the system with the highest crop productivity per $m^2$. Also the cumulative relative productivity (LER) is the highest for each location and for each crop. However, in this conclusion for this purpose, the energy consumption per scenario is not taken into account. This is discussed in the following paragraph.

### 4.4.2. Energy & productivity

For the case when both the productivity per area and the energy consumption are important, the efficacy is a more relevant measure to use. This measure takes into account both the crop production as the energy consumption of a scenario. In both Kiruna and Delft, for lettuce, the crop production per $kWh$ is the highest for scenario 3. This greenhouse scenario uses LED technology and has a checkerboard PV module configuration on top of the greenhouse roof. For the cultivation of lettuce, the efficacy of scenario 3 is 1.6 times higher than the reference greenhouse in both locations. For Abu Dhabi, the fully covered greenhouse has the highest efficacy for the cultivation of lettuce. The differences in efficacy for the cultivation of tomato in Kiruna and Delft are less significant among scenarios 2, 3 and 4.

### 4.4.3. Costs

This paragraph describes the main conclusion for the economically best scenarios, while also taking into account the crop production and the energy consumption of the scenarios. At locations where there is little supplemental light needed due to the large amount of sunlight available throughout the year, greenhouse scenario 4 is economically the best choice. For locations like Abu Dhabi goes: the larger the part of the roof covered with PV modules is, the lower the costs per crop production are over time. For locations where the amount of supplemental lighting needed is significant, both scenario 2 and 3 have the lowest costs per crop produced over a period of 20 years. This goes for both lettuce and tomato.

## 4.5. Discussion optimal greenhouse scenario

In the previous section the conclusion regarding the optimal greenhouse design is discussed. In this section, the sensitivity of the results are tested by varying significant parameters. Then the approach and the reliability of the conclusions of the optimal greenhouse scenario analysis are discussed.

### 4.5.1. Sensitivity analysis

The parameters that have a significant influence on the sensitivity of the results are discussed in this section. In this section, the effect of the greenhouse glass transmission, LED efficacy, the photosynthetic rate, the PV energy production and the other energy demanding processes is tested.

#### Glass transmission

The first parameter that is tested for sensitivity is the light transmission of the greenhouse glass. It has been assumed that the transmission of the glass has an average value of 70%. However, literature shows that this value is conservative [132] and that it is not unlikely for the transmission to be 80% on average. This increase

does not have an effect on the performance of scenario 4, since LED lighting is the sole source of light for the crops. Increasing the transmission results in that less supplemental lighting is needed and therefore the energy demand decreases. When increasing the transmission by 14.2% from 70% to 80%, the efficacy of scenario 1, 2 and 3 for lettuce in Delft increases by 2.4%, 0.8% and 0.6%, respectively. For Abu Dhabi and Kiruna, the increase of the efficacies is comparable small.

**LED efficacy**

The second parameter that plays an important role is the efficacy of the light fixtures that are assumed. In the model, the efficacy of the whole LED system is taken as 2.5 $\mu mol/m^2 s$. When reducing this efficacy to 2.0 $\mu mol/m^2 s$, the results for scenario 2, 3 and 4 change. However, this significant reduction, does still lead to the same conclusion regarding the optimal greenhouse system for all three locations for the both crops. By decreasing the LED efficacy with 20% (from 2.5 to 2.0) the total energy demand for scenarios 2, 3 and 4 increases with 11.0%, 14.5% and 15.1%, respectively for the lettuce in Delft. This strong correlation is because the lighting system has a significant share in the total energy demand for Delft and the efficacy of the LED determines the energy demand for the light. The efficacy of the total greenhouse system in Delft decreases with 9.1%, 12.0% and 11.1% for scenario 2, 3 and 4, respectively.

**Photosynthetic rate**

An important parameter for the crop production is the rate of photosynthesis. In the model, it is assumed that the photosynthetic rate of the crops is the highest for the LED light and the lowest for sunlight. To check the effect of the photosynthetic rate on the final results, in this sensitivity analysis it is assumed that the photosynthetic rate over the PPFD is equal for all light sources. This is visualized in figure 4.26. The trends for sunlight and the HPS light take the trend of photosynthetic rate of the LED light. By doing this, the advantage of the LED spectrum regarding the photosynthetic efficiency is taken away. The resulting efficacy of the different scenarios for lettuce in Delft is shown in figure 4.27. Comparing this figure with the results shown in figure 4.14, it can be concluded that the efficacy of each scenario increases significantly. This is because the photosynthetic rate as a result of sunlight is significantly higher. It can be concluded that also when removing the effect of the spectrum of the specific light sources on the photosynthetic rate, the efficacy of scenario 3 (checkerboard PV module configuration) is still the highest.

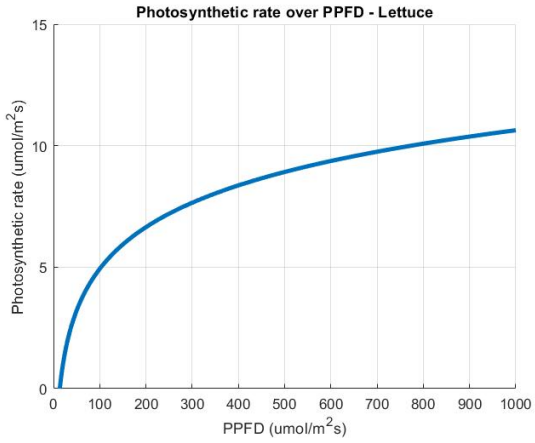


Figure 4.26: Photosynthetic rate versus the PPFD for lettuce

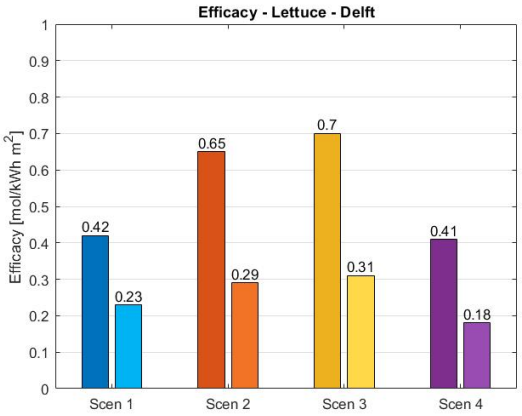


Figure 4.27: Efficacy of different scenarios at equal photosynthetic rates for all light sources

**PV energy production**

To test the effect of the PV energy production on the analysis results, the efficiency of the PV modules is decreased from 20% to 15%. For the cultivation of lettuce in Delft, this 25 % decrease leads to a 4.0% and 3.9% decrease in the efficacy of scenario 3 and 4 respectively. For Delft, a change in PV production does not have a strong effect on the efficacy. Executing the same sensitivity analysis on the scenarios in Abu Dhabi, a decrease of 2.7% and 3% is found. The decrease for Abu Dhabi is less significant compared to Delft, because the total energy demand is higher for the greenhouses in Abu Dhabi. The decrease in efficacy found for Kiruna is negligible.

**Other energy demanding processes**
In the analysis, a subdivision is made with the results that only take into account the energy needed for lighting and the results that take into account all significant energy demanding processes. This subdivision already tests the effect of adding other energy consuming processes. As discussed, the ratios between the results for the different scenarios is comparable for the "light energy" and "all energy" analysis. This is mainly caused by the fact that the energy needed for artificial lighting has a large share in the total energy demand, especially in Kiruna and Delft. Besides that, as discussed in section 3.5, the assumptions regarding the amount of energy needed for the processes besides lighting, are conservative for the scenarios that have the best performance with respect to the assumptions made for the reference greenhouse.

### 4.5.2. Discussion and improvements

This section discusses the approach used to find the results and the results of the analysis themselves. First of all, in this analysis the crop production is measured in the amount of photons used for photosynthesis annually. The rate of photosynthesis is an important measure for plant growth. However, the plant growth is dependent on other factors as well. A better measure to quantify the crop production would be to use structural (e.g. sucrose, starch glucose) and non structural (e.g. cell walls, cytoplasm) dry weight. To determine this, the model described by Van Henten (1994) [169] could be used. Furthermore, data for the other energy demanding processes is retrieved from different studies. However, data for a system that uses both supplemental lighting and PV modules on top of the greenhouse, is not available. A first step to model the energy dynamics within the greenhouse more accurately could be to use KASPRO [170]. KASPRO is an advanced, dynamic model to calculate the climate in greenhouses based on the energy and mass balance of greenhouse elements. However, the effect of PV modules on the greenhouse climate is not taken into account in KASPRO.

At the moment, the model used to determine the performance of the different scenarios assumes that the illuminated crop area is fully covered with crops. As discussed, in reality, this would have to mean that the crops are frequently rearranged to guarantee a fully covered area. This means that it is likely that more light and therefore energy is wasted by not reaching the plants. Besides that, the model uses an overhead lighting system. For crops that mainly grow in the vertical direction, the lower leaves receive significantly less light than the leaves on top. This effect is neglected in this model.

Furthermore, in this study, the different scenarios are tested for two types of crops and three locations with a significant different climate. The main conclusion that goes for all variables is that scenario 2, 3 and 4 perform better than the reference greenhouse. It is expected that this conclusion can be drawn for various crops and different locations worldwide. However, to what extent which greenhouse scenario performs best will depend on the type crop and the climate of the location. More data and additional models are needed to accurately determine this. Besides that, in this study, a Venlokas with specific dimensions is assumed. The PV system configuration is based on the dimensions of this structure. However, not all greenhouses with a Venlokas configuration have the same dimensions. Using a greenhouse structure with different dimensions potentially changes to configuration of the PV arrays on top of the greenhouse. However, for all locations, the efficacy of scenario 2 (only LED) and scenario 3 (checkerboard PV module configuration and LED) was higher than the reference greenhouse and scenario 4 (fully covered with PV modules). From these results it can be concluded that the optimal design of a greenhouse, with other dimensions than the greenhouse structure assumed in this research, would be in between scenario 2 and 3. In case the different structure does not allow for the same checkerboard PV module configuration because it is smaller in size, a PV configuration in which (less than) half of the greenhouse is covered in combination with LED lighting would be the most optimal greenhouse design. It is important, however, that the homogeneity of sunlight falling on the crops over a day is assured with this PV coverage. For a greenhouse with larger dimensions, the PV configuration could be extended or the same number of PV modules can be used, but with a larger spacing between the modules. In both cases it is expected that the design will have a better efficacy than the reference greenhouse.

Furthermore, the factor used to determine the amount of global radiation that reaches in scenario 3 (with the checkerboard PV configuration) could be more accurate. A value of 0.65 was found using daily integrals. By assuming a constant value, an average is taken between the direct and diffuse radiation. At moments when a square meter receives more direct radiation than diffuse radiation, the value of 0.65 results might result in an overestimation of the photosynthetic rate of the plant at this specific moment in time. This is because crops absorb and use photons more efficiently at a low PPFD, as shown in figure 3.20. A more accurate approach

would be to create a grid on the greenhouse floor (crop level) and determine the hourly radiation reaching each element for every hour of the year. Using the amount of radiation for an average element for every hour as an input to determine the photosynthetic rate per hour, would be a more reliable approach. For even more realistic results, the direct radiation and diffuse radiation could be separated.

Another factor that could be made more accurate is the light transmission of the greenhouse glass. In the model, the average value of 70% is assumed. However, the transmission of light through a medium is dependent on the angle of incidence of the light beam. By assuming a value of 0.7 for every angle of incidence, for a moment with high intensity radiation with a low angle of incidence, the amount of radiation that reaches the crops at a specific moment is underestimated. The relation between the angle of incidence and the light transmission for a specific type of glass is shown in figure 4.28. By using this relation in the simulation, the amount of radiation that reaches the crops can be determined more accurately. In order to use this relation the altitude of the sun is needed for every hour of the year for each analysed location.

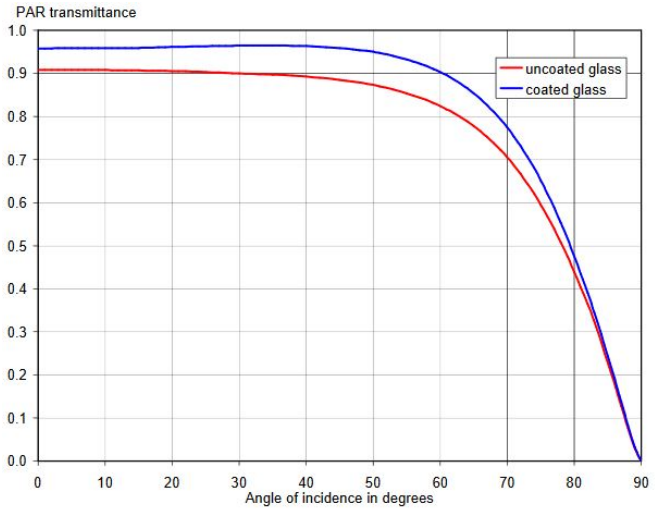


Figure 4.28: Relation between the transmission of coated and uncoated glass and the angle of incidence of the incoming light

Lastly, the economic analysis executed for the different greenhouse scenarios can also be improved. The analysis assumes a constant electricity and gas price over time. More detailed energy cost (prediction) data could be used to get a more realistic result. However, due to the higher energy demand in the reference greenhouse, it is still expected that after a period of 20 years, the cumulative costs for the other scenarios are lower. In case the energy price decreases, the moment at which the scenarios with the higher investment costs cross the line of the reference greenhouse, becomes later in time. With higher energy prices, scenarios 2, 3 and 4 become a better economical choice even faster. Furthermore, in this analysis the earnings of the produced crops are not taken into account. Additional data would be needed to predict the price of lettuce and tomato over time. Including this parameter in the analysis would allow for an estimation of the payback time of each system.

# 5

# Plant factory

In the previous chapter the performance of four greenhouse scenarios was analysed for three locations and two types of crops. In this chapter, another system for crop cultivation is described, namely: the plant factory. The research question that is discussed in this chapter is: what is the potential of plant factories compared to greenhouses? This question is worked out for the crop lettuce.

First, the main characteristics of a plant factory are discussed and the difference with greenhouses is elaborated on. Subsequently, the design and yield of a PV system on the plant factory roof is described. Then, the performance of the plant factory is analysed and compared with the performance of the greenhouse scenarios described in the previous chapter. Lastly, a general conclusion is drawn for the results of the plant factory and the reliability of the results is discussed.

## 5.1. System characteristics

In contrast with greenhouses, plant factories, also known as vertical farms, are closed, multi-storey crop production systems which are designed to maximise production density [95]. Because of this closed system, plant factories are solely dependent on artificial light technologies and since this way of cultivation is relatively new, mainly LED technology is used. The next sections elaborate on the dimensions of the external and internal structure of the plant factory used in this study. Also, the lighting system present is explained and the energy requirements of the plant factory, besides lighting are touched upon.

### 5.1.1. Structure

To make a fair comparison between the greenhouse scenarios and the plant factory, the dimensions of the horizontal surface of the plant factory are the same as the area of the greenhouse, being 40 x 26.4 $m$. The height of the plant factory is assumed to be 10 $m$, but does not further play a role in this analysis. These dimensions are shown in figure 5.1a. It is assumed that the plant factory is a highly insulated box and has no light transmission. Inside the plant factory, the area used for crop cultivation is the same as for the greenhouse scenarios. However, since artificial light is the only light source that is used, multiple storeys of crops can be installed. In this study, it is assumed that the plant factory has a total of five storeys, as shown in figure 5.1b. Theoretically, this means that the production per $m^2$ is five times higher for the plant factory compared to the greenhouses, which only use one layer of crops.

### 5.1.2. Lighting

As mentioned, because of the closed system, the plant factory only makes use of artificial lighting. In this study, a LED lighting system is assumed. Similar to greenhouse scenario 4, the lamps are placed close to the crops. The spectral output of the LED is dependent on type of crop cultivated. Again, it is assumed that the LED fixture is able to output the required spectrum. The efficacy of the LEDs is taken 2.5 $\mu mol/J$ and the electricity demand for the LEDs for one storey of the plant factory is assumed to be equal to the light's electricity demand for scenario 4.

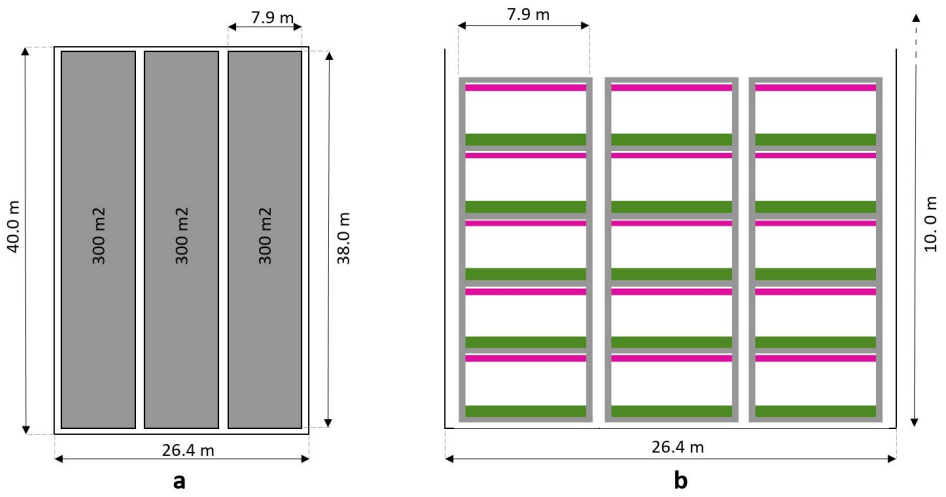


Figure 5.1: Top view of plant factory dimensions (a) and side view of plant factory including 5 levels of crops and lighting systems (b)

### 5.1.3. Other energy requirements

Compared to the semi-closed greenhouse, in the closed system of the plant factory, the energy demand processes besides lighting are different. First of all, because of the well insulated system and the heat produced by the lamps, no additional energy is needed for heating. On the other hand, the lack of natural ventilation results in a high demand for cooling and water vapor removal inside the vertical farm [95], compared to the greenhouse scenarios. The energy demanding processes taken into account for the plant factory are the dehumidification to maintain the humidity of the air, sensible cooling of the air and the cooling of the LED fixtures. The magnitude of these energy demanding processes is assumed to be equal for each location, because of the highly insulated system and is presented in table 5.1. The data for these other energy demanding processes for lettuce is retrieved from the study done by Graamans et al. in 2017 [152], where a comparison is between the performance of greenhouses and plant factories in three different climates (Kiruna, Delft and Abu Dhabi). This study assumes a plant factory with five storeys.

Table 5.1: Relevant energy demanding processes in plant factory for cultivation of lettuce in Kiruna, Delft and Abu Dhabi

| | **Sensible cooling** | **Dehumidification** | **LED cooling** |
|---|---|---|---|
| **Annual energy demand (kWh/m$^2$)** | 90 | 541 | 215 |

### 5.1.4. Model assumptions

The model used to determine the performance of the plant factory is mainly based on the model used to simulate the greenhouse scenarios. As mentioned above, it is assumed that the energy demand and crop production is equal for the three locations. Also the method to determine the rate of photosynthesis and thus the amount of photons used for photosynthesis annually is determined with the same relation as in scenario 4. This relation between the PPFD and the rate of photosynthesis for LEDs is presented in table 3.4. Just like in the greenhouse scenarios, the other parameters having an effect on the rate of photosynthesis, like the temperature and the $CO_2$ concentration are assumed to be optimal and thus do not limit the photosynthetic rate. Furthermore, the same measures are used to indicate the performance of the plant factory compared to the greenhouses, namely: energy consumption, crop production, efficacy and Land Equivalent ratio. The economics of the plant factory system are not determined in this study due to the lack of available data. As discussed, due to the availability of data, the comparison of the plant factory is only done for the crop lettuce.

## 5.2. PV system

As described above, the plant factory is assumed to be a box with an horizontal roof surface of 1056 $m^2$ (40x26.4$m$). This unused area can be used for the installation of a PV system. For the design of the PV system

on the plant factory roof, it is assumed that the whole rooftop area is freely available and that the horizon is free of objects. The next paragraphs describe the steps taken and the assumptions made for the design of the PV system on the roof of the plant factory for Delft, Kiruna and Abu Dhabi.

For the location of Delft in the Netherlands, the relative energy yield is determined for a south facing PV array with tilt angles ranging from 30 to 43 degrees as shown in figure 5.2. The irradiance data is again retrieved from Meteonorm and for this calculation specifically annual data is used. It can be concluded that in Delft, the tilt angle of the PV array with an orientation of 180° with the highest PV energy production annually is 39°. To design a PV system on the roof of the plant factory, taking into account mutual shading, an iterative process is used.

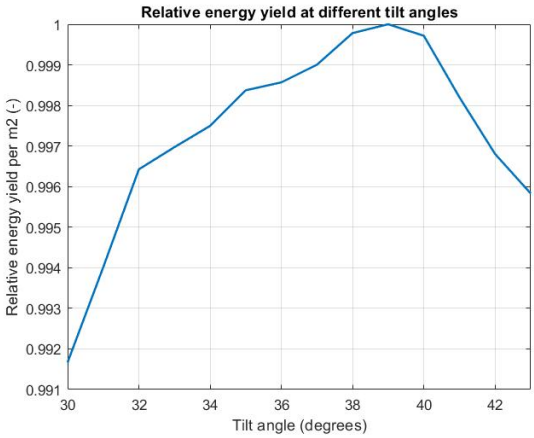


Figure 5.2: Relative energy yield of PV array at different tilt angles with an azimuth of 180°

## Row spacing

To determine the optimal row spacing, it is assumed that there is no mutual shading between $10h$ and $14h$ at the winter solice, the 21st of December. For these moments, the sun altitude and azimuth are shown in table 5.2. This data is retrieved from the SunCalc tool [171]. The following equation is used to determine the shadow length of a PV module having a tilt angle of 39° and facing South [172]:

$$d = l(cos\theta_M + sin\theta_M \; cot\, a_S \; cos(A_M - A_S)), \tag{5.1}$$

where $d$ is the shadow length of the module, $l$ the length of the PV module in $m$, $\theta_M$ the tilt angle of the module, $a_S$ the altitude of the sun, $A_M$, the orientation of the PV modules and $A_s$ the Azimuth of the sun. All angles are measured in *degrees*. In order to minimize the shading losses due to the strings, the PV modules are placed in landscape orientation. This results in $l$ being 1 $m$ (the width of the module is 1.6 $m$).

Filling in the values from table 5.2 in this equation, shadow lengths of 4.83 $m$ and 3.33 $m$ for $10h$ and $14h$, respectively. A Sun Path simulation is done in Rhinoceros using the DIVA plugin to check these values. With this Sun Path simulation, one is able to display sun paths and shadows of objects at a specified moment in time and location. The result of this simulation for one PV module is shown in figure 5.3. The results of the simulation are the same as the values determined with equation 5.1.

Table 5.2: Altitude and azimuth of the sun at 21st of December in Delft

| **Time (h)** | **Altitude (°)** | **Azimuth (°)** |
|---|---|---|
| 10:00 | 6.785 | 143.4 |
| 14:00 | 12.59 | 198.6 |

It can be concluded that in order to prevent mutual shading at the winter solice between $10h$ and $14h$, a row spacing of at lest 4.83 $m$ is needed. This spacing is used in the 3D design of the PV system on top of the plant factory. When using a row spacing of 4.83 $m$, a total of nine PV arrays can be installed and one array consists of 16 modules. The PV modules have an azimuth of 180°. A radiation mapping simulation for a year is done

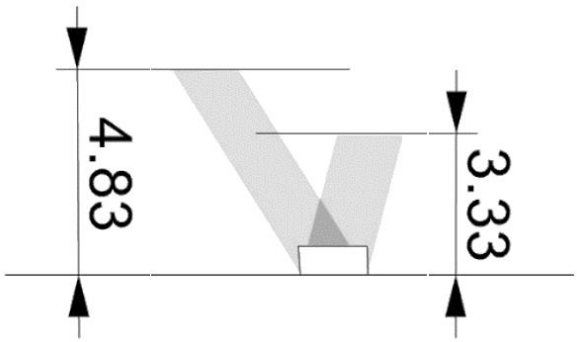


Figure 5.3: Shadow lengths at 10h and 14h at the 21st of December in Delft, the Netherlands

for this setup using hourly irradiance data from Meteonorm. The result of this radiation mapping is shown in figures 5.4 and 5.5. Figure 5.4 shows the 3D view of PV arrays on the plant factory roof and the sum of the radiation over the year on both the plant factory outer surface and the PV modules. Figure 5.5 gives a top view that focuses on the bottom right corner of the plant factory roof. In this figure, the reduced radiation due to shading of the PV array is visible. At a distance of approximately 2.5 $m$, the effect of shading becomes negligible. This means that the row spacing of 4.83 $m$ is a conservative assumptions. The next iteration is done with an array spacing of 2.48 $m$. Besides the smaller array spacing, North facing PV modules are added to

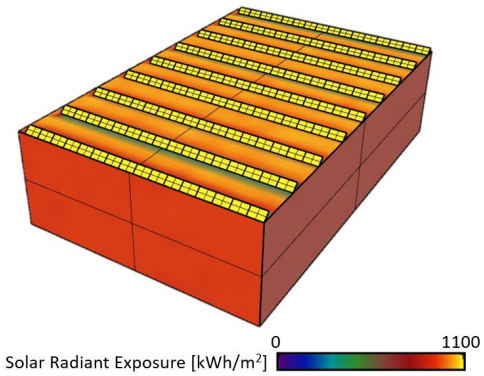


Figure 5.4: Iteration 1: Radiation mapping of PV arrays facing South on top of plant factory

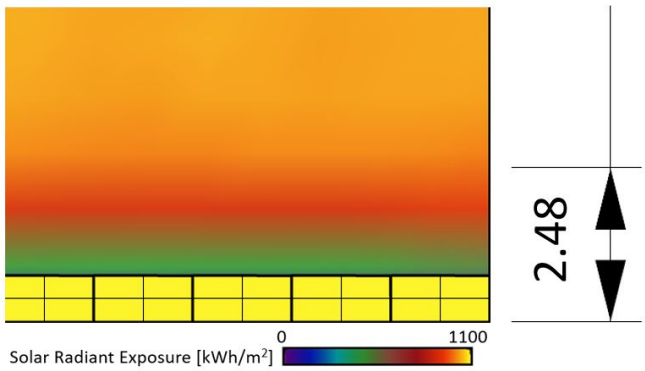


Figure 5.5: Top view of plant factory showing the reduced radiation on the plant factory roof due to shadowing by the PV array

the PV system. These modules have the same angle as the South facing modules and the highest edge of the modules are connected. In this way, the addition of the North facing arrays does not result in extra shading and the system has a higher energy yield. By doing this, the total amount of PV modules becomes 256. The radiation mapping of this configuration is shown in figure 5.6. It can be seen that the total radiation falling on the South facing arrays is still the same as in the first iteration. Assuming a module efficiency of 20% and an effective area of 95%, the annual yield of the total PV system is 210 MWh. Dividing this yield by the total surface area of the plant factory, a yield of 198 $kWh/m^2$ is found.

In practice, however, PV arrays on rooftop are often installed with a tilt angle of 15° to be able to withstand high wind loads. Despite the fact that this tilt angle is not the optimal angle for most of the world, this way of mounting is done worldwide [173, 174]. High wind loads can deform, move and lift the frame of the PV module and array, what can lead to damaging of the PV system. For locations in the Netherlands, the yield of a PV system with a tilt angle of 15° instead of 39° is approximately 5% lower [173]. For all locations, Delft, Kiruna and Abu Dhabi, a PV system is used consisting of arrays with an tilt angle of 15°.

The lower tilt angle of the PV array results in that the array spacing can be reduced. A new array spacing of $2m$ is assumed and both South facing and North facing arrays are included in the system. Similar to iteration 2 with the tilt angle of 39°, the arrays having a opposing orientation, are tip connected. The PV system

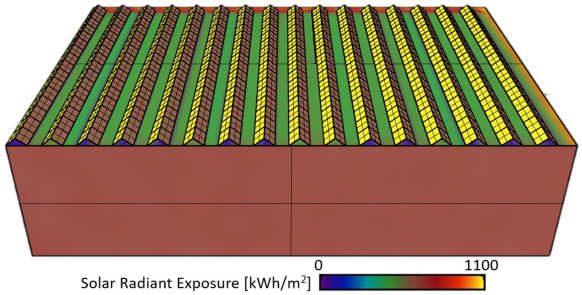


Figure 5.6: Iteration 2: Radiation mapping of PV arrays facing both North and South on top of plant factory

mounted on top of the plant factory is shown in figure 5.7. The system has a total of 672 modules, of which half is facing South. The simulations show that the yield of the South facing arrays is not reduced by shading, since the first array (with the highest sky view factor) has approximately the same annual radiation as the arrays in the middle. For Delft, the annual radiation received by the South facing arrays is circa 1150 $kWh/m^2$ and circa 870 $kWh/m^2$ for the North facing arrays, as shown in figure 5.8. The results for the radiation mapping simulations for Kiruna and Abu Dhabi are shown in figures 5.9 and 5.10, respectively. For Kiruna, the annual radiation received by the South facing arrays is circa 930 $kWh/m^2$ and circa 630 $kWh/m^2$ for the North facing arrays. In Abu Dhabi, the annual radiation received by the South facing arrays is circa 2120 $kWh/m^2$ and circa 1800 $kWh/m^2$ for the North facing arrays. For Abu Dhabi, the tilt angle of 15 degrees is in the optimal range. A tilt angle between 10 and 20 degrees towards the south is found to be optimum for PV systems in this location [175].

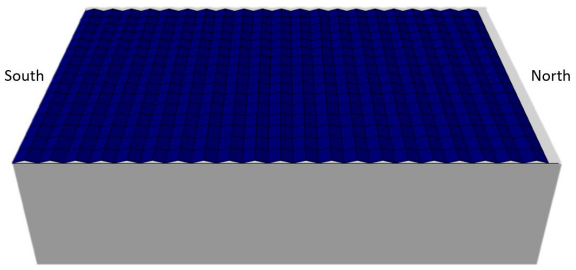


Figure 5.7: 3D view of plant factory with South and North facing PV arrays at a 15° tilt angle

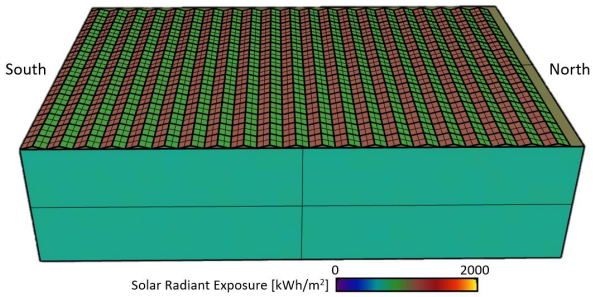


Figure 5.8: 3D view of radiation mapping of plant factory in Delft

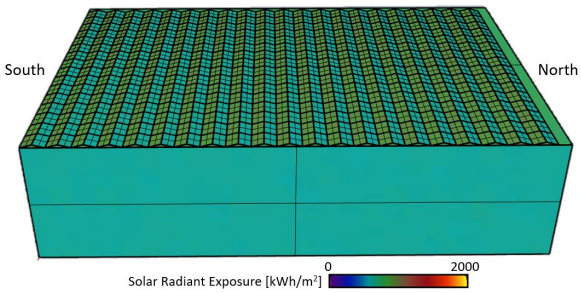


Figure 5.9: 3D view of radiation mapping of plant factory in Kiruna

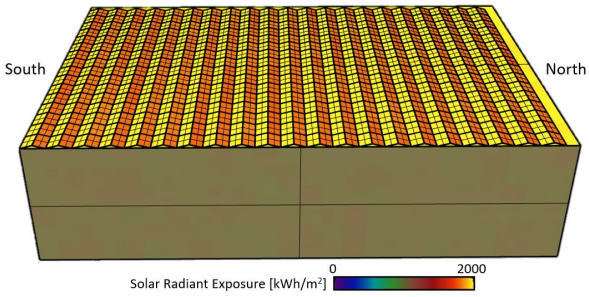


Figure 5.10: 3D view of radiation mapping of plant factory in Abu Dhabi

The total annual energy yield of the PV systems for the three locations is presented in table 5.3. As expected, the production of the system is the highest for Abu Dhabi and the lowest in Kiruna. This table also shows the energy production per $m^2$. This value is determined by dividing the total energy yield by the area of the plant

factory. The energy produced per $m^2$ is used in the performance analysis of the plant factory. Comparing the energy yield of this PV system in Delft with the energy yield for the system with a tilt angle of 39°, which was 198 $kWh/m^2$, it can be concluded that the yield is indeed approximately 5% lower for the system with a tilt angle of 15°.

Table 5.3: Energy production of PV system on plant factory in Kiruna, Delft and Abu Dhabi

| | **Kiruna** | **Delft** | **Abu Dhabi** |
|---|---|---|---|
| **Total annual energy production (MWh)** | 151 | 200 | 385 |
| **Average energy production (kWh/m$^2$)** | 143 | 188 | 364 |

## 5.3. Results

This sections presents and discusses the performance of the plant factory for the cultivation of lettuce and compares it to the performance of the greenhouse scenarios. The analysis is done for all three locations. Subsequently, the energy demand, crop production, efficacy and Land Equivalent Ratio are discussed below.

### 5.3.1. Energy consumption

In figures 5.11, 5.12 and 5.13, the energy consumption for the four scenarios and the plant factory are presented for Kiruna, Delft and Abu Dhabi, respectively. In each bar chart, the left bar of the two bars (lighter bar) of each scenario stands for the energy demand for the lighting and the PV energy produced. The right bar displays the energy demand taking into account the other energy demanding processes as well. In figure 5.11, it can be seen that the energy demand for both measures is significantly higher for the plant factory compared to the greenhouse scenarios in Kiruna. This is mainly caused by the fact that the plant factory has five storeys and the electricity demand for the lighting is five times as high. Because this graph also takes into account the PV energy produced per $m^2$ and there is only one layer of PV modules per $m^2$, the electricity demand for the lighting (dark bar) minus PV energy for the plant factory is more than five times higher than scenario 4.

Figure 5.12 shows that the energy demand for the plant factory in Delft is lower than for the plant factory in Kiruna. This is because the energy yield of the PV system in Delft is higher, as displayed in table 5.3. Furthermore, the same conclusions as in Kiruna, can be drawn for the energy demand of the plant factory in Delft compared to the greenhouses scenarios. Focusing on the energy demand for the plant factory in Abu Dhabi, in figure 5.13, the energy demand is again lower than the plant factory in both Kiruna and Delft, because of the higher PV energy production. For this figure, it can also be concluded that the difference in energy demand between the plant factory and the greenhouses is less significant in Abu Dhabi than for the other two locations. This is caused by the high energy demand of the greenhouse scenarios in Abu Dhabi, which is the result of the large amount of forced ventilation and dehumidification that is needed due to the warm climate.

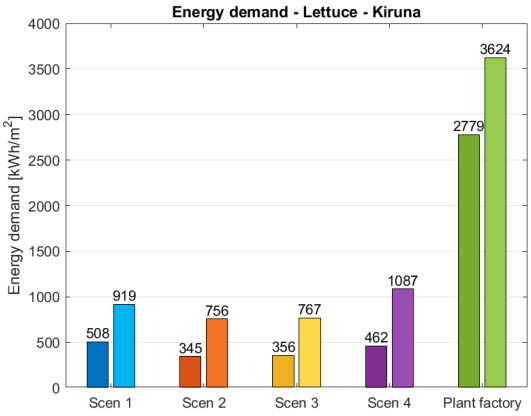


Figure 5.11: Annual energy demand of supplemental light (dark colored bars - left) and all energy demand processes (light colored bars - right) for cultivation of lettuce in Kiruna

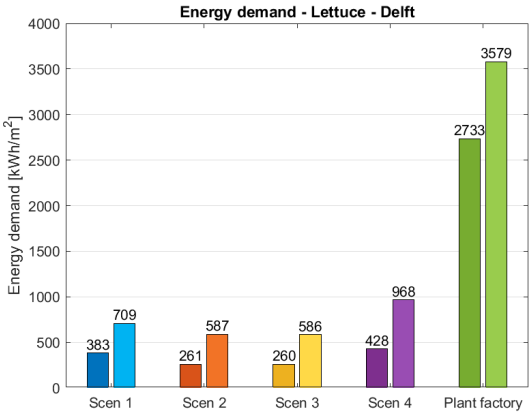


Figure 5.12: Annual energy demand of supplemental light (dark colored bar - left) and all energy demand processes (light colored bars - right) for cultivation of lettuce in Delft

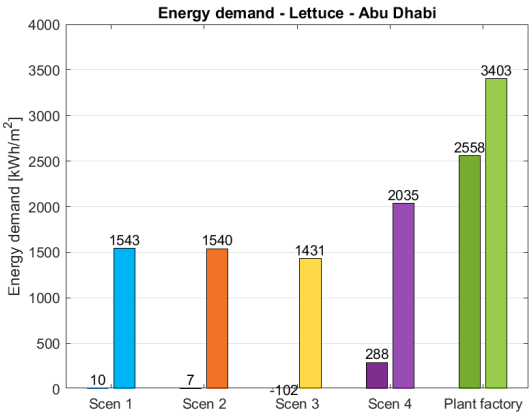


Figure 5.13: Annual energy demand of supplemental light (dark colored bar - left) and all energy demand processes (light colored bars - right) for cultivation of lettuce in Abu Dhabi

## 5.3.2. Crop production

Figures 5.14, 5.15 and 5.16 show the crop production determined in the number of photons used for photosynthesis annually. It can be seen that the number of photons is equal for the plant factories at the different locations. This is because the plant factory is assumed to be a completely closed system and the same amount of lighting is used in each system. The number of photons used in the plant factory is exactly five times the number for scenario 4. This is because the same lighting setup is used, but the plant factory has five storeys and thus five times the production. This goes for all locations.

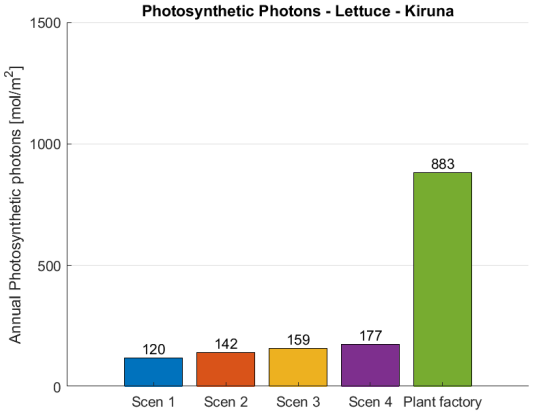


Figure 5.14: The amount of photons used for photosynthesis annually for lettuce in Kiruna

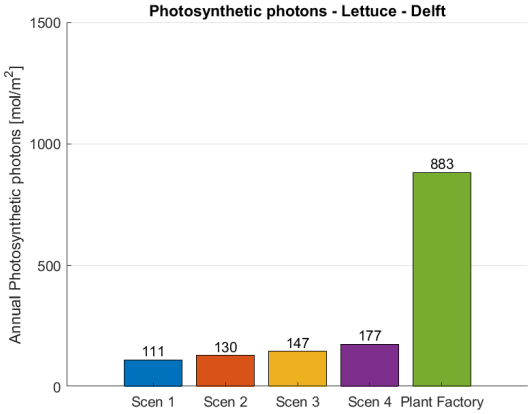


Figure 5.15: The amount of photons used for photosynthesis annually for lettuce in Delft

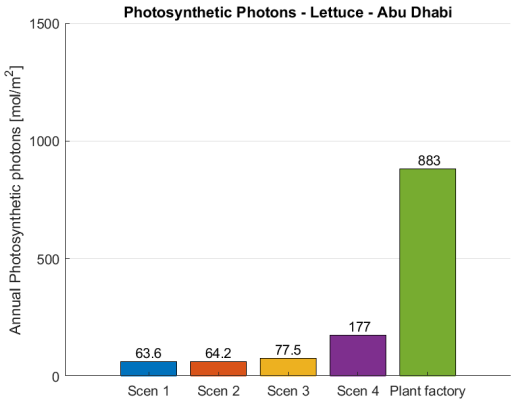


Figure 5.16: The amount of photons used for photosynthesis annually for lettuce in Abu Dhabi

### 5.3.3. Efficacy

The two quantities discuss above, the crop production and energy consumption, are used to determine the efficacy of the system, which is given in $mol/kWh$. As discussed in the two paragraphs, on the one hand, the energy demand is significantly higher for the plant factory. On the other hand, the crop production in the plant factories is also significantly higher compared to the greenhouse scenarios. Figures 5.17, 5.18 and 5.19 show the ratio between these two quantities. It can be seen that the values for the efficacy are not significantly different from the greenhouse scenarios.

Figure 5.17 shows the efficacy for the cultivation of lettuce in Kiruna. When only taking into account the energy needed for the supplemental lighting, scenario 3, with the checkerboard PV system on top, has the highest efficacy. However, when taking into account all energy dynamics, the plant factory has the highest efficacy. This is mainly because the closed, well insulated, plant factory does not need energy to maintain the indoor air temperature. The semi-closed greenhouses, however, do need a significant amount of energy to maintain the temperature. Focusing on the efficacy for the different systems in Delft (shown in figure 5.18), when only taking into account the energy needed for the supplemental lights, scenario 3 performs best. However, when taking into account the other energy demanding processes as well, the difference becomes less significant. Still, scenario 3 has a minimally higher efficacy than the plant factory.

Comparing the results for Abu Dhabi, when only taking into account the energy needed for supplemental lighting, the values for the efficacy explode because of the little amount of additional light that is needed due to the large amount of sunlight available. Focusing on the efficacy including all energy demanding processes, it can be seen that the plant factory has a significantly higher efficacy than the greenhouse scenarios. On the one hand, this is because the greenhouse scenarios require a large amount of energy to cool the system, which is not the case for the well insulated plant factory. On the other hand, the energy yield of the PV system on top of the plant factory is significantly higher than the PV systems present in greenhouse scenario 3 and 4.

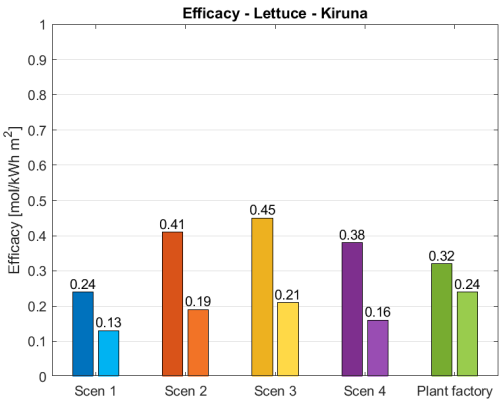


Figure 5.17: The efficacy including only the supplemental lighting energy (dark bar) and the efficacy including the total energy demand (light bar) for lettuce in Kiruna

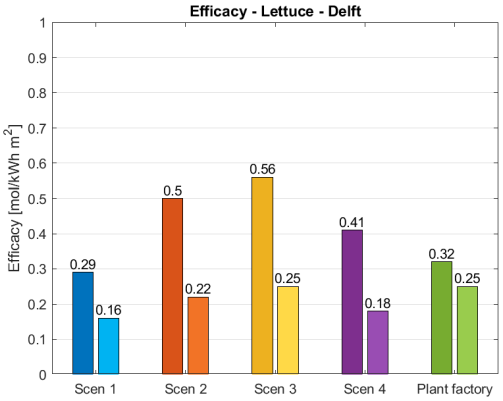


Figure 5.18: The efficacy including only the supplemental lighting energy (dark bar) and the efficacy including the total energy demand (light bar) for lettuce in Delft

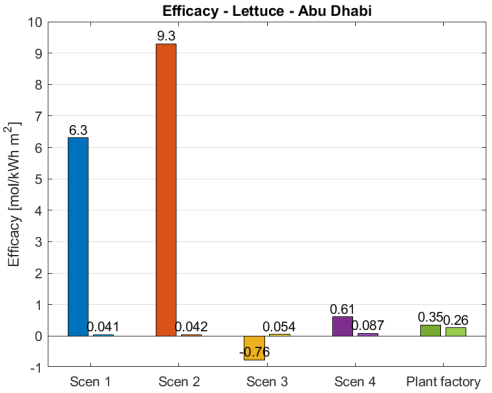


Figure 5.19: The efficacy including only the supplemental lighting energy (dark bar) and the efficacy including the total energy demand (light bar) for lettuce in Abu Dhabi

### 5.3.4. Land Equivalent Ratio

The figures 5.20, 5.21 and 5.22 display the LER of the plant factory compared to the greenhouse scenarios in Kiruna, Delft and Abu Dhabi. As discussed in the previous chapter, the difference the LER for the various greenhouses is small. For the plant factory, the LER is exactly the same for all locations, namely 6. This is because the crop production in the plant factory is location independent due to the closed system. The five storeys result in a production of 5x1 per square meter, while in the greenhouses the production was 1 per square meter. The other component is the PV energy produced. It is assumed that the PV production on top of the greenhouse is maximal for the specified area. This results in the relative PV production to be 1. Combining these two production factors, the combined production value of 6 or 600% is found. Compared to the greenhouse scenarios in all locations, this is a significant increase and thus mainly caused by the high production per area because of the multiple stories. Increasing the number of storeys ($N$) will increase the LER with $N+1$.

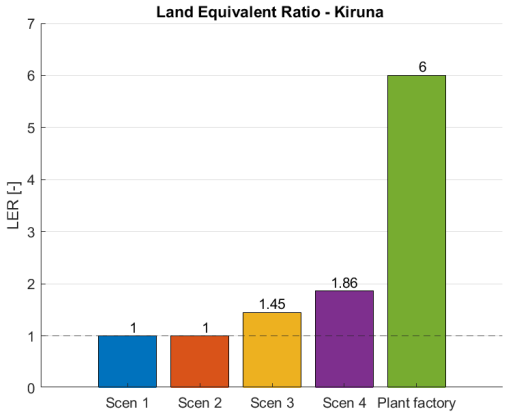


Figure 5.20: Land Equivalent Ratio for the cultivation systems in Kiruna

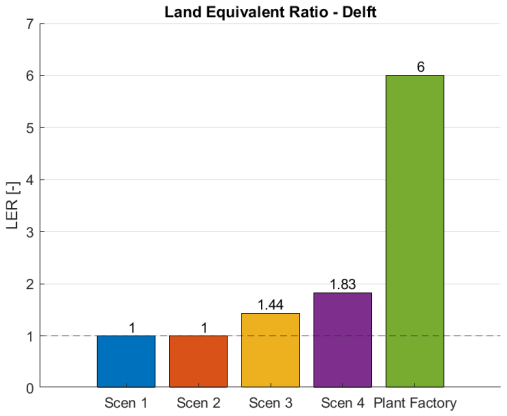


Figure 5.21: Land Equivalent Ratio for the cultivation systems in Delft

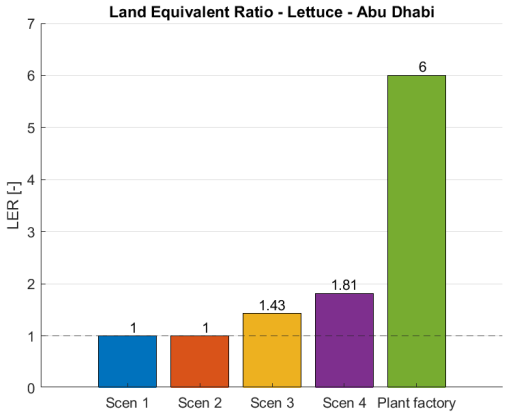


Figure 5.22: Land Equivalent Ratio for the cultivation systems in Abu Dhabi

## 5.4. Conclusion

The sub-question discussed in this chapter is: what is the potential of plant factories compared to greenhouses? The main conclusion that can be drawn from the previous sections is that the production of crops per $m^2$ can be significantly increased by cultivating in a plant factory. Because a plant factory is a closed system and does not make use of sunlight, layers of crops can be placed on top of each other. The high productivity per area is mainly dependent on the number of storeys that is used in the vertical farm. With this option of using multiple layers of crops, a plant factory outperforms all greenhouse scenarios when it comes to productivity. However, the evident shortcoming of the plant factory is the high energy (electricity) demand for artificial lighting. By using five storeys, five times the amount of electricity is needed for lighting. The electricity demand is partly compensated by the installation of the PV system on top of the plant factory, but is still significantly higher than the greenhouse scenarios, that use sunlight as a source of light as well.

In the more extreme climates of Kiruna and Abu Dhabi, the efficacy of the plant factory is higher than the efficacy of the greenhouse scenarios. This difference is most significant in Abu Dhabi. In Delft, the efficacy of the plant factory is approximately equal to the efficacy of greenhouse scenario 3, that has a checkerboard PV module configuration on top. The conclusion that plant factories have a better relative performance compared to greenhouses in extreme climates is in line with the conclusions drawn by Graamans et al. (2017). Figure 5.23 shows an estimation of the advantages of plant factories versus greenhouses based on the relative water scarcity (blue) and electricity use efficiency (red). It is clear that the relative electricity use efficiency is the highest at locations with a very high or very low latitude. At the end of this chapter, in table 5.4, an overview is given of all the results discussed in this and the previous chapter for the two crops, the three locations and the four scenarios and plant factory.

When choosing between cultivation in a plant factory or in a (refurbished) greenhouse, other factors besides the crop production and energy consumption might be taken into account as well. An advantage of plant factories is that they can be placed inside a city, which reduces the potential transportation distance to the customer and thus costs and energy [176]. Greenhouses on the other hand are typically placed hundreds to thousands of kilometers away for most urban centers, because the land is invariably cheaper the further away from the city [177]. However, it must be noted that for some countries, like the Netherlands, this distance is much shorter and the energy and costs needed for transportation are not significant. Another advantage of cultivation in a plant factory is that the water use can be significantly reduced. In the Netherlands, production in plant factories could reduce water consumption to 95% compared to greenhouses [152]. Besides that, the closed production environment minimises the risk of disease infiltration and the need of protective chemicals.

On the other hand, the investment costs and costs for the electricity are significantly higher for the plant factory compared to greenhouses. Refurbishing the reference greenhouse to the more energy efficient greenhouse with a checkerboard PV module configuration on top, is expected to be a lower investment than the installation of a plant factory. With the predicted decrease of the costs for LED technology and the increase in LED efficiency, plant factories are expected to become economically more feasible [176].

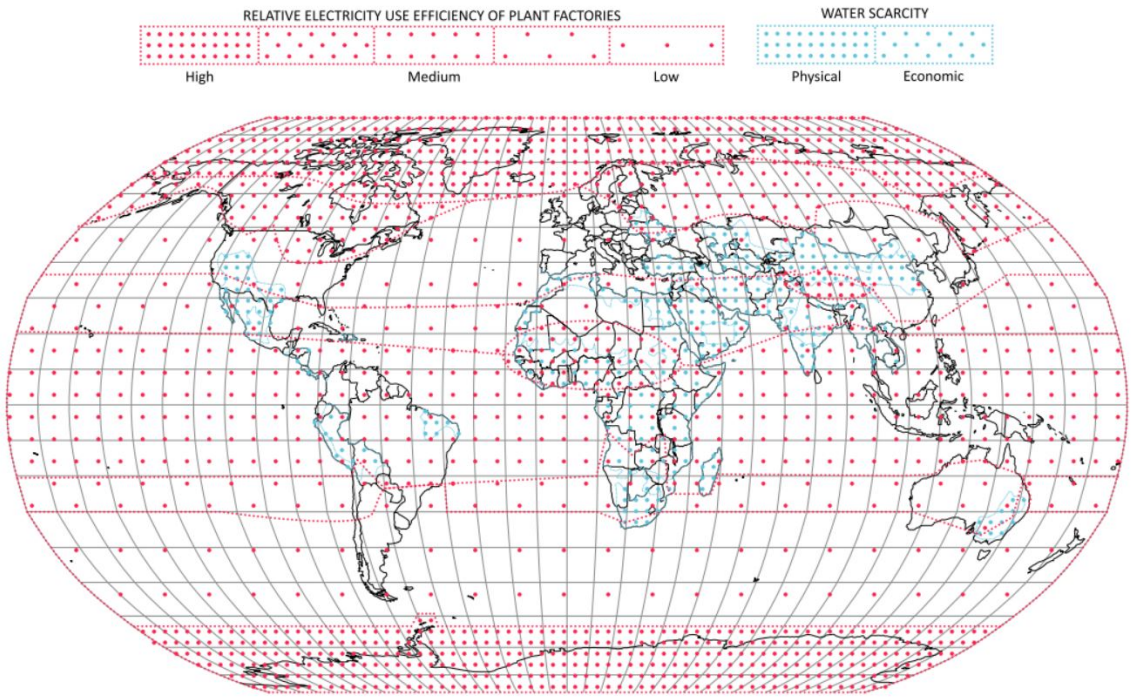


Figure 5.23: Estimation of advantages of plant factories compared to greenhouses based on relative water scarcity (blue) and electricity use efficiency (red) [152]

## 5.5. Discussion - plant factory

Since the general model that is used for the analysis of the plant factory is the same as the model used to analyze the greenhouse scenarios, the shortcomings of the model described in the discussion of the results in the previous chapter, also go for the model used in the plant factory analysis. This section discusses the results of the plant factory specifically and does not describe subjects regarding the model that already have been described in the previous chapter.

The analysis for the plant factory focused on lettuce. However, comparable results regarding the high energy intensity but also high crop production are expected for other crops, like tomato. The production of crops per square meter is five times higher for the plant factory with respect to the greenhouse scenario, because of the multiple storeys. More data is needed for other crops to simulate the performance of the plant factory and to determine the payback time of the system for different crops at different locations. However, at the moment, little information is available regarding other crops and many growth cycles and trial and error processes are needed to get a better understanding of the needs of the specific crop. Also, more information is needed regarding the amount of energy needed besides the energy for supplemental lighting. In fact, currently a limited amount of crop types is cultivated in vertical farms (mainly leafy greens and herbs [178]) and therefore little information is available regarding the (energy) requirements to maintain the indoor climate for different types of crops [176].

Furthermore, for the design of the PV system on the roof of the plant factory, an empty roof surface is assumed. In line with this assumption, the PV modules cover as much of the roof area as possible. However, in practice, not the whole roof area is available for the placement of PV modules, because of the presence of for example cooling systems. Also, normally it is practically not possible to mount the PV modules directly at the rooftop edge due to the presence of structural components or fences. If it would be spatially possible to install the modules at the edge, modules still need to be placed at least 30 $cm$ from the edge to prevent possible damaging of the modules due to wind loads [179]. However, this potential reduction of PV modules and therefore energy production is negligible compared to the total yield of the PV system.

The plant factory has not been included in the economic analysis. However, it is expected that the investment of a plant factory and the costs for electricity are significantly higher than the costs needed to refurbish a greenhouse to the design of scenario 3 (with the highest efficacy among the greenhouse scenarios)[176]. The profitability of a plant factory is again also dependent on the climate and country it is used in. As discussed before, in a more extreme climate, the well insulated plant factory generally has a higher production and requires less energy to maintain the indoor climate than the greenhouse scenarios. However, the vertical farm sector faces major challenges and many vertical farm companies have gone bankrupt as they struggle with the power costs of maintaining a controlled environment 24/7 [178].

Table 5.4: Overview of the results for the two tested crops, three different locations and five scenarios (1: Reference greenhouse, 2: Greenhouse with LED, 3: Greenhouse with LED and checkerboard PV system, 4: Greenhouse with LED and full PV system, 5: Plant factory

| **Crop** | **Location** | **Scenario** | **Energy demand (kWh/m2)** | **Crop production (mol/m2)** | **Efficacy (mol/kWh)** | **LER (-)** |
|---|---|---|---|---|---|---|
| Lettuce | Kiruna | 1 | 919 | 120 | 0.13 | 1.00 |
| | | 2 | 756 | 142 | 0.19 | 1.00 |
| | | 3 | 767 | 159 | 0.21 | 1.45 |
| | | 4 | 1087 | 177 | 0.16 | 1.86 |
| | | PF | 3624 | 883 | 0.24 | 6.00 |
| | Delft | 1 | 709 | 111 | 0.16 | 1.00 |
| | | 2 | 587 | 130 | 0.22 | 1.00 |
| | | 3 | 586 | 147 | 0.25 | 1.44 |
| | | 4 | 968 | 177 | 0.18 | 1.83 |
| | | PF | 3579 | 883 | 0.25 | 6.00 |
| | Abu Dhabi | 1 | 1543 | 63.6 | 0.041 | 1.00 |
| | | 2 | 1540 | 64.2 | 0.042 | 1.00 |
| | | 3 | 1431 | 77.5 | 0.054 | 1.43 |
| | | 4 | 2035 | 177 | 0.087 | 1.81 |
| | | PF | 3403 | 883 | 0.26 | 6.00 |
| Tomato | Kiruna* | 1 | 740 | 167 | 0.23 | 1.00 |
| | | 2 | 503 | 211 | 0.42 | 1.00 |
| | | 3 | 540 | 230 | 0.43 | 1.45 |
| | | 4 | 632 | 273 | 0.43 | 1.86 |
| | Delft | 1 | 888 | 158 | 0.18 | 1.00 |
| | | 2 | 700 | 192 | 0.23 | 1.00 |
| | | 3 | 742 | 215 | 0.21 | 1.44 |
| | | 4 | 1114 | 273 | 0.14 | 1.83 |
| | Abu Dhabi* | 1 | 46 | 108 | 2.35 | 1.00 |
| | | 2 | 31 | 109 | 3.48 | 1.00 |
| | | 3 | 9 | 132 | 14.13 | 1.43 |
| | | 4 | 458 | 273 | 0.6 | 1.81 |

*For the results of tomato in Kiruna and Abu Dhabi, only the energy needed for artificial lighting is taken into account due to the absence of data. These results do not take into account other energy demanding processes.

# 6

# Conclusions & outlook

In this chapter, the main conclusions of this report are discussed on the basis of the research questions presented in the introduction chapter. Besides the conclusions, the outlook to future research is elaborated on.

## 6.1. Conclusions

This section presents the main conclusions that can be drawn from the work presented in this study. The conclusions are discussed using the research questions. The main research question of this study was:

*What is the most space and energy efficient LED-based agrivoltaic system for the cultivation of lettuce and tomato in three different climates?*

In order to be able to answer this research question, multiple sub-questions were defined. Below, the conclusions are discussed per sub-question. Since each sub-question is linked to a chapter and every chapter ends with a conclusion for the specific sub-question, in this section, only the general conclusion per sub-question is discussed.

1. *What is the state of the art of the developments of crop cultivation within greenhouses?*
   This question has been discussed in the literature review in chapter 1. In this chapter, it was concluded that there have been various important developments in agriculture over the last decades. First of all, a lot of research has been done finding the optimal lighting conditions for crops. However, optimal conditions have not been fully determined yet and research is still ongoing to better understand the reaction of plants under different lighting conditions. Despite this, it can be concluded that LED is a suitable lighting technology to grow crops in an efficient way. Furthermore, research has been done finding the right balance between the amount of PV modules used and the amount of light that reaches the crops in an agrivoltaic setup. It was found that a checkerboard PV module arrangement led to the best spatial distribution of light at the crop level in greenhouses. The interaction between these main developments (LED technology and agrivoltaics) and the optimization of a combined system had not been studied yet. This research gap formed the core of this study.

2. *What are the requirements for an artificial lighting system for optimal crop cultivation?*

   This question is discussed in the chapter *Light Simulation Model* and is worked out by means of the design of a light simulation model. The requirements for a lighting system used for the cultivation of crops is dependent on the needs of plants. The plant's lighting requirements can be subdivided into the quality and the quantity of light or the spectral distribution and the amount of photons reaching the crops per time period. These parameters are crop dependent and therefore each crop has it's own optimal values. Besides these two characteristics, the homogeneity of the lamp's output is important for equal crop development on a specified surface. It can be concluded that LED lighting is the most suitable lighting technology for this application. The light simulation tool developed in this study is able to design LED configurations that satisfy these requirements and LED configurations for multiple

crop species can be created. The results found with the model are close to the results of practical measurements and therefore it can be concluded that the model has the potential to be used for the design of lighting systems for crop cultivation.

3. *How can LED and PV technology be arranged in a greenhouse system?*

   In chapter 3, four greenhouse scenarios are designed. The first scenario is a reference greenhouse that uses HPS lighting as addition to sunlight. The second scenario is comparable to the reference greenhouse, but uses LED lighting instead of HPS lighting. The third scenario is a greenhouse that uses LED lighting and also has a checkerboard PV array configuration installed on the roof. In this greenhouse, the amount of sunlight reaching the crops is reduced, but the LED lamps ensure a sufficient amount of light reaches the crops. The fourth scenario is a greenhouse that is fully covered with PV modules and therefore no sunlight is able to enter the greenhouse. LED lamps are the source of light for the crops. In the third and fourth scenarios, c-Si modules are installed on the tilted roof of the greenhouse. Regarding the PV systems present in scenario 3 and 4, it is assumed that the electricity produced by the PV systems is dumped on the grid. Besides that, the electricity needed for the systems driven by electricity, is drawn from the grid. There is no storage system present in these systems.

4. *What is the optimal LED-based agrivoltaic greenhouse design for different climates*

   This sub-question is discussed in chapter 4. In order to determine the optimal greenhouse system, the purpose of the greenhouse system plays an important role. When the purpose of a greenhouse is to have the highest productivity per area, while the energy consumption is less important, the fourth greenhouse scenario that only uses LED lighting as lighting source and that is fully covered with PV modules is the optimal system for Kiruna (SWE), Delft (NLD) and Abu Dhabi (UAE) and both lettuce and tomato. Compared to the lettuce production in the reference greenhouse, scenario 4 produces 1.5, 1.6 and 2.8 times better in Kiruna, Delft and Abu Dhabi, respectively. For tomato, comparable ratios are found. LED light with the right spectrum leads to a higher photosynthetic rate than the light from HPS lamps and sunlight. This means that the more LED light with respect to sunlight reaches the crops, the higher the crop production. Besides the highest crop production, greenhouse scenario 4 also produces most PV energy.

   However, when the purpose of the greenhouse is to have a high crop production and a low energy consumption, the third greenhouse scenario with LED lighting and a checkerboard PV modules configuration performs best in Kiruna and Delft for lettuce. For both locations, scenario 3 has an efficacy that is 1.6 times higher than the efficacy of the reference greenhouse. For the cultivation of lettuce in Abu Dhabi, the efficacy for scenario 4 is the highest.

   Other than the two purposes described before, when the cumulative investment and energy costs per production unit is the most important requirement for the greenhouse, the optimal greenhouse scenario is location dependent. For locations, like Abu Dhabi, with a warm climate and where there is a lot of sunlight available, scenario 4 is the best choice economically. At locations where the amount of supplemental lighting needed is significant, both scenario 2 (with LED lighting) and scenario 3 (with a checkerboard PV module configuration and LED lighting) have the lowest costs per crop produced over a period of 20 years. This conclusion can be drawn for both lettuce and tomato.

5. *What is the potential of plant factories compared to greenhouses?*

   In chapter 5, the potential of the cultivation of lettuce in plant factories was discussed and the performance of the plant factory was compared to the performance of the greenhouse scenarios presented in chapter 4. The main answer to this question is that the production of crops per area can be significantly increased by using a plant factory. The most important reason for this is that a plant factory is a closed and well insulated system that does not make use of sunlight and is only dependent on artificial lighting. Because of this, layers of crops can be placed on top of each other, creating a vertical farm. The production per area is therefore dependent on the number of storeys used inside the plant factory. The plant factory analyzed in this study had five storeys. Regarding the productivity per area, the plant factory outperforms the four greenhouse scenarios significantly. The plant factory produced 5.0 times

more crops than the best producing greenhouse (scenario 4) for all locations. However, inherent to the high productivity is the high energy demand of the plant factory, mainly as a results of the amount of artificial lighting needed. The PV energy production by the PV system installed on the roof of the plant factory partly compensates for the high energy demand, but the energy demand is significantly higher than for the greenhouse scenarios.

The efficacy of the plant factory, which is the ratio between the productivity and the energy consumption, is higher than the greenhouse scenarios in Kiruna and Abu Dhabi. This difference is most significant in Abu Dhabi, where the efficacy of the plant factory is 3.0 times higher than the greenhouse with the highest efficacy (scenario 4). It can be concluded that a plant factory have a better relative performance compared to greenhouses in extreme climates. The efficacy of a plant factory in Delft, however, was found to be approximately equal to the efficacy of greenhouse scenario 3, with a checkerboard PV module configuration.

Besides the high productivity compared to the greenhouses, cultivation within a plant factory has other advantages compared to greenhouses, like the significantly reduced water consumption and the absence of plant diseases and therefore no need of chemical pesticides. On the other hand, the economic feasibility of plant factories is insecure at the moment. Also, the available knowledge on how to cultivate crops efficiently in a closed system as a plant factory is still lacking for the majority of the crops. Today, mainly leafy greens and herbs are grown in plant factories. With the expected developments in crop cultivation with artificial lighting and the developments in LED technology, it is expected that plant factories become more economically feasible in the future.

Summarizing the answers to the sub-questions to answer the main research question, it can be concluded that for the cultivation of lettuce and tomato in Delft, the refurbishment of a reference greenhouse to a greenhouse that uses LED lighting and has a checkerboard PV module configuration installed on the roof is the best option regarding space and energy efficiency. Changing a conventional greenhouse to LED-based agrivoltaic greenhouse, the efficacy of the system is increase by 56%. For more extreme climates, like Abu Dhabi and Kiruna, a plant factory is the system with the highest productivity per specified area and efficacy when cultivating lettuce. Compared to a conventional greenhouse, the efficacy is increased with 534% and 85% for Abu Dhabi and Kiruna, respectively.

In general, this works shows that the production of food and renewable energy do not have to be in competition for the same piece of land; they can be combined in one system while increasing the cumulative productivity per square meter and the total efficacy of the system.

## 6.2. Outlook

In this section, an outlook is given to potential further research regarding this study. As broadly discussed in this research, more research has to be done regarding the optimal lighting conditions for different type of crops. Mainly for closed systems in which no sunlight is used, finding the right lighting conditions seems to be crucial. Also, to better estimate the growth of the plant, existing models to simulate plant growth could be used for the analysis done, like the model described by van Henten (1994) [169]. Besides existing models, new models should be developed to simulate the response of specific crops to various lighting conditions. The development of these kind of models, is inherent to the knowledge available regarding optimal lighting conditions for crops. Furthermore, as discussed, the model does not assume the fact that for high plants, the lower leaves possibly receive too little light because of shading of top leaves. For these kind of crops, like tomato, the growth rate can be increased when using intracanopy lighting [180]. In this concept, besides overhead lighting, lamps are placed in between the crops to also illuminate the leaves located at the lower part of the plant.

Furthermore, the potential of PV systems installed on the greenhouse and plant factory should be further researched. For example, the model described in this study can be combined with a model that assesses the PV potential of actual rooftops using aerial imagery and LiDAR, as described by de Vries et al. (2020) [181]. In this way, the potential of greenhouse roofs with a different shape than the reference greenhouse can be determined and integrated in the analysis. Furthermore, in this study, fixed and conventional PV modules are used. With the current developments in PV technology and the already broad availability of different types

of PV energy generating devices, new combinations of LED-based agrivoltaic systems can be researched. For example, the potential of a greenhouse that combines sun tracking PV modules with LED lighting. Goa et al. (2019) [182] and Valle et al. (2017) [183] found that by using sun tracking PV arrays on a greenhouse improved both the PV energy production and the annual average global irradiance and uniformity on the target plane compared to fixed PV modules. The combination with an LED lighting system could further improve the performance of the greenhouse system. Also the potential of semi-transparent organic solar cells, part of recent studies [184], which transmit light in the PAR region and convert part of the other light into electricity, could be part of further research. Furthermore, the integration of new generation PV modules (500W) [185] could be a relevant addition to the greenhouses discussed. Besides that, the potential of the integration of other PV techniques in the greenhouse design could be further studied. In 2019, van Staalduinen [134] discussed possible techniques, namely: Dye sensitized solar cells as a replacement of greenhouse glass, semi-transparent crystalline modules, flexible modules and bi-facial modules. Also the potential of the implementation of a storage system in the PV system could be part of future research.

Besides these developments of PV technologies, the potential of the use of fiber optic cables could be researched. These cables can be used in plant factories to let sunlight through while being able to maintain a well insulated system. In this way, the freely available sunlight can be used, while the energy needed to maintain the internal temperature stays minimal. Furthermore, while this research focuses on LED technology, the potential of the use of other artificial light sources for crop cultivation should be part of future studies as well. For example the growth of crops under single-wavelength laser light might unlock advantages for highly energy-efficient horticulture [186].

# Bibliography


[1] N. Alexandratos and J. Bruinsma. World agriculture towards 2030/2050. 2012.

[2] R. Green, S. Cornell, J. Scharlemann, and A. Balmford. Farming and the fate of wild nature. 2005.

[3] FAOSTAT. Database on agriculture. 2012.

[4] A. Kahan. Eia projects nearly 50% increase in world energy usage by 2050, led by growth in asia. 2019.

[5] L. Stevens, B. Anderson, C. Cowan, K. Colton, and D. Johnson. The footprint of energy: land use of u.s. electricity production. 2017.

[6] M. Elborg. Reducing land competition for agriculture and photovoltaic energy generation – a comparison of two agro-photovoltaic plants in japan. 2015.

[7] K. Jaspers. 'nederland subsidieert fossiele sector jaarlijks met 7,6 miljard', 2017. URL `https://www.fluxenergie.nl/nederland-subsidieert-fossiele-sector-jaarlijks-met-76-miljard/?gdpr=accept`.

[8] A. Sikkema. Case for radical change in agriculture sector, 2017. URL `https://resource.wur.nl/en/show/Case-for-radical-change-in-agriculture-sector.htm`.

[9] A. Dieleman. Led lighting in greenhouse horticulture, 2015. URL `https://www.wur.nl/en/newsarticle/LED-lighting-in-greenhouse-horticulture.htm`.

[10] M. Jones and G. Jones. *Advanced Biology*. Cambridge University Press, 1997.

[11] L.P. Vernon, E.R. Shaw, T. Ogowas, and D. Raveed. Structure of photosystem i and photosystem ii of plant chloroplasts. 1971.

[12] A. Ried, B. Hessenberg, H. Metzler, and R. Ziegler. Distribution of excitation energy among photosystem i and photosystem ii in red algae. 1977.

[13] G. Weaver and M.W. van Iersel. Photochemical characterization of greenhouse-grown lettuce (lactuca sativa l. 'green towers') with applications for supplemental lighting control. *HortScience*, 2019.

[14] D.O. Hall and K.K. Rao. *Photosynthesis*. Cambridge University Press, 1999.

[15] N.O.G. Jorgensen. Effect of gamma and uv-b/c radiation on plant cells. *Encyclopedia of Inland Waters*, 2009.

[16] A.W.D. Larkum, S.E. Douglas, and J.A. Raven. Photosynthesis in algae. 2003.

[17] A. Smets, K. Jäger, O. Isabella, R. van Swaaij, and M. Zeman. *Solar Energy*. 2015.

[18] R.J. Ritchie. Modelling photosynthetic photon flux density and maximum potential gross photosynthesis. 2010.

[19] C Matthew. Complex inorganic colored pigments: Comparison of options and relative properties when faced with elemental restrictions. 2016.

[20] G. Boyle. *Renewable energy: power for a sustainable future*. Oxford University Press, 2nd edn. edition, 2004.

[21] A.E. Stapleton. Ultraviolet radiation and plants: burning questions.

[22] E. Kovács and Á. Keresztes. Effect of gamma and uv-b/c radiation on plant cells. *Elsevier*, 2001.

[23] I. Ashdown. Photometry and photosynthesis, 2019. URL https://www.allthingslighting.org/index.php/2019/02/15/photometry-and-photosynthesis/.

[24] R. Emerson and C.M. Lewis. The dependence of the quantum yield of chlorella photosynthesis on wave length of light. *American Journal of Botany*, 1943.

[25] S. Zhen and B. Bugbee. Far-red photons have equivalent efficiency to traditional photosynthetic photons: Implications for redefining photosynthetically active radiation. 2020.

[26] J.R. Evans. The dependence of quantum yield on wavelength and growth irradiance. *Functional Plant Biology*, 1987.

[27] S.W. Hogewoning, E. Wientjes, P. Douwstra, G. Trouwborst, W. van Ieperen, R. Croce, and J. Harbinson. Photosynthetic quantum yield dynamics: from photosystems to leaves. 2012.

[28] W.H. Hoover. The dependence of carbon dioxide assimilation in a higher plant on wavelength of radiation. *Smithsonian Institute*, 2012.

[29] K. Inada. Action spectra for photosynthesis in higher plants. *Plant and Cell Physiology*, 1976.

[30] K.J. McCree. The action spectrum, absorptance and quantum yield of photosynthesis in crop plants. *Elsevier*, 1971.

[31] S. Dutta Gupta. *Light Emitting Diodes for Agriculture*. Springer, 2017.

[32] J.M Anderson, W. Soon Chow, and Y. Park. The grand design of photosynthesis: Acclimation of the photosynthetic apparatus to environmental cues. 1995.

[33] T. Ouzounis, E. Rosenqvist, and C.O. Ottosen. Spectral effects of artificial light on plantphysiology and secondary metabolism: a review. *HortScience*, 2015.

[34] Anonymous. Par, ppf, ypf, ppfd and dli, 2019. URL https://www.horti-growlight.com/par-ppf-ypf-ppfd-dli.

[35] H. Hashimoto, W. Soon Chow, and Y. Park. Carotenoids and photosynthesis. 2016.

[36] R. Croce, M.G. Müller, R. Bassi, and A.R. Holzwarth. Carotenoid-to-chlorophyll energy transfer in recombinant major light-harvesting complex (lhcii) of higher plants. 2001.

[37] R.G. Walters and P. Horton. Acclimation of arabidopsis thaliana to the light environment: Changes in photosynthetic function. 1995.

[38] J.F.H. Snel, M.A. Bruins, W. van Ieperen, S.W. Hogewoning, and L.F.M. Marcelis. Fotosynthese-efficiency bij verschillende golflengten. 2011.

[39] R. Emerson. Dependence of yield of photosynthesis in long-wave red on wavelength and intensity of supplementary light. 1957.

[40] X. Chen, L. Wang, T. Li, and W. Guo. Sugar accumulation and growth of lettuce exposed to different lighting modes of red and blue led light. 2019.

[41] Y. Kuno, H. Shimizu, and H. Nakashima. Effects of irradiation patterns and light quality of red and blue light-emitting diodes on growth of leaf lettuce (lactuca sativa l.“greenwave”). *Control in Biology*, 2017.

[42] A. Lobiuc, V. Vasilache, M. Oroian, and T. Stoleru. Blue and red led illumination improves growth and bioactive compounds contents in acyanic and cyanic ocimum basilicum l. microgreens. *Molecules*, 2017.

[43] G. Pennisi, E. Sanyé-Mengual, F. Orsini, and A. Crepaldi. Modelling environmental burdens of indoor-grown vegetables and herbs as affected by red and blue led lighting. 2019.

[44] C. Piovene, F. Orsini, S. BOsi, R. Sanoubar, and V. Bregola. Optimal red: blue ratio in led lighting for nutraceutical indoor horticulture. *Elsevier*, 2015.

[45] K.H. Son and M.M. Oh. Leaf shape, growth, and antioxidant phenolic compounds of two lettuce cultivars grown under various combinations of blue and red light-emitting diodes. *HortScience*, 2013.

[46] S. Zhen and M.W. van Iersel. Far-red light is needed for efficient photochemistry and photosynthesis. *Elsevier*, 2016.

[47] T. Han, V. Vaganov, S. Cao, Q Li, Ling. L, X. Cheng, L Peng, C. Zhang, A.N. Yakovlev, Y. Zhong, and M. Tu. Improving "color rendering" of led lighting for the growth of lettuce. 2017.

[48] H. Kim, R.M. Wheeler, and C.A. Mitchell. Plant productivity in response to led lighting. *HortScience*, 2008.

[49] M. Chen and R. E. Blankenship. Expanding the solar spectrum used byphotosynthesis. 2006.

[50] B Demmig-Adams, C.M. Cohu, O. Muller, and W.W. Adams. Modulation of photosynthetic energy conversion in nature: From seconds to seasons. 2012.

[51] K. Maxwell and G.N. Johnson. Chlorophyll fluorescence: A practical guide. 2000.

[52] N.R. Baker. Chlorophyll fluorescence: A probe of photosynthesis in vivo. 2008.

[53] Y.A. Berkovich, I.O. Konovalova, S.O. Smolyanina, A.N. Erokhin, Bassarskaya E.M. Avercheva, O.V., G.V. Kochetova, T.V. Zhigalova, O.S. Yokovleva, and I.G. Tarakanov. Led crop illumination inside space greenhouses. *Elsevier*, 2017.

[54] M.G. Lefsrud, D.A. Kopsell, R.M. Augé, and A.J. Both. Biomass production and pigment accumulation in kale grown under increasing photoperiods. *Hortscience*, 2006.

[55] M. Dorais. The use of supplemental lighting for vegetable crop production: light intensity, crop response, nutrition, crop management, cultural practices. 2003.

[56] H.V. Koontz and R.P. Prince. Effect of 16 and 24 hours daily radiation (light) on lettuce growth. *Hortscience*, 1986.

[57] W.W. Garner. Comparative responses of long-day and short-day plants to relative length of day and night. *Plant Physiology*, 1933.

[58] M. Brechner and A.J. Both. Hydroponic lettuce handbook. 2013.

[59] J. Holley, B. Poel, S. Hulick, P Shaw, and M Yelton. Using a high yield photoperiod to increase lettuce production by 40%. 2019.

[60] Anonymous. The history of greenhouses, 2019. URL `http://www.thediygreenhouse.com/the-history-of-greenhouses/`.

[61] J.T. Fletcher. *Diseases of greenhouse plants*. Longman, 1984.

[62] D. Waaijenberg and S. Hemming. Haalbaarheid optimale foliekassen voor energie-extensieve teelten : Deelrapport: Inventarisatie mogelijke foliekasconstructies. 2006.

[63] J.A. Dieleman. Energie-efficiënte glastuinbouw dankzij led. 2016.

[64] AP Holland. Blackout and light emission screens, 2019. URL `http://www.apholland.nl/en/screening/black-out-light-emission-screens/`.

[65] Anonymous. Kasconstructies, . URL `https://library.wur.nl/WebQuery/file/lom/lom_t43df9824_002.html`.

[66] F. Kempkes and G Swinkels. Analyse kastransmissievan een helder-diffuus en een referentie kas. 2015.

[67] T. Nacima, T. Bartzanas, D.K. Fidaros, and C. Kittas. Influence of heating system on greenhouse microclimate distribution. 2010.

[68] H. Mangon. Production de la matière verte des feuilles sous l'influence de la lumière électrique. 1861.

[69] E.W. Muijzenberg. A history of greenhouses. 1980.

[70] P. Pinho and L. Halonen. Agricultural and horticultural lighting. 2014.

[71] R.S Simpson. Lighting control - technology and applications. 2003.

[72] R.M. Wheeler, C.L. Mackowiak, and J.C. Sage. Soybean stem growth under high-pressure sodium with supplemental blue lighting. 1991.

[73] J.R. Biard and G.E. Pittman. Semiconductor radiant diode. 1962.

[74] Y. Nanishi. The birth of the blue led. 2014.

[75] S. Nakamura, T. Mukai, and M. Senoh. High-brightness ingan/algan double-heterostructure blue-green-light-emitting diodes. 1994.

[76] S. Kasap. Pn junction devices and light emitting diodes. 2001.

[77] E.F. Schubert. Light-emitting diodes. 2003.

[78] A. Tokuno, Ito S. Araki H. Ibaraki, Y., K. Yoshimura, and K. Osaki. Disease suppression in greenhouse tomato by supplementary lighting with 405 nm led. 2012.

[79] Anonymous. De belichtingsnavigator. 2014.

[80] J.A. Nelson and B. Bugbee. Economic analysis of greenhouse lighting: Light emitting diodes vs. high intensity discharge fixtures. 2014.

[81] Y. Park and E. Runkle. Spectral effects of light-emitting diodes on plant growth, visual color quality, and photosynthetic photon efficacy: White versus blue plus red radiation. 2018.

[82] P.M. Pattison, M. Hansen, and J.Y. Tsao. Led lighting efficacy: Status and directions. 2017.

[83] A. Goetzberger and A. Zastrow. On the coexistence of solar-energy conversion and plant cultivation. 1981.

[84] C. Dupraz, H. Marrou, G. Talbot, L. Dufour, A. Nogier, and Y. Ferard. Combining solar photovoltaic panels and food crops for optimising land use: Towards new agrivoltaic schemes. 2011.

[85] Dricus. Agrivoltaics, 2019. URL `https://sinovoltaics.com/learning-center/technologies/agrivoltaics/`.

[86] C.S. Allardyce, C. Fankhauser, S.M. Zakeeruddin, M. Grätzel, and P.J. Dyson. The influence of greenhouse-integrated photovoltaics on crop production. 2017.

[87] S. Amaducci, X. Yin, and M. Colauzzi. Agrivoltaic systems to optimise land use for electric enerfgy production. 2018.

[88] P.R. Malu, U.S. Sharma, and J.M. Pearce. Agrivoltaic potential on grape farms in india. 2017.

[89] M. Cossu, L. Murgia, L. Ledda, P.A. Deligios, A. Sirigu, F. Chessa, and A. Pazzona. Solar radiation distribution inside a greenhouse with south-oriented photovoltaic roofs and effects on crop productivity. 2014.

[90] A. Yano, M. Kadowaki, A. Furue, N. Tamaki, T. Tanaka, E. Kiraki, Y. Kato, F. Ishizu, and S. Noda. Shading and electrical features of a photovoltaic array mounted inside the roof of an eastewest oriented greenhouse. 2010.

[91] M. Kadowaki, A. Yano, T. Tanaka, F. Ishizu, and S. Noda. Effects of greenhouse photovoltaic array shading on welsh onion growth. 2012.

[92] H. Fatnassi, C. Poncet, R. Brun, M.M. Muller, and N. Bertin. Cfd study of climate conditions under greenhouses equipped with photovoltaic panels. 2014.

[93] A. Marucci and A. Cappuccini. Dynamic photovoltaic greenhouse: Energy efficiency in clear sky conditions. 2016.

[94] F. de Zwart, S. Hemming, M. Ruijs, and T. Gieling. Benutting van zonne-energie in de tuinbouw – een strategische verkenning. 2011.

[95] L. Graamans, M. Tenpierik, A. van den Dobbelsteen, and C. Stanghellini. Plant factories: Reducing energy demand at high internal heat loads through façade design. 2020.

[96] J. Hirama.

[97] G. Spencer. Indoor vertical farming in asia and beyond: Digging deep in data, 2018. URL https://news.microsoft.com/apac/features/indoor-vertical-farming-digging-deep-data/.

[98] Anonymous. Dialux, 2020. URL https://www.dial.de/en/home/.

[99] Valoya. Optimal numbers of luminaires for an optimal result, 2019. URL https://www.valoya.com/light-planning/.

[100] Valoya. Solutions for vertical farming. 2019.

[101] F. Bantis, T. Ouzounis, and K. Radoglou. Artificial led lighting enhances growth characteristics and total phenolic content of ocimum basilicum, but variably affects transplant success. 2016.

[102] G.W. Stutte, S. Edney, and T. Skerritt. Photoregulation of bioprotectant content of red leaf lettuce with light-emitting diodes. 2009.

[103] M. Johkan, K. Shoji, F. Goto, and S. Hashida. Blue light-emitting diode light irradiation of seedlings improves seedling quality and growth after transplanting in red leaf lettuce. 2010.

[104] D. Sergejeva, I. Alsina, M. Duma, L. Dubova, I. Augspole, I. Erdberga, and K. Berzina. Evaluation of different lighting sources on the growth and chemical composition of lettuce. 2018.

[105] M.J. Lee, S.Y. Park, and M.M. Oh. Growth and cell division of lettuce plants under various ratios of red to far-red light-emitting diodes. 2015.

[106] Q. Li and C. Kubota. Effects of supplemental light quality on growth and phytochemicals of baby leaf lettuce. 2009.

[107] K.P. Ferentinos, L.D. Albright, and D.V. Ramani. Se—structures and environment: Optimal light integral and carbon dioxide concentration combinations for lettuce in ventilated greenhouses. 2000.

[108] N. Lu, T. Maruo, M. Johkan, M. Hohjo, S. Tsukagoshi, Y. Ito, T. Ichimura, and Y. Shinohara. Effects of supplemental lighting with light-emitting diodes (leds) on tomato yield and quality of single-truss tomato plants grown at high planting density. 2012.

[109] A. Brazaityte, P. Duchovskis, V. Akvile, and G. Sauoline. The effect of light-emitting diodes lighting on the growth of tomato transplants. 2010.

[110] D.A. Demers and A. Gosselin. Growing greenhouse tomato and sweet papper under supplemental lighting: optimal photoperiod, negative effects of long photoperiod and their causes. 2002.

[111] R.G. Hurd. Long-day effects on growth and flower initiation of tomato plants in low light. 1973.

[112] J. Gerard. Will tomatoes grow without darkness?, 2017. URL https://homeguides.sfgate.com/tomatoes-grow-darkness-67767.html.

[113] Anonymous. Typical ppfd and dli values per crop, . URL https://www.horti-growlight.com/typical-ppfd-dli-values-per-crop.

[114] Anonymous. Daily light integral should be guide for optimal vegetable production, 2019. URL https://www.redusystems.com/en/innovation/daily-light-integral-guide-for-optimal-vegetable-production/.

[115] A.P. Torres and R.G. Lope. Measuring daily light integral in a greenhouse. 2012.

[116] E. van der Zwart. Understanding led wavelength for horticulture. 2018.

[117] M. Kim. Origin of efficiency droop in gan-based light-emitting diodes. 2007.

[118] H. Fu and Y. Zhao. Nitride semiconductor light-emitting diodes (leds). pages 299 – 325, 2018.

[119] D. Zhu and C.J. Humphreys. Solid-state lighting based on light emitting diode technology. 2016.

[120] F.P. Incropera, D.P. Dewitt, and T.L. Bergman. *Fundamentals of Heat and Mass Transfer*. John Wiley Sons, 2006.

[121] D. Bickford and S. Dunn. *Lighting for plant growth*. 1972.

[122] T. Orth, M. Krahl, P. Parlevliet, and N. Modler. Optical thermal model for led heating in thermoset-automated fiber placement. 2018.

[123] U. Gross, K. Spindler, and E. Hahne. Shapefactor-equations for radiation heat transfer between plane rectangular surfaces of arbitrary position and size with parallel boundaries. 1981.

[124] K. Li, Q. Yang, Y. Tong, and R. Cheng. Using movable light-emitting diodes for electricity savings in a plant factory growing lettuce. 2014.

[125] Anonymous. Reliability oriented design of led-based light sources, 2016. URL `https://www.led-professional.com/resources-1/articles/reliability-oriented-design-of-led-based-light-sources`.

[126] G. Hao, M. Taniguchi, K. Nakaya, and S. Inoue. Optimization of p-electrode pattern for algan-based deep-ultraviolet light-emitting diodes. 2015.

[127] X.J. Fan. Development, validation, and application of thermal modeling for a mcm power package. 2003.

[128] X. Qu, H. Wang, X. Zhan, F. Blaabjerg, and H.S. Chung. A lifetime prediction method for leds considering real mission profiles. 2017.

[129] P. Goodman, S. Subramanya, and Landau. Busting myths about led reliability. 2008.

[130] Avantes. What is a spectrometer?, unknown. URL `https://www.avantes.com/products/what-is-a-spectrometer`.

[131] Valoya.

[132] E.G.O.N. Janssen, H. Oversloot, W.D. van der Wiel, and L. Zonneveldt. Optimaal kasdek. 2006.

[133] P.A. van Weel and J.O. Voogt. Natuurkundige analyse van de vocht- en energie balans van een tuinbouwkas. 2012.

[134] J. van Staalduinen. Haalbaarheid transparante zonnepanelen. 2019.

[135] Anonymous. Zonnepanelen op uw kas, 2020. URL `https://www.gakon.nl/nl/tuinbouw/kassenbouw/solar-kassen`.

[136] Anonymous. Kas systemen, 2020. URL `http://solarkassen.nl/site/nl/solar/left-menu/montagesystemen/kas-systeem`.

[137] A. Bosio, G. Rosa, and N. Romeo. Past, present and future of the thin film cdte/cds solar cells. 2018.

[138] Y. Han, Y. Pan, T. Zhao, and C. Sun. Evaluating buildings' solar energy potential concerning urban context based on uav photogrammetry. 2019.

[139] L. Ghobad, A.H. Ardakan, J. Hu, and W. Place. Comparison of climate-based daylighting in two integrated simulation tools: Diva and openstudio:. 2013.

[140] C.F. Reinhart and P.F. Breton. Diva for rhino version. 2011.

[141] C.F. Reinhart and O. Walkenhorst. Validation of dynamic radiance-based daylight simulations for a test office with external blinds. e. 2001.

[142] M. Cossu, A. Cossu, P.A. Deligios, L. Ledda, Z. Li, H. Fatnassi, C. Poncet, and A. Yano. Assessment and comparison of the solar radiation distribution inside the main commercial photovoltaic greenhouse types in europe. 2018.

[143] Anonymous. Plant lighting efficiency and efficacy: mols per joule, 2019. URL `https://www.redusystems.nl/nl/innovatie/elke-procent-meer-licht-in-de-winter-is-pure-winst/`.

[144] C.A. Gueymard, D. Myers, and K. Emergy. Proposed reference irradiance spectra for solar energy systems testing. 2002.

[145] J.C. Sager and J.C. Mc Farlane. Radiation. 2002.

[146] T. Markus. We komen steeds dichter bij het 1:1 vervangen van son-t. 2018.

[147] E. Runkle and B. Bugbee. Plant lighting efficiency and efficacy: mols per joule, 2017. URL `https://gpnmag.com/article/plant-lighting-efficiency-and-efficacy`.

[148] D. Walker. The measurement of rate of photosynthesis as a function of photon flux density and the significance and implication of these measurements. 1989.

[149] M.U.F. Kirschbaum. Does enhanced photosynthesis enhance growth? lessons learned from co2 enrichment studies. 2011.

[150] R. Brakels. Installing solar panels on a flat roof — all the angles covered. 2018.

[151] C.L Chang and K.P. Chang.

[152] L. Graamans, E. Baeza, A. van den Dobbelsteen, I. Tsafaras, and C. Stanghellini. Plant factories versus greenhouses: Comparison of resource efficiency. 2018.

[153] G. Hussey. Growth and development in the young tomato: Iii. the effect of night and day temperatures on vegetative growth. 1965.

[154] K. Hikosaka and N. Hirotsu. The excess light energy that is neither utilized in photosynthesis nor dissipated by photoprotective mechanisms determines the rate of photoinactivation in photosystem ii. 2003.

[155] E. Runkle. Interactions of light, co2 and temperature on photosynthesis. 2015.

[156] N. Domurath, F.G. Schroeder, and S. Glatzel. Light response curves of selected plants under different light conditions. 2012.

[157] K.J. Bergstrand, A. Suthaparan, L. Mortensen, and H.R. Gisleroed. Photosynthesis in horticultural plants in relation to light quality and co2 concentration. 2016.

[158] R. Matsuda, T. Yamano, K. Murakami, and K. Fujiwara. Effects of spectral distribution and photosynthetic photon flux density for overnight led light irradiation on tomato seedling growth and leaf injury. 2016.

[159] A. van Gelder, M. Warmenhoven, and M. Grootscholten. Het nieuwe telen tomaat 2010. 2012.

[160] J.C. Bakker. Luchtvochtigheid. 1993.

[161] P.A. van Weel, H.F. de Zwart, and J.O. Voogt. Vochtbeheersing in kassen en terugwinning van latente energie. 2016.

[162] J.D. Mondol, Y.G. Yohanis, and B. Norton. Optimal sizing of array and inverter for grid-connected photovoltaic systems. 2006.

[163] T. Georgitsioti, N. Pearsall, I. Forbes, and G. Pillai. A combined model for pv system lifetime energy prediction and annual energy assessment. 2019.

[164] B. Vromans. Led belichting in de aardbeienteelt. 2008.

[165] E. Runkle. Investment considerations for greenhouse lighting. 2017.

[166] J. Eaves and S. Eaves. Comparing the profitability of a greenhouse to a vertical farm in quebec. 2017.

[167] Eurostat. Statistieken over aardgasprijzen, 2019. URL https://ec.europa.eu/eurostat/statistics-explained/index.php?title=Natural_gas_price_statistics/nl#Aardgasprijzen_voor_niet-huishoudelijke_verbruikers.

[168] R. Fu, D. Feldman, and R. Margolis. U.s. solar photovoltaic system cost benchmark: Q1 2018. 2018.

[169] E.J. Van Henten. Validation of a dynamic lettuce growth model for greenhouse climate control. 1994.

[170] H.F. de Zwart. Analyzing energy-saving options in greenhouse cultivation using a simulation model. 1996.

[171] V. Agafonkin. Suncalc, 2020. URL https://www.suncalc.org/.

[172] A. Smets, K. Jäger, O. Isabella, R. van Swaaij, and M. Zeman. *Solar Energy*. 2015.

[173] Anonymous. Ballast zonnepanelen plat dak, belangrijke weetjes, 2019. URL https://www.zonnepanelen.net/ballast-zonnepanelen-plat-dak/.

[174] ecogeneration. The australian solar mounting systems guide. 2020.

[175] M Yousif and C.K. Lee. Installation of solar pv systems. 2017.

[176] K. Al-Kodmany. The vertical farm: A review of developments and implications for the vertical city. 2018.

[177] D. Despommier. Farming up the city:the rise of urban vertical farms. 2013.

[178] H. Claver. Vertical farming sector struggles with costs. 2020.

[179] J.H. Cain and D. Banks. Wind loads on rooftop photovoltaic panel systems installed parallel to roof planes. 2016.

[180] F.T. Tewolde, K. Shiina, T. Maruo, M. Takagaki, T. Kozai, and W. Yamori.

[181] T.N.C. de Vries, J. Bronkhorst, M. Vermeer, J.C.B. Donker, S.A. Briels, H. Ziar, M. Zeman, and O. Isabella.

[182] Y. Gao, J. Dong, O. Isabella, R. Santbergen, H. Tan, M. Zeman, and G. Zhang. Modeling and analyses of energy performances of photovoltaic greenhouses with sun-tracking functionality. 2019.

[183] B. Valle, T. Simonneau, F. Sourd, P. Pechier, P. Hamard, T. Frisson, M. Ryckewaert, and A. Christophe. Increasing the total productivity of a land by combining mobile photovoltaic panels and food crops. 2017.

[184] E. Ravishankar, R.E. Booth, C. Saravitz, H. Sederoff, H.W. Ade, and B.T. O'Connor. Achieving net zero energy greenhouses by integrating semitransparent organic solar cells. 2020.

[185] K. Hofmeister. Opening the new 500w+ module era. 2020.

[186] A. Ooi, A. Wong, K.T. Ng, C. Marondedze, C. Gehring, and B.S. Ooi. Growth and development of arabidopsis thaliana under single-wavelength red and blue laser light. 2016.